



DUDLEY WIGHT LIBRARY
NAVAL POSTGRADUATE SCHOOL
MONTEREY, CALIFORNIA 93943-6002

NAVAL POSTGRADUATE SCHOOL

Monterey, California



THESIS

DIGITALLY CONTROLLED "PROGAMMABLE"
ACTIVE FILTERS

by

Panagiotis Andresakis

December 1985

Thesis Advisor:

Sherif Michael

Approved for public release; distribution is unlimited.

T224636

REPORT DOCUMENTATION PAGE

1. REPORT SECURITY CLASSIFICATION		1b. RESTRICTIVE MARKINGS	
2. SECURITY CLASSIFICATION AUTHORITY		3. DISTRIBUTION/AVAILABILITY OF REPORT Approved for public release; distribution is unlimited.	
4. DECLASSIFICATION/DOWNGRADING SCHEDULE		5. MONITORING ORGANIZATION REPORT NUMBER(S)	
6. PERFORMING ORGANIZATION REPORT NUMBER(S)		7a. NAME OF MONITORING ORGANIZATION Naval Postgraduate School	
7. NAME OF PERFORMING ORGANIZATION Naval Postgraduate School		6b. OFFICE SYMBOL (if applicable) Code 62	
8. ADDRESS (City, State, and ZIP Code) Monterey, CA 93943-5100		7b. ADDRESS (City, State, and ZIP Code) Monterey, CA 93943-5100	
9. NAME OF FUNDING/SPONSORING ORGANIZATION		8b. OFFICE SYMBOL (if applicable)	
10. ADDRESS (City, State, and ZIP Code)		9. PROCUREMENT INSTRUMENT IDENTIFICATION NUMBER	
10. SOURCE OF FUNDING NUMBERS		10. SOURCE OF FUNDING NUMBERS	
		PROGRAM ELEMENT NO.	PROJECT NO.
		TASK NO.	WORK UNIT ACCESSION NO.

TITLE (Include Security Classification)

DIGITALLY CONTROLLED "PROGRAMMABLE" ACTIVE FILTERS

PERSONAL AUTHOR(S)
ANDRESAKIS, Panagiotis

11. TYPE OF REPORT Master's Thesis	13b. TIME COVERED FROM _____ TO _____	14. DATE OF REPORT (Year, Month, Day) 1985 December	15. PAGE COUNT 201
---------------------------------------	--	--	-----------------------

SUPPLEMENTARY NOTATION

COSATI CODES			18. SUBJECT TERMS (Continue on reverse if necessary and identify by block number) digitally controlled analog filter
FIELD	GROUP	SUB-GROUP	

ABSTRACT (Continue on reverse if necessary and identify by block number)

In this research a general purpose digitally controlled analog filter is presented. The novel design is a cascade of second-order sections that are individually programmed to achieve any filtering topologies. Two-binary words are used to control the pole frequency ω_p and selectivity Q_p of each section independently. Each second-order section is a Generalized-Immittance Converter (GIC) biquads which are known for their high stability and low active and passive sensitivity. CMOS switches are used to electronically relocate the minimum number of passive elements to achieve function programmability. Switches are also used to select the number of cascaded sections to realize higher order transfer functions.

20. DISTRIBUTION/AVAILABILITY OF ABSTRACT <input checked="" type="checkbox"/> UNCLASSIFIED/UNLIMITED <input type="checkbox"/> SAME AS RPT. <input type="checkbox"/> DTIC USERS		21. ABSTRACT SECURITY CLASSIFICATION Unclassified	
22a. NAME OF RESPONSIBLE INDIVIDUAL Sherif Michael		22b. TELEPHONE (Include Area Code) (408) 646-2252	22c. OFFICE SYMBOL Code 62Mi

Approved for public release; distribution is unlimited.

Digitally Controlled "Programmable" Active Filters

by

Panagiotis Andresakis
Lieutenant Hellenic Navy
B.S., Hellenic Naval Academy 1977

Submitted in partial fulfillment of the
requirements for the degree of

MASTER OF SCIENCE IN ELECTRICAL ENGINEERING

from the

NAVAL POSTGRADUATE SCHOOL

December 1985

John N. Dyer
Dean of Science and Engineering

ABSTRACT

In this research a general purpose digitally controlled analog filter is presented. The novel design is a cascade of second order sections that are individually programmed to achieve any filtering topologies. Two-binary words are used to control the pole frequency ω_p and selectivity Q_p of each section independently. Each second-order section is a Generalized-Immittance Converter (GIC) biquads which are known for their high stability and low active and passive sensitivity. CMOS switches are used to electronically relocate the minimum number of passive elements to achieve function programmability. Switches are also used to select the number of cascaded sections to realize higher order transfer functions.

TABLE OF CONTENTS

I. INTRODUCTION.....14

 A. THE NEED FOR AN ACTIVE PROGRAMMABLE FILTER....14

 B. LINEAR SYSTEMS.....16

 C. FILTERS AS A SPECIAL CLASS OF LINEAR SYSTEMS..18

 D. ACTIVE FILTERS FUNDAMENTALS.....18

 E. GENERALIZED IMMITTANCE CONVERTER.....19

II. THEORETICAL ANALYSIS.....21

 A. BIQUADRATIC TRANSFER FUNCTIONS.....21

 1. Low Pass.....22

 2. High Pass.....23

 3. Band Pass.....23

 4. Notch.....23

 5. All Pass.....24

 B. SENSITIVITY FUNCTIONS.....24

 1. Magnitude Function Deviation.....25

 2. Classical Sensitivity.....26

 3. Gain Sensitivity Product.....27

 4. Determining the Variability of the
 Transfer Function Magnitude.....28

- C. PROPOSED GIC FILTER, ANALYSIS.....29
 - 1. Low Pass Realization.....34
 - 2. High Pass Realization.....36
 - 3. Band Pass Realization.....37
 - 4. Notch Realization.....38
 - 5. All Pass Realization.....38
- D. SENSITIVITY ANALYSIS.....39
- E. STABILITY.....52
- III. PROGRAMMABLE GENERALIZED IMMITTANCE CONVERTER
FILTER.....53
 - A. GENERAL.....53
 - B. THE PROPOSED GIC PROGRAMMABLE FILTER.....54
 - C. THE REALIZED GIC PROGRAMMABLE FILTER.....61
- IV. COMPUTER SIMULATION.....69
 - A. INTRODUCTION.....69
 - B. STIMULATION RESPONSE(S).....70
 - 1. Low Pass Realization..... 70
 - 2. High Pass Realization.....80
 - 3. Band Pass Realization.....84
 - 4. Notch Realization.....88
 - 5. All Pass Realization.....101

V.	REALIZATION OF THE PROGRAMMABLE GIC FILTER.....	105
A.	EXPERIMENTAL RESULTS.....	105
1.	Low Pass.....	105
2.	High Pass.....	107
3.	Band Pass.....	122
4.	Notch.....	122
5.	All Pass.....	142
B.	CONCLUSION.....	142
VI.	COMBINING HIGHER ORDER SECTIONS.....	149
VII.	APPLICATIONS OF THE PROPOSED GIC PROGRAMMABLE FILTER IN FREQUENCY HOPPING SYSTEMS.....	167
A.	BACKGROUND.....	167
1.	General Description of FH Systems.....	167
2.	Signal Generation.....	168
a.	Direct Synthesis.....	168
b.	Indirect Synthesis.....	170
B.	PROPOSED USES.....	173
VIII.	CONCLUSION.....	177
	APPENDIX A: PROGRAM USED TO STIMULATE THE IDEAL GIC PROGRAMMABLE FILTER.....	179
	APPENDIX B: PROGRAM USED TO SIMULATE THE NONIDEAL GIC PROGRAMMABLE FILTER.....	185
	APPENDIX C: PAPER PRESENTED AT THE 19TH ANNUAL ASILOMAR CONFERENCE ON CIRCUITS, SYSTEMS AND COMPONENTS.....	191
	LIST OF REFERENCES.....	196
	INITIAL DISTRIBUTION LIST.....	200

LIST OF TABLES

2.1	Elements Identification for Realizing the Most Commonly Used Transfer Functions.....	41
3.1	The Elements Identification for Different Realization of the GIC Filter.....	56
3.2	The Truth Table of the Switches Logic Used to Select the Filtering Function.....	59
3.3	The Four Bitwords that control Fp and the Corresponding Capacitor.....	65
3.4	The Four Bitwords that control Rq and Qp.....	66
4.1	The Resulting Qp Values for the Different Introduced Rq Values in the Computer Simulation.....	71
4.2	The Resulting p Values for the Different Introduced G Values.....	72
4.3	The 25 Possible Combinations of Transfer Function Realizations.....	73
4.4	Data from Figs. (4.3) and (4.4) Indicating the Affect of Frequency Dependency of Ai (i-1, 2)	79
4.5	Data Illustrating the Ideal vs. the Nonideal Responses of the HPF.....	86
4.6	Data Indicating the Ideal vs. the Nonideal Responses of the BPF Realization.....	97

LIST OF FIGURES

2.1	Active Filter Configuration Using the GIC.....	30
2.2	The Circuit of 2.1 Prepared for Nodal Analysis.	31
2.3(a)	The CGIC Implementation Using Op. Amps.....	40
2.3(b)	Symbolic Representation of the CGIC with Created 3G and 4G.....	40 40
2.3(c)	The Basic Confirguration.....	40
3.1	The Generalized Immittance convertor GIC Implementation Using Op. Amplifiers.....	55 55
3.2	Schematic Diagram of the Programmable GIC Filter Showing the Controlled Noder.....	57 57
3.3	Different Elements Realizations and the Corresponding Switches Used for Digitally Selecting the Filtering Type.....	58 58
3.3(a)	The CMOS Logic Diagram Used to Control the Analog CMOS Switches of Fig. (3.4) and Realize the Truth Table of Table (3.2).....	60 60
3.4	The complete Circuit Diagram of the Programmable GIC Filter.....	60 60
3.5	The Two Capacitor Banks Realizations for the Programming of p	62 62
3.6	The Resistor Bank used to Realize R_q Needed for the Programming of Q_p	63 63

3.7	The Constructed Blocks of Capacitor's Controlling the fp.....	67
3.8	The Constructed Block of Resistance Controlling Qp.....	68
4.4	Ideal LPF Amplitude Response.....	75
4.2	Ideal LPF Amplitude Response.....	76
4.3	Ideal vs. Nonideal CPF Amplitude Response for Q=2 and Variety of Frequencies.....	77
4.4	Ideal vs. Nonideal LPF Amplitude Response for Frequencies (7.96k and 30.1k) and a Variety of Q's.....	78
4.5	Ideal HPF Amplitude Response for a Variety of Q's.....	81
4.6	Ideal HPF Amplitude Response.....	82
4.7	Nonideal HPF Amplitude Response.....	83
4.8	Ideal vs. Nonideal HPF Amplitude Response.....	85
4.9	Ideal vs. Nonideal HPF Amplitude Response.....	87
4.10	Ideal BPF Amplitude Response.....	89
4.11	Ideal BPF Amplitude Response.....	90
4.12	Ideal BPF Amplitude Response.....	91
4.13	Ideal BPF Amplitude Response.....	92
4.14	Nonideal BPF Amplitude Response.....	93
4.15	Nonideal BPF Amplitude Response.....	94
4.16	Ideal vs. Nonideal BPF Amplitude Response.....	95
4.17	Ideal vs. Nonideal BPF Amplitude Response.....	96
4.18	Ideal Notch Amplitude Response.....	98
4.19	Ideal Notch Amplitude Response.....	99

4.20	Ideal vs. Nonideal Amplitude Response.....	100
4.21	Ideal vs. Nonideal Amplitude Response.....	103
4.22	Ideal vs. Nonideal Phase Response.....	104
5.1	LPF Amplitude Response.....	106
5.2	LPF Amplitude Response.....	108
5.3	LPF Amplitude Response.....	109
5.4	LPF Amplitude Response.....	110
5.5	LPF Amplitude Response.....	111
5.6	LPF Amplitude Response.....	112
5.7	LPF Amplitude Response.....	113
5.8	LPF Amplitude and Phase Response.....	114
5.9	LPF Amplitude and Phase Response.....	115
5.10	HPF Amplitude Response.....	116
5.11	HPF Amplitude Response.....	117
5.12	HPF Amplitude Response.....	118
5.13	HPF Amplitude Response.....	119
5.14	HPF Amplitude Response.....	120
5.15	HPF Amplitude Response.....	121
5.16	HPF Amplitude and Phase Response.....	123
5.17	HPF Amplitude and Phase Response.....	124
5.18	HPF Amplitude and Phase Response.....	125
5.19	HPF Amplitude and Phase Response.....	126
5.20	BPF Amplitude Response.....	127
5.21	BPF Amplitude Response.....	128
5.22	BPF Amplitude Response.....	129
5.23	BPF Amplitude Response.....	130
5.24	BPF Amplitude Response.....	131

5.25	BPF Amplitude Response.....	132
5.26	BPF Amplitude Response.....	133
5.27	BPF Amplitude Response.....	134
5.28	BPF Amplitude and Phase Response.....	135
5.29	BPF Amplitude and Phase Response.....	136
5.30	BPF Amplitude and Phase Response.....	137
5.31	BPF Amplitude and Phase Response.....	138
5.32	BPF Amplitude and Phase Response.....	139
5.33	Notch Filter Amplitude Response.....	140
5.34	Notch Filter Amplitude Response.....	141
5.35	Notch Filter Phase and Amplitude Response.....	143
5.36	Notch Filter Amplitude Response.....	144
5.37	Notch Filter Amplitude Response.....	145
5.38	All Pass Filter Amplitude Response.....	146
5.39	All Pass Filter Amplitude Response.....	147
5.40	All Pass Filter Amplitude and Phase Response...	148
6.1	Cascade GIC Programmable Filter.....	149
6.2	LPF Fourth Order vs. Second Order Ideal Response from Computer Simulation.....	151
6.3	Network with Logic Realizing up to the 8th Order LP, HP, BP, N and AP Transfer Functions	152
6.4	Fourth Order vs. Second Order Experimental LPF Responses.....	153
6.5	Ideal Fourth vs. Second Order HPF Responses From Computer Simulation.....	154
6.6	Fourth Order vs. Second Order Experimental HPF Responses.....	155

6.7	Fourth Order vs. Second Order BPF Amplitude Responses from Computer Simulation.....	157
6.8	Fourth Order vs. Second Order Experimental BPF Responses.....	158
6.9	Fourth Order vs. Second Order Notch Filter Amplitude Responses from Computer Simulation.	160
6.10	All Pass Fourth Order vs. Second Order Amplitude Responses from Computer Simulation.	162
6.11	Chevychev Response.....	163
6.12	Chevychev Response.....	164
6.13	BP-BD Amplitude Response.....	165
6.14	BP-BD Amplitude Response.....	166
7.1	Block Diagram of Frequency Hopping Modem.....	169
7.2	Diagram of a Direct Frequency Synthesizer.....	171
7.3	Indirect Signal Synthesis Using a Phase-Locked Loop.....	172
7.4	Proposed Receiver of a F.H. System Using the Programmable GIC Filter.....	174
7.5	Practical BPF Realizations of the Composite GIC	176

ACKNOWLEDGEMENTS

Totally devoted to my father.

I also would like to express my gratitude to Professor Sherif Michael for all his teaching and understanding.

I. INTRODUCTION

A. THE NEED FOR AN ACTIVE PROGRAMMABLE FILTER

The availability of an analog filter with digitally controlled "programmable" coefficients has been the goal of many researchers due to its several attractions. One possibility of a compact, versatile analog filter under remote control opens up many novel and independent application areas. Also, when a programmable filter is combined with a permanent referenced memory which is user-programmable, this would form an economical and versatile device for dedicated stand-alone applications. The need for such a device was motivated by advancement in thick and thin film technologies and continuous upgrading of systems specifications to take advantage of the available technologies to the limits.

Linear analog filtering finds many applications, such as speech processing (recognition or synthesis), geology, instrumentation, communications, process control, adaptive balancing, etc. There has been much emphasis on performing the filtering function digitally, largely because of the ease of varying and optimizing the transfer function. However, for many reasons, such as cost, size, signal processing complexity, and bandwidth, it would be desirable to perform

the filter function with linear components yet retain the flexibility of varying the filter parameters digitally.

Recently, the advantages of combining linear components (operational amplifiers, resistors and capacitors) and non linear elements (switches) have been demonstrated using switched capacitor techniques [36-38]. In this research, we are presenting the results of realizing a continuous active device using linear elements and switches controlled by digital signals to achieve a fully programmable filter [32]. Several programming features of the proposed filter are reported. The first feature is the ability of the network to realize the most common filtering functions (function programmability) namely: Low Pass (LP), Band Pass (BP), High Pass (HP), All Pass (AP) and Notch (N) functions, using the minimal set of elements. The second feature is the ability of the network to program (independently) the key parameters of the filtering function chosen (parameter programmability) namely: the pole resonant frequency (ω_p) and selectivity (Q_p). Finally, the ability to program the network to cascade several sections to achieve higher order filter. All of the above programmability features are performed independently to realize a universal filtering network. In order to demonstrate the idea of this research, it is necessary to introduce some theoretical back ground.

B. LINEAR SYSTEMS

The box at Fig. (1.1) illustrates the concept of the linear system. In the time domain, the system is characterized by its impulse response $y(t)$, which is the output signal $y(t)$ produced in response to an impulse. For an arbitrary input signal $u(t)$, the output signal $y(t)$ is given by the well known convolution integral.

$$y(t) = \int_{-\infty}^{+\infty} y(t-\tau) u(\tau) d\tau \quad (1.1)$$

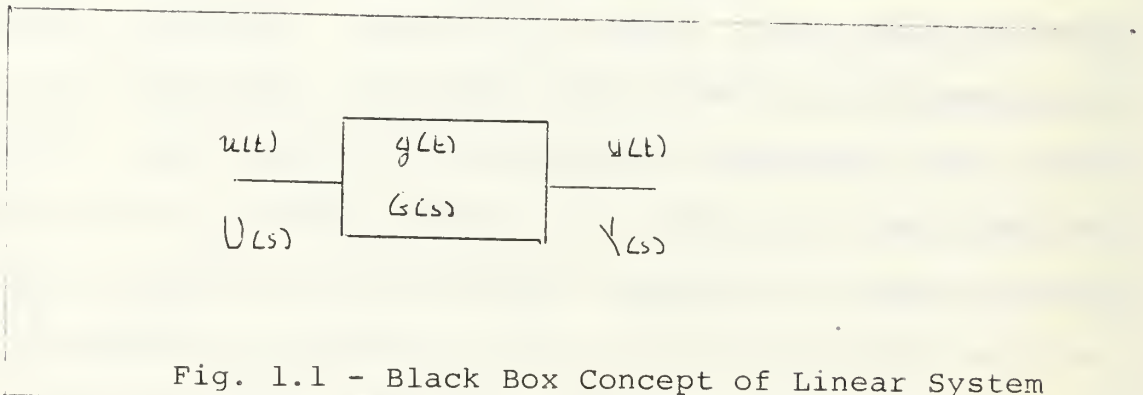


Fig. 1.1 - Black Box Concept of Linear System

The system transfer function $G(s)$ is the Laplace transform of $g(t)$, thus:

$$G(s) = \int_0^{\infty} g(t) e^{-s t} dt \quad (1.2)$$

where $s = \sigma + j\omega$

Under the laplace transformation 1.1) becomes:

$$Y(s) = G(s) \cdot U(s) \quad (1.3)$$

so that the transfer function $G(s)$ is the ratio of the output variable to the input variable.

$$G(s) = \frac{Y(s)}{U(s)} \quad (1.4)$$

The most general types of linear systems are consisting of a finite number of lumped, linear and time-invariant elements. The system is characterized by an N th order ordinary linear differential equation which results, in most general cases, a transfer function $G(s)$ which is a real rational polynomial function of the complex variable s . Thus we can write $G(s)$ in general as

$$G(s) = \frac{P(s)}{E(s)} = \frac{p_M s^M + p_{M-1} s^{M-1} + \dots + p_0}{e_N s^N + e_{N-1} s^{N-1} + \dots + e_0} = \frac{\sum_{k=0}^M p_k s^k}{\sum_{k=0}^N e_k s^k} \quad (1.5)$$

where p_k and e_k are real numbers so that $G(s)$ is real for real s , and the roots of the polynomial $P(s)$ and $E(s)$ must be

real or occur in conjugate pair.

Also by proper multiplications $G(s)$ can take the form

$$G(s) = \frac{P(s)}{E(s)} = C \cdot \frac{\prod_{k=1}^M (s - s_{2k})}{\prod_{k=1}^N (s - s_{1k})} \quad (1.6)$$

where C is a constant extracted from $G(s)$ such that $E(s)$ and $P(s)$ become monic polynomials (leading coefficients equal to unity), s_{2k} are the transmission zeros and s_{1k} are the natural modes at the system.

C. FILTERS AS A SPECIAL CLASS OF LINEAR SYSTEMS

Linear systems can be distinguished into "SPECTRAL SHAPING NETWORKS" and "FILTERS." The role of filters is one of selecting signals while the role of spectral shaping networks is that of modifying the input signal spectrum in an arbitrary, but predescribed manner. Specifically, we desire that a filter should do as little as possible shaping on signals in its passband; any shaping it is considered a distortion of the signal. On the other hand, networks which perform pulse forming fall within the spectral shaping category.

D. ACTIVE FILTER FUNDAMENTALS

The distinction between passive and active filters is that the first do not require a power source to perform their function while the second do. The motivation behind active

RC filters lies in the desire to have inductorless filter realizations. It is well known that of the three passive R,C&L elements, the inductor is the most nonideal one. This is especially true at low frequencies, where inductors become quite bulky and have increased losses or equivalently lower Q-factors.

E. GENERALIZED IMMITTANCE CONVERTOR

One of the methods of active RC filters design consists of simulating the inductances in the LC ladder by active RC networks. This simulation can be based on the principle that we want to find a one port network having an input impedance.

$$Z_{11} = s*L$$

Various active elements as well as synthesis procedures employing them have been proposed [1-9]. A partial list includes:

- (1) Negative Impedance Converter (NIC)
- (2) Negative Impedance Inverter (NIV)
- (3) Postive Impedance Converter (PIC)
- (4) Gyrator
- (5) Generalized Impedance Converter (GIC)
- (6) Curent Conveyor (CC),and
- (7) Operational Amplifier (OA)

Although the introduction of these elements has stimulated research in the area of active network theory, very few elements have made their way to large scale

production to become available as off-the-shelf items. The reason for this is mostly an economic one. For a device to become available at low cost, it has to be used in substantially large quantities. It follows that such a device has to be versatile enough to be of use in a number of applications, of which active filter design is only one. The analog circuit design area has found these attributes in the IC operational amplifiers (Op. Amp.)

The IC Op. Amp. is currently the most popular linear active element. It is available from a large number of manufacturers, at reasonable cost and with good performance characteristics. Furthermore, elements engineers have become accustomed to the use of Op. Amp. It is therefore, only natural that the Op. Amp. is becoming the most popular active element in the design of active RC filters, and can be found in NIC's, PIC's, GIC's, and other circuit realizations.

II. THEORETICAL ANALYSIS

A. BIQUADRATIC TRANSFER FUNCTIONS

The filter as a special class of linear system has a transfer function expressed in a polynomial quotient form given as

$$T(s) = \frac{P(s)}{E(s)} = \frac{P_M S^M + P_{M-1} S^{M-1} + \dots + P_0}{g_N S^N + g_{N-1} S^{N-1} + \dots + g_0} = \frac{\sum_{k=0}^M P_k S^k}{\sum_{k=0}^N g_k S^k} \quad (2.1)$$

where P_k and g_k are real numbers so that $T(s)$ is real for s , and the roots of the polynomials $P(s)$ and $E(s)$ must either be real or occur in conjugate pairs. Also, in general, the degree of the numerator ($\text{deg}[P(s)] = M$) is less than or equal to the degree of denominator ($\text{deg}[E(s)] = N$) and the roots of $E(s)$ are in the open-half S -plane. The $E(s)$ is known as the characteristic polynomial or natural mode polynomial of the linear system, and the degree of $E(s)$, that is N , is the order or degree of the system.

A general second-order transfer function or "biquad" function may be written as

$$T(s) = \frac{P_2 s^2 + P_1 s + P_0}{s^2 + g_1 s + g_0} = \frac{P(s)}{E(s)} \quad (2.2)$$

where $P(s)$ is the loss-pole, or more appropriately here, the transmission-zero polynomial, and $E(s)$ is the natural pole polynomial mode as discussed above. It is a usual practice to express the denominator in terms of ω_p and Q_p , where ω_p is the natural-mode or resonance frequency and Q_p is the natural-mode or quality factor. Thus (2.2) becomes

$$T(s) = \frac{P_2 s^2 + P_1 s + P_0}{s^2 + \frac{\omega_p}{Q_p} s + \omega_p^2} \quad (2.3)$$

The numerator coefficients determine the location of the transmission zeros and hence, the type of filter function the biquad provides. Special cases of interest are:

1. Low Pass (LP)

For which $P_1=P_2=0$, thus two transmission zeros are at infinity

$$T(s) = \frac{P_0}{s^2 + \frac{\omega_p}{Q_p} s + \omega_p^2} \quad (2.4)$$

2. High Pass (HP)

For which $p_0=p_1=0$, thus two transmission zeros are at infinity, and

$$\bar{T}(s) = \frac{P_2 s^2}{s^2 + \frac{\omega_p}{Q_p} s + \omega_p^2} \quad (2.5)$$

3. Band-Pass (BP)

For which $P_0=P_2=0$, thus one transmission zero is at infinity while the other is at the origin, and

$$\bar{T}(s) = \frac{P_1 s}{s^2 + \frac{\omega_p}{Q_p} s + \omega_p^2} \quad (2.6)$$

4. Notch (N)

For which $P_1=0$ and the two transmission zeros are at $s = \pm j\omega_n$, $\omega_n \begin{matrix} < \text{LPN} \\ > \text{HPN} \end{matrix} \omega_p$ (depending if we have low-pass-notch or high-pass-notch), leading to

$$\bar{T}(s) = P_2 \cdot \frac{s^2 + \omega_n^2}{s^2 + \frac{\omega_p}{Q_p} s + \omega_p^2} \quad (2.7)$$

5. All Pass (AP)

For which the pair of zeros are at the mirror image location of the pair of poles, that is

$$T(s) = \frac{s^2 - \frac{\omega_p}{Q_p} s + \omega_p^2}{s^2 + \frac{\omega_p}{Q_p} s + \omega_p^2} \quad P_2 \quad (2.8)$$

B. SENSITIVITY FUNCTIONS

A concern about the design of a filter is how close the resulting response will be to the ideal or desired function. The reason for response deviation from the ideal is the finite tolerances of the RC elements, as well as the nonideal performance of the active elements. In the latter case, not only the gain changes or tolerances have to be considered but the effect of the "limited amplifier bandwidth" on the filter response must also be evaluated. Although effects of initial component tolerances may be "trimmed out" during the initial filter alignments or tuning process, a sensitive design will deviate from the required specifications as time process, due to component variations with temperature, aging, humidity, etc. Note also that a sensitive design might be extremely difficult to tune in the first place, or the initial adjustment will be quite uneconomical.

The answer to tolerance question can be obtained through sensitivity studies. Considerable emphasis has been placed, in the active filter literature, on the study of sensitivity

functions and relations. some of the most useful and widely accepted sensitivity functions are the:

1. Magnitude Function Deviation

Assure a filter designed to meet a certain magnitude characteristics $T(s)$ or $T(j\omega)$. One is concerned with the deviation in $|T(j\omega)|$, that is $\Delta|T(j\omega)|$ both in passband and in stopband. Usually it is desirable to express the expected deviation in dB. The deviation $D(\omega)$ dB in the magnitude function may be evaluated as follows. Let the function $|T(j\omega)|$ change to $[|T(j\omega)| + \Delta|T(j\omega)|]$, then

$$D(\omega) = 20 \log \frac{|T(j\omega) + \Delta T(j\omega)|}{|T(j\omega)|}, (db) \quad (2.9)$$

or

$$D(\omega) = 8.68 \ln \left[1 + \frac{\Delta|T(j\omega)|}{|T(j\omega)|} \right], (db) \quad (2.10)$$

and for small variability (2.10) can be approximated as,

$$D(\omega) \approx 8.68 \frac{\Delta|T(j\omega)|}{|T(j\omega)|}, (db) \quad (2.11)$$

Thus, the deviation in the magnitude response in nepers is equal to the per unit variability in the magnitude of the transfer function. The problem now reduces to that of evaluating the per unit change in $|T(j\omega)|$. This is not an easy problem since $T(j\omega)$ is a function of many elements with different tolerances and tolerance statistics. Furthermore, the per unit change is function of frequency.

2. Classical Sensitivity

Lets recall the definition of the classical sensitivity, S_x^y where y is a variable of interest, usually a function of many parameters of which x is one, then

$$S_x^y \triangleq \frac{\partial y}{\partial x} \frac{x}{y} = \frac{\partial(\ln y)}{\partial(\ln x)} \quad (2.12)$$

Note that from the above definition, S_x^y is the limit to as $Dx \rightarrow 0$. thus, for small variations,

$$S_x^y \approx \frac{\Delta y/y}{\Delta x/x} \quad (2.13)$$

The usefulness of the classical sensitivity function is evident from (2.13). The per unit or percentage change in

y, due to a given per unit or percentage change in x, can be easily obtained by multiplication with S, i.e.,

$$\left(\frac{\Delta y}{y}\right) \approx S_x^y \left(\frac{\Delta x}{x}\right) \quad (2.14)$$

3. Gain Sensitivity Product

An important consideration in the evaluation of the sensitivity of a filter parameter as considered in [2] with respect to the closed loop gain is the tolerance on the closed loop due to the open loop gain variability.

Thus, the gain-sensitivity-product, $G.S_K^Y$ is defined as:

$$G.S_K^Y \triangleq K.S_K^Y \quad (2.15)$$

where k is the closed loop gain. We can extend (2.15) to the open loop gain as:

$$G.S_{A_0}^Y \triangleq A_0.S_{A_0}^Y \quad (2.16)$$

and also we can note that:

$$G \cdot S_k^x = G \cdot S_{A_0}^x \quad (2.17)$$

and thus then ultimate good is the variability or tolerance rather than the sensitivity, the gain-sensitivity product is a better index for comparing different designs.

4. Determining the Variability of the Transfer Function Amplitude

Assure that the active filter has ℓ resistors, m capacitors and n amplifiers. Let the amplifier k have an open loop gain A_{0k} and, possibly, a closed loop gain K_k . The variability of the magnitude function as given by the Reference [10] is:

$$\begin{aligned} \frac{\Delta |T(j\omega)|}{|T(j\omega)|} &= \sum_{i=1}^{\ell} S_{P_i} |T(j\omega)| \left(\frac{\Delta R_i}{R_i} \right) + \sum_{j=1}^m S_{C_j} |T(j\omega)| \left(\frac{\Delta C_j}{C_j} \right) + \\ &+ \sum_{k=1}^n G \cdot S_{K_k} |T(j\omega)| \left(\frac{\Delta A_{0k}}{A_{0k}^2} \right) \end{aligned} \quad (2.18)$$

Note that each of the sensitivity functions is (2.13) is a function of frequency. In a high order filter realization, the different sensitivity functions might be difficult to evaluate.

C. PROPOSED GIC FILTER ANALYSIS

In order to obtain the transfer functions of the proposed programmable filter [13] shown at Fig. (2.1), nodal analysis was used as follows:

(1) The circuit of Fig. (2.1) was replaced by the one of Fig. (2.2) in which the two operational amplifiers were replaced by the two equivalent dependent voltage sources as can be seen, every element (node, admittance, voltage source, etc.) was labeled and every element was associated to a current direction and a voltage polarity.

(2) The kirchoff current law was written for every node except:

(a) The reference,

(b) any node connected to the reference by a voltage source.

<u>Node</u>	<u>K.C.L.</u>	
1	$i_7 = -i_3$	(2.19)
2	$i_2 = i_5 + i_6$	(2.20)
3	--	
4	--	
5	$i_4 = i_7 + i_8$	(2.21)
6	--	
7	--	

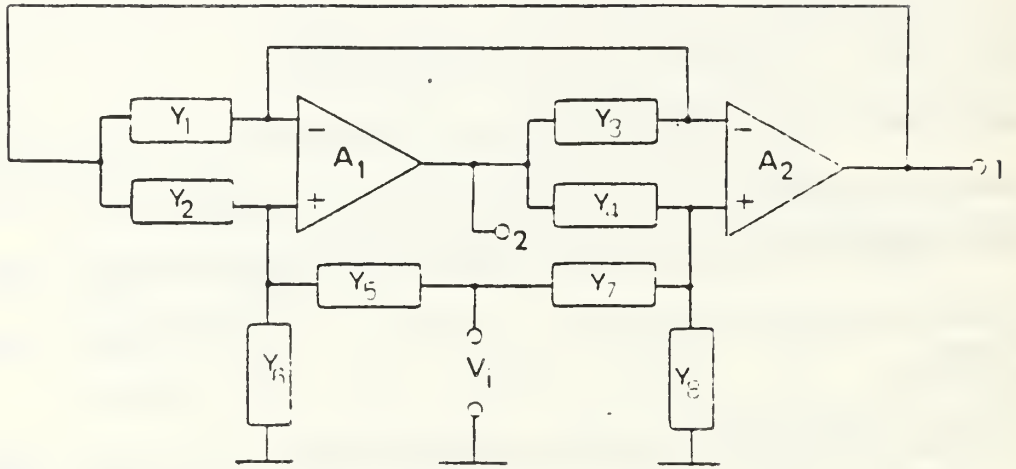


Fig. 2.1 Active Filter Configuration Using the GIC

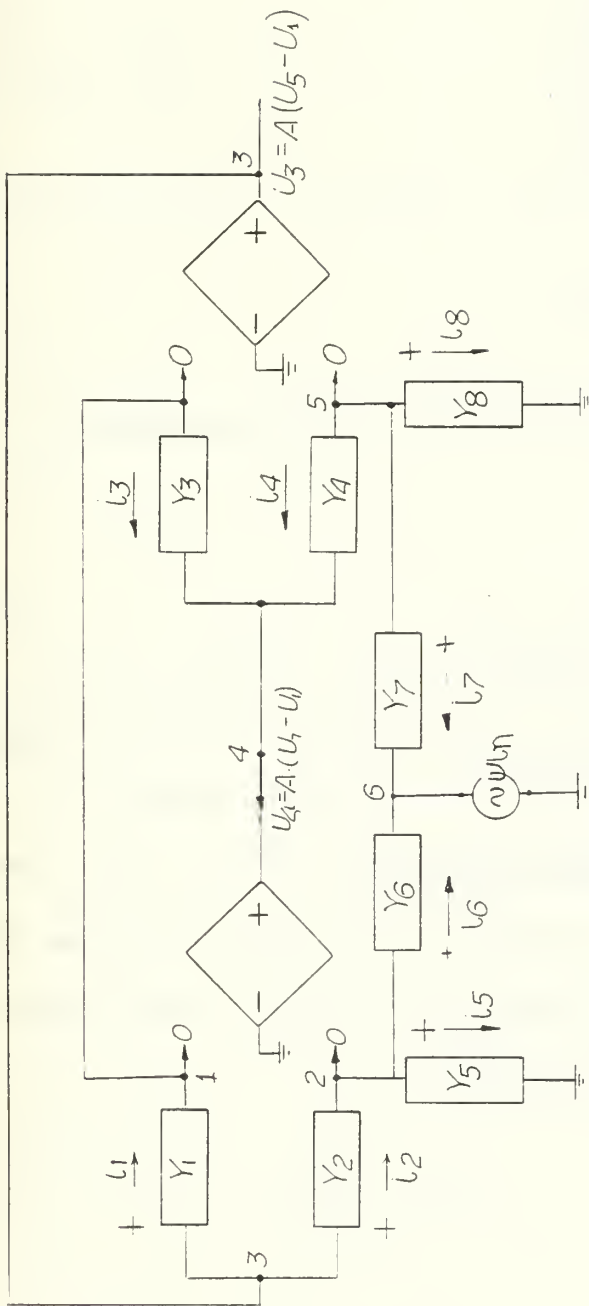


Fig. 2.2 - The Circuit of 2.1 prepared for Nodal Analysis

(3) Every admittance current was expressed in terms of nodal voltages:

$$i_1 = Y_1[\nu_3 - \nu_1] \quad (2.22)$$

$$i_2 = Y_2[\nu_3 - \nu_2] \quad (2.23)$$

$$i_3 = Y_3[\nu_4 - \nu_1] \quad (2.24)$$

$$i_4 = Y_4[\nu_4 - \nu_5] \quad (2.25)$$

$$i_5 = Y_5[\nu_2 - \nu_6] \quad (2.26)$$

$$i_6 = Y_6[\nu_2] \quad (2.27)$$

$$i_7 = [Y_7[\nu_5 - \nu_6] \quad (2.28)$$

$$i_8 = Y_8[\nu_5] \quad (2.29)$$

(4) The source dependencies were listed expressed in terms of nodal voltages,

$$\nu_4 = A_1[\nu_2 - \nu_1] \quad (2.30)$$

$$\nu_5 = A_2[\nu_5 - \nu_1] \quad (2.31)$$

and then (substitute) where necessary.

(5) A matrix equation having the unknown voltages ν_3 , ν_4 , and ν_5 related with the desired transfer functions T_1 , T_2 , T_3 , of the filter was obtained as:

$$\begin{bmatrix} Y_1 \left[1 + \frac{1}{A_2} \right] + \frac{Y_3}{A_2} & Y_2 & -Y_3 - Y_1 \\ Y_2 \left[1 + \frac{1}{A_1} \right] + \frac{Y_5}{A_2} + \frac{Y_6}{A_1} & -\frac{Y_2}{A_1} - \frac{Y_5}{A_1} - \frac{Y_6}{A_1} & -Y_2 - Y_5 - Y_6 \\ 0 & Y_4 & -Y_7 - Y_8 - Y_4 \end{bmatrix} \begin{bmatrix} \nu_3 \\ \nu_4 \\ \nu_5 \end{bmatrix} = \begin{bmatrix} 0 \\ -Y_5 \nu_{i2} \\ Y_7 \nu_{i2} \end{bmatrix} \quad (2.32)$$

and by substituting $T_1 = \frac{V_3}{V_{i2}}$, $T_2 = \frac{V_4}{V_{i2}}$ and $T_3 = \frac{V_5}{V_{i2}}$
the above matrix equation takes the following form:

$$\begin{bmatrix} Y_1 \left[1 + \frac{1}{A_1} \right] + \frac{Y_3}{A_2} & Y_3 & -Y_3 - Y_1 \\ Y_2 \left[1 + \frac{1}{A_1} \right] + \frac{Y_5}{A_2} + \frac{Y_6}{A_1} & -\frac{Y_2}{A_1} - \frac{Y_5}{A_1} - \frac{Y_6}{A_1} & -Y_5 - Y_6 - Y_5 \\ 0 & Y_4 & -Y_7 - Y_8 - Y_4 \end{bmatrix} \begin{bmatrix} T_1 \\ T_2 \\ T_3 \end{bmatrix} = \begin{bmatrix} 0 \\ -Y_5 \\ -Y_7 \end{bmatrix} \quad (2.33)$$

So the above matrix equation gives the 3 different responses of the programmable filter as functions of the Y_1, \dots, Y_7 admittances and A_1, A_2 (Gains) the two Op. Amps. In ideal case [$A_1=A_2=\infty$] the equation takes the form:

$$\begin{bmatrix} Y_1 & Y_3 & -Y_3 - Y_1 \\ Y_2 & 0 & -Y_2 - Y_5 - Y_6 \\ 0 & Y_4 & -Y_4 - Y_7 - Y_5 \end{bmatrix} \begin{bmatrix} T_1 \\ T_2 \\ T_3 \end{bmatrix} = \begin{bmatrix} 0 \\ -Y_5 \\ -Y_7 \end{bmatrix} \quad (2.34)$$

which expressed the different realizations discussed by [31].

Now we can express the above matrix equation for the nonideal case in which A_1 and A_2 are finite and frequency dependent $A_1 = W_1/s$, $A_2 = W_2/s$ where W_1 and W_2 are the Gain Bandwidth Products (GBWP) of the Op. Amps. A_1 , A_2 , respectively.

$$\begin{bmatrix}
 Y_1 \left[1 + \frac{s}{W_2} \right] + \frac{Y_3}{W_2} s & Y_3 & -Y_3 - Y_1 \\
 Y_2 \left[1 + \frac{s}{W_2} \right] + \frac{s}{W_2} [Y_5 + Y_6] & -\frac{s}{W_1} [Y_2 + Y_5 + Y_6] & -Y_2 - Y_5 - Y_6 \\
 0 & Y_4 & -Y_4 - Y_2 - Y_8
 \end{bmatrix}
 \begin{bmatrix}
 T_1(s) \\
 T_2(s) \\
 T_3(s)
 \end{bmatrix}
 =
 \begin{bmatrix}
 0 \\
 -Y_5 \\
 -Y_7
 \end{bmatrix}
 \quad (2.35)$$

1. Low Pass (LP) Realization

Can be obtained through $T_2(s)$ by substituting $Y_6 = Y_7 = 0$, and if we consider the ideal case where ($A_1 = A_2 = \infty$), then

$$T_2(s) = \frac{Y_1 Y_5 (Y_4 + Y_8)}{Y_1 Y_4 Y_5 + Y_2 Y_5 Y_8} \quad (2.36)$$

If we further substitute the values of the remaining admittances as proposed in [4], that is $Y_1=G_1$, $Y_2=sC_2$, $Y_3=sC_3+G_3$, $Y_4=G_4$, $Y_5=G_5$, $Y_8=G_8$ then (2.36) takes the form

$$T_2(s) = \frac{G_1 G_5 (G_4 + G_8)}{G_1 G_4 G_5 + G_3 G_8 C_2 s + G_8 C_2 C_3 s^2} \quad (2.37)$$

which is the form of a low pass transfer function as indicated by (2.4) where

$$P_0 = G_1 G_5 (G_4 + G_8) / C_2 C_3 G_8 \quad (2.38)$$

$$\omega_p^2 = \frac{G_1 G_4 G_5}{C_2 C_3 G_8} \quad (2.39)$$

and

$$\frac{\omega_p}{Q_p} = \frac{G_3}{C_3} \quad (2.40)$$

2. High Pass (HP) Realization

This one is obtained through $T_1(s)$ substituting the following values of the admittances: $Y_1=G_1$, $Y_2=G_2$, $Y_3=sC_3$, $Y_r=G_4$, $Y_5=0$, $Y_6=G_6$, $Y_7=sC_7$, and $Y_8=G_8$, and if we assume ideal case ($A_1=A_2 \rightarrow \infty$), the

$$T_1(s) = \frac{s^2 C_3 C_7 (G_2 + G_4)}{G_6 G_1 G_4 + C_3 G_2 G_8 s + G_2 C_3 C_7 s^2} \quad (2.41)$$

expresses the H.P. filter of (2.5) where

$$\omega_p^2 = \frac{G_1 G_4 G_6}{G_2 C_3 C_7} \quad (2.42)$$

$$\frac{\omega_p}{Q_p} = \frac{G_8}{C_7} \quad (2.43)$$

and

$$p_2 = \frac{G_2 + G_4}{G_3} \quad (2.44)$$

3. Band Pass (BP) Realization

This is also derived from $T_1(s)$ by substituting the following values of admittances: $Y_1=G_1$, $Y_2=G_2$, $Y_3=sC_3$, $Y_4=G_4$, $Y_5=0$, $Y_6=G_6$, $Y_7=G_7$, and $Y_8=sC_8$, and if we assume ideal case ($A_1=A_2 \rightarrow \infty$), then

$$T_1(s) = \frac{sC_3G_7(G_2+G_6)}{G_1G_4G_6 + sG_2G_7C_2 + C_3C_8G_7s^2} \quad (2.45)$$

which is the form of a BP transfer function as given by (2.5)

where

$$\omega_p^2 = \frac{G_1G_4G_6}{G_2C_3C_8} \quad (2.46)$$

$$\frac{\omega_p}{Q_p} = \frac{G_7}{C_8} \quad (2.47)$$

and

$$p_1 = \frac{G_7(G_2+G_6)}{C_8G_2} \quad (2.48)$$

4. Notch (N) Realization

$T_2(s)$ expressed the Notch response if the following substitutions have been made. $Y_1=G_1$, $Y_2=G_2$, $Y_3=sC_3$, $Y_4=G_4$, $Y_6=0$, $Y_5=G_5$, $Y_7=sC_7$, $Y_8=G_8$, and again assuming ideal case ($A_1=A_2 \rightarrow \infty$),

$$T_2(s) = \frac{s^2 C_3 C_7 G_2 + G_1 G_5 (G_4 + G_8)}{s^2 C_3 C_7 G_2 + C_3 G_2 G_8 s + G_1 G_4 + G_5} \quad (2.49)$$

which is the form of a N transfer function as defined by (2.7) where

$$\omega_n^2 = \frac{G_1 G_5 (G_4 + G_8)}{C_3 C_7 G_2} \quad (2.50)$$

$$\omega_p^2 = \frac{G_1 G_4 G_5}{C_3 C_7 G_2} \quad (2.51)$$

and

$$\frac{\omega_p}{Q_p} = \frac{G_8}{C_7} \quad (2.52)$$

5. All Pass (AP) Realization

This is derived from $T_1(s)$ with the following admittances substitutions. $Y_1=G_1$, $Y_2=G_2$, $Y_3=sC_3$, $Y_4=G_4$,

Y5=G5, Y6=0, Y7=sC7 and Y8=G8, and if once more we assume ideal case, then

$$T_1(s) = \frac{s^2 C_3 C_7 G_2 - s C_3 G_5 G_8 + G_1 G_4 G_5}{s^2 C_3 C_7 G_2 + s C_3 G_2 G_8 + G_5 G_1 G_4} \quad (2.53)$$

which is the response of an All Pass filter as (2.8) indicates where:

$$\frac{\omega_P}{\omega_{QP}} = \frac{G_8}{C_7} \quad (\text{for nonminimum phase}) \quad (2.54)$$

and

$$\omega_P^2 = \frac{G_1 G_4}{C_3 C_7} \quad (\quad - \quad - \quad) \quad (2.55)$$

Table 2.1 shows all the realizations proposed by [31]. In our research for designing a programmable filter the No. 1, 3, 7, 9, and 12 realizations were used since they offer the minimum admittance elements change to shift from one to another.

D. SENSITIVITY ANALYSIS

Consider the CGIC circuit shown in Figure (2.2(a)) [12]. Assuming ideal Op. Amps., the chain matrix of the CGIC can be obtained as

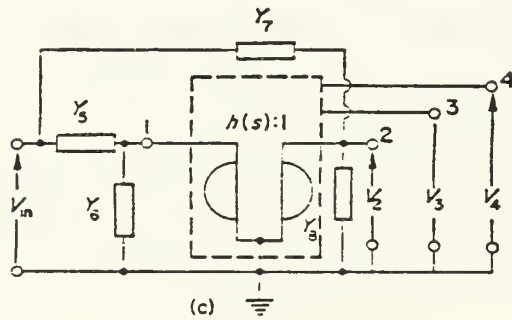
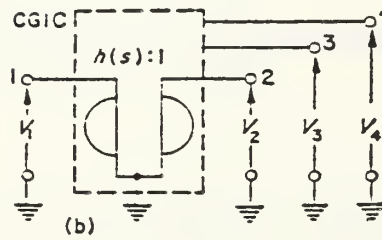
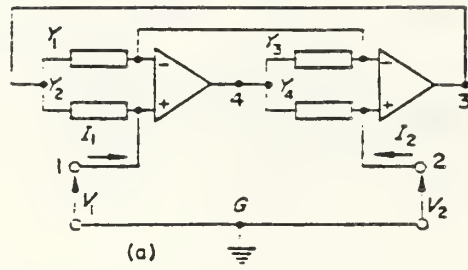


Fig. 2.3 (a) The CGIC Implementation Using Op. Amps.
 (b) Symbolic Representation of the CGIC with created ports 3G and 4G
 (c) The Basic Configuration.

Element identification for realizing the most commonly used transfer functions

Cr. No	$A(s)$	V_1	V_2	V_3	V_4	V_5	V_6	V_7	V_8	Transfer function
(1) LP	$\frac{sC_2(sC_1+G_2)}{G_1G_4}$	G_1	sC_2	sC_1G_3	G_4	G_5	0	0	G_8	$T_{22} = \frac{G_1G_5(G_4+G_8)}{G_1G_5G_4 + sC_2G_3G_8 + s^2C_1C_3G_8}$
(2) LP	$\frac{G_2G_3}{sC_1(sC_4+G_4)}$	sC_1	G_2	G_3	sC_4	0	G_6	G_7	$s(C_8+G_8)$	$T_{32} = \frac{G_2G_3G_7(1+G_6/G_2)}{G_2G_3(G_7+G_8) + s(C_1G_6+G_4+G_7G_2) + s^2C_1G_6}$
(3) HP	$\frac{sC_3G_2}{G_1G_4}$	G_1	G_2	sC_3	G_4	0	G_6	sC_7	$s(C_8+G_8)$	$T_{11} = \frac{s^2C_3C_7(G_2+G_4)}{G_1G_4G_4 + sC_3G_2G_4 + s^2(C_7+G_8)G_2C_3}$
(4) HP	$\frac{sC_3G_2}{G_1G_4}$	G_1	G_2	sC_3	G_4	0	0	0	0	$T_{10} = \frac{s^2C_3C_7(G_2+G_4)}{G_1G_4G_4 + sC_3G_2G_4 + s^2C_3C_7(G_2+G_4)}$
(5) BP	$\frac{s^2C_2C_3}{G_1G_4}$	G_1	G_2	sC_3	G_4	sC_5	G_6	0	G_8	$T_{22} = \frac{sC_5(1+G_6/G_4)G_1G_4}{G_1G_4G_6 + sC_5G_1G_4 + s^2C_2C_3G_8}$
(6) BP	$\frac{G_2G_3}{sC_1(sC_4+G_4)}$	sC_1	G_2	G_3	sC_4+G_4	0	G_6	sC_7	G_8	$T_{11} = \frac{s(G_2G_3 + (1+G_6/G_2))}{G_2G_3G_8 + s(C_7G_2G_3 + C_1G_6G_4) + s^2C_1C_4G_6}$
(7) BP	$\frac{sC_3G_2}{G_1G_4}$	G_1	G_2	sC_3	G_4	0	G_6	G_7	$s(C_8+G_8)$	$T_{21} = \frac{sC_3G_7(G_2+G_4)}{G_1G_4G_4 + sC_3G_2(G_7+G_8) + s^2C_3C_8G_2}$
(8) N	$\frac{G_2G_3}{s^2C_1C_4}$	sC_1	G_2	G_3	sC_4	G_5	0	G_7	sC_8	$T_{22} = \frac{s^2G_3(G_2+G_4) + G_2G_3G_7}{s^2C_1G_5G_4 + sC_8G_2G_3 + G_2G_3G_7}$
(9) N	$\frac{sG_2C_3}{G_1G_4}$	G_1	G_2	sC_3	G_4	G_5	0	sC_7	G_8	$T_{22} = \frac{s^2C_3(G_2+G_4)G_5(G_4+G_8)}{s^2C_3G_2G_4 + sC_7G_5G_4 + G_5G_4G_8}$
(10) N	$\frac{sG_2C_3}{G_1G_4}$	G_1	G_2	sC_3	G_5	G_5	G_6	sC_7	sC_7	$T_{31} = \frac{(1 + [(G_6+G_5)(C_7+G_8)]) (C_7 + (C_7+G_8))}{s^2 + s[G_6(C_7+G_8) + (G_6+G_5)] + (G_6+G_5)(C_7+G_8)}$
(11) AP	$\frac{G_2G_3}{s^2C_1G_4}$	sC_1	G_2	G_3	sC_4	G_5	G_6	G_7	sC_8	$T_{11} = \frac{s^2C_1C_4 - sG_5G_3C_8 + G_5G_3(G_2+G_4)}{s^2C_1C_4(G_5+G_6) + s(G_6G_2G_3 + G_5G_3G_7)}$
(12) AP	$\frac{sG_2C_3}{G_1G_4}$	G_1	G_2	sC_3	G_4	G_5	G_6	sC_7	G_8	$T_{21} = \frac{s^2G_3(G_2+G_4) - sC_7G_5G_8 + G_5G_4G_8}{s^2C_3C_7G_2 + sC_7G_5G_8 + (G_5+G_4)G_1G_4}$

* These elements can be set equal to zero

Table 2.1 - Elements identification for Realizing the Most Commonly Used Transfer Functions

$$[a] = \begin{bmatrix} 1 & 0 \\ 0 & h(s) \end{bmatrix} \quad (2.56)$$

where $h(s)$, the admittance conversion function, is given by:

$$h(s) = Y_2 Y_3 / (Y_1 Y_4) \quad (2.57)$$

Two new ports can be created across terminals 3G and 4G as shown symbolically in Fig. (2.3 (b)).

A synthesis procedure is now described which uses the configuration of Fig. (2.3(c)). The transfer functions between the input and output terminals 2, 3, and 4 are readily obtained as

$$V_3/V_1 = T_1 = [Y_5 + h(s) \{Y_7(1 + Y_6/Y_2) - Y_5 Y_8/Y_2\}] / D(s) \quad (2.58)$$

$$V_4/V_1 = T_2 = \{Y_5(1 + Y_6/Y_4) - Y_6 Y_7/Y_4 + h(s) Y_7\} / D(s) \quad (2.59)$$

$$V_2/V_1 = T_3 = \{Y_5 + h(s) Y_7\} / D(s) \quad (2.60)$$

where

$$D(s) = (s + Y_6 + h(s))(Y_7 + Y_8) \quad (2.61)$$

The conversion function $h(s)$ and Y_5 - Y_8 can be selected in many different ways and it is found that any second-order transfer function can be realized [12].

Letting

$$Y_i = sC_i + G_i$$

where $i=1, 2, 3, \text{ or } 4$, we have from (2.57)

$$h(s) = (sC_2 + G_2)(sC_3 + G_3) / (sC_1 + G_1)(sC_4 + G_4) \quad (2.62)$$

Clearly by omitting one or more conductances and/or capacitances a number of specific conversion functions can be generated.

Most frequently, filters are designed by using Butterworth, Chebychev, Bessel or elliptic approximations in which the transmission zeros are located at the origin, imaginary axis or at infinity. Consequently, the transfer

function can be expressed as a product of a second-order transfer functions of the form

$$T(s) = \frac{a_2 s^2 + a_1 s + a_0}{b_2 s^2 + b_1 s + b_0} \quad (2.63)$$

where $a_1=a_2=0$, $a_0=a_1=0$, $a_0=a_2=0$ or $a_1=0$ for low pass (LP), high pass (HP), band pass (BP) or notch (N) section, respectively.

The coefficients a_i 's of $T(s)$ for these sections are all positive. These sections can be realized by choosing $h(s)$ in a simple manner such as $k_1 s$, $k_2 s$, $k_3 s^2 + k_4 s$ or their reciprocals. The different k_i 's ($i=1, 2, 3$, or 4) are positive constants. By comparing (2.58-2.61) with (2.63), circuits 1-10 in Table 2.1 can be obtained. Circuits 3, 4 and 7 can be regarded as realizations of simple RLC networks [31].

All pass transfer functions are often needed for delay equalization and these can be realized by using second-order transfer functions of the type give by (2.63) where $a_2=b_2$, $a_1=b_1$, and $a_0=b_0$. Second-order sections of this class can be obtained from circuits 11 and 12 of Table 2:1.

Figures (2.3(a)), (2.3(b)), and Table 2.1 show that with the exception of circuit 10, the response is obtained from the output of an operational amplifier. Owing to the low

output resistance of the amplifier, any number of sections can be cascaded without isolating amplifiers.

An important criterion of a realization is its sensitivity to element variations. The pole Q factor and the undamped frequency of oscillation from the transfer function of (2.63) are defined as

$$Q_p = \sqrt{b_0 b_1} / b_1, \quad \omega_p = \sqrt{b_0 / b_2} \quad (2.64)$$

For a Notch section, the Notch frequency is defined by

$$\omega_n = (a_0 / a_2)^{1/2} \quad (2.65)$$

and the multiplier constant can be taken to be

$$H_N = a_0 / b_0 \quad \text{or} \quad a_2 / b_2 \quad (2.66)$$

for $\omega_n > \omega_p$ or $\omega_n < \omega_p$, respectively.

Similarly for the LP, HP, and BP sections

$$H_{LP} = a_0 / b_0, \quad H_{HP} = a_2 / b_2 \quad \text{and} \quad H_{BP} = a_1 / b_1 \quad (2.67)$$

For an All Pass Section, let

$$Q_1 = \frac{(a_0 a_2)^{1/2}}{a_1}, \quad \omega_2 = (a_0 | a_2)^{1/2} \text{ and } H_{AP} = a_2 / b_2 \quad (2.68)$$

The sensitivity of a quantity x with respect to variations in an element e is given by

$$S_e^x = \frac{e}{x} \frac{\partial x}{\partial e}$$

For ideal amplifiers, the use of (2.64)-(2.68) and Table (2.1) leads to

$$0 \leq |S_e^x| \leq 1 \quad (2.69)$$

where x represents any one of the quantities defined by (2.64)-(2.68) and e represents any capacitance or conductance. In addition, it can be shown that

$$\sum S_e^x = 0$$

and

$$\sum |S_e^{Q_1}| = \sum |S_e^{Q_2}| = 4 \quad (2.70)$$

For amplifiers with a finite open-loop gain A, according to [31] the circuit of (Fig. 1(c)) gives

$$U_k/U_i = N_k(s) / D(s) \quad (2.71)$$

where $k=2, 3, 4$, and

$$\left. \begin{aligned} D(s) &= F_1 Y_1 + F_2 Y_3 + (1+F_1)(1+F_2) \left(Y_1/A_1 + Y_3/A_2 + Y_1/A_1 A_2 + Y_3/A_1 A_2 \right) \\ F_1 &= (Y_5 + Y_6) / Y_2 \\ F_2 &= (Y_7 + Y_8) / Y_4 \end{aligned} \right\} \quad (2.72)$$

Consider realizations in which $h(s) = k/s$, such as the circuits 7(BP), 3(HP), 9, 10(N), where

$$Y_1 = G_1, Y_2 = G_2, Y_3 = sG_3, Y_4 = G_4, Y_5 = G_5, Y_6 = G_6, Y_7 = s(G_7 + G_8) \text{ and } Y_8 = s(G_8 + G_8)$$

$$(2.73)$$

For real amplifier gains such that

$$A_1 = A_2 = A_0 \text{ and } A_0 \gg 1$$

(2.72) gives

$$D(s) = F_1 Y_1 + F_2 Y_3 + (1+F_1)(1+F_2) (Y_1 + Y_3) / A_0 \quad (2.74)$$

From (2.64), (2.73), and (2.74), the Q-factor and the undamped frequency of oscillation can be obtained as

$$Q_{pa} = Q_p \left\{ 1 + \frac{X_4}{X_1 A_0} \right\}^{1/2} \left\{ 1 + \frac{X_5 G_4}{(C_7 + C_8) A_0} \right\}^{1/2} / \left\{ 1 + \frac{C_3 X_4 + G_1 X_5}{C_3 X_2 A_0} \right\},$$

$$\omega_{pa} = \omega_p \left\{ \left(1 + \frac{X_4}{X_1 A_0} \right) / \left(1 + \frac{X_5 G_4}{(C_7 + C_8) A_0} \right) \right\}^{1/2} \quad (2.75)$$

where

$$Q_p = \left\{ (G_5 + G_6) (C_7 + C_8) G_1 G_4 / (C_7 + C_8)^2 G_2 G_3 \right\},$$

$$\omega_p = \left\{ (G_5 + G_6) G_1 G_4 / (C_7 + C_8) G_2 C_3 \right\}^{1/2},$$

$$X_1 = (G_5 + G_6) / G_2, \quad (2.76)$$

$$X_2 = (C_7 + C_8) / G_4,$$

$$X_3 = (C_7 + C_8) / G_1,$$

$$X_5 = (1 + X_1) / X_3 \quad \text{and} \quad X_4 = (1 + X_1) (1 + X_2)$$

The sensitivities of Q_{pa} and ω_{pa} with respect to the amplification A_0 can be written as

$$S_{A_0}^{Q_{pa}} = \frac{-1}{2A_0} \left[\frac{X_4}{X_1} + \frac{X_5}{X_3} - \frac{2X_4}{X_2} - \frac{2G_1}{C_3} \frac{X_5}{X_2} \right],$$

$$S_{A_0}^{\omega_{pa}} = \frac{1}{2A_0} \left[\frac{X_5}{X_3} - \frac{X_4}{X_1} \right] \quad (2.77)$$

The use of (2.77) and (2.78) leads to

$$S_{A_0}^{Q_{pa}} = \frac{-1}{2A_0} \left[\left(1 + \frac{1}{X_1} \right) (1 + X_2) + (1 + X_1) \left\{ 1 - 2 \left(1 + \frac{1}{X_2} \right) - \frac{2Q_p^2 X_2}{X_1} \right\} \right] \quad (2.78)$$

by assuming that

$$\left(1 + \frac{1}{x_1}\right) - x_1 \ll 2x_2(1+x_1) + 2Q_p^2 x_2 \left(1 + \frac{1}{x_1}\right) \quad (2.79)$$

Eq.(2.78) reduces to

$$S_{A_0}^{Q_{pa}} = \frac{Q_p}{A_0} \left[Q_p x_2 \left(1 + \frac{1}{x_1}\right) + (1+x_1) (Q_p x_2) \right] \quad (2.80)$$

Straight forward differentiation shows that $S_{A_0}^{Q_{pa}}$ is minimum when

$$x_1 = 1, \quad x_2 = 1/Q_p \quad (2.81)$$

From (2.79) and (2.81) the analysis is valid provided that $4Q_p + 4/Q_p \gg 1$ which is clearly satisfied in practice.

From (2.80) and (2.81) the minimum sensitivity to variations in A_0 is derived as

$$S_{A_0}^{Q_{pa}} = 4Q_p / A_0 \quad (2.82)$$

The corresponding value of $S_{A_0}^{wpa}$ is given by

$$S_{A_0}^{Qpa} = -\frac{1}{A_0 Q_p} \quad (2.83)$$

LP realizations as circuits 1 and 2 can be obtained by using a conversion function of the form or its reciprocals. The admittances Y_1 to Y_8 are chosen as

$$Y_1 = G_1, Y_2 = sC_2, Y_3 = s(C_3 + G_3), Y_4 = G_4, Y_5 = G_5, Y_6 = Y_7 = 0, Y_8 = G_8 \quad (2.84)$$

in order to obtain a conversion function of the form $k_{35} \frac{z^2 + k_{45}}{z^2 + k_{45}}$

Now Q_{pa} and ω_{pa} are obtained as

$$Q_{pa} = \frac{Q_p \left\{ 1 + (1 + G_8/G_4)(1 + G_3/G_1)/A_0 \right\}^{1/2} \left\{ 1 + (1 + G_4/G_8)/A_0 \right\}^{1/2}}{1 + (1 + G_4/G_8)(1 + G_1/G_3)/A_0 + (1 + G_4/G_8)(G_3 G_5 / G_3 (2 A_0))} \quad (2.85)$$

$$\omega_{pa} = \omega_p \left\{ 1 + (1 + G_8/G_4)(1 + G_3/G_1)/A_0 \right\}^{1/2} \left\{ 1 + (1 + G_4/G_8)/A_0 \right\}^{1/2} \quad (2.86)$$

$$\left. \begin{aligned} Q_0 &= \left\{ (C_3 G_1 G_4 G_5) / (C_2 G_3^2 G_8) \right\}^{1/2} \\ \omega_p &= \left\{ (G_1 G_4 G_5) / (C_2 C_3 G_8) \right\}^{1/2} \end{aligned} \right\} \quad (2.87)$$

The sensitivity of Q_{pa} with respect to variations in A_o can be minimized following the approach used earlier. It is found that for minimum sensitivity [31]

$$G_4 = G_8, \quad G_1 = Q_p G_3 \quad (2.88)$$

The minimum value of $S_{A_o}^{Q_{pa}}$ can be shown to be

$$S_{A_o}^{Q_{pa}} = 4Q / A_o \quad (2.89)$$

and the corresponding value of $S_{A_o}^{\omega_{pa}}$ is given by

$$S_{A_o}^{\omega_{pa}} = -1 / A_o Q_p \quad (2.90)$$

The above sensitivity analysis can be extended to realizations using any other type of conversion function [31].

Equation (2.69) shows that the sensitivities to passive element variations are independent of the selectivity. Furthermore, the sensitivities with respect to variations in the amplifier gain are low. The proposed realizations are

seen to have similar sensitivity properties as the low sensitivity realizations reported in [21-27].

E. STABILITY

It has been shown elsewhere [20] that some networks using GIC's can be conditionally stable where a circuit can lock in an unstable mode during activation (just after switching on the power supply). In this section the stability properties of the configuration show in Fig. (2.2(c)) are examined.

The natural frequencies of the circuit in Fig.(2.3(c)) are the zeros of the characteristic polynomial $D(s)$ as given by (2.72). The differential open-loop gain of a frequency compensated Op. Amp., in a bounded frequency range $0 \leq \omega \leq \omega_c$

$$A = A_0 \cdot \omega_c / (s + \omega_c)$$

where A_0 and ω_c are the d.c. gain and the cutoff frequency respectively, and $0 \leq A_0 \leq A_{max}$. In the frequency range $\omega \ll \omega_c$ the amplifier gains A_1 and A_2 can be assumed to be real. For any second-order transfer function the coefficients of $D(s)$ are seen to remain positive for any attainable pair of A_1 and A_2 . This is due to the absence of negative terms in $D(s)$. Therefore, the zeros of $D(s)$ will remain the left-half s -plane and low frequency unstable modes cannot arise during activation.

III. PROGRAMMABLE GIC FILTER

A. GENERAL

Signal processing devices evolved considerably over the last several years. The progress was motivated by the advancement in film and semiconductor technologies, as well as the continuous upgrading of systems specifications to take advantage of the available technologies to the limits.

Linear filtering finds many applications, such as speech processing (recognition or synthesis), geology, instrumentation, communications, process control, adapting balancing, etc. There has been much emphasis on performing the filter function digitally, largely because of the ease of varying and optimizing the transfer. However, and for many reasons, such as cast size signal processing complexity, and bandwidth, it would be desirable to perform the filter function with linear components, yet retain the flexibility of varying the filter parameters digitally.

Recently, several advantages of combining linear components (amplifiers and capacitors) and nonlinear elements (switches) have been demonstrated using MOS switched capacitor techniques [31, 32]. Here, we are presenting the results of realizing a continuous active device using linear elements and switches controlled by digital signals to achieve fully programmable filters.

Our research addressed two different aspects of programmability namely;

(1) Programming the filter topology using a minimal set of elements to obtain any type of filtering function desired, e.g., LP, HP, BP, N and AP.

(2) Programming the filter's transfer function parameters, (pole resonant frequency ω_p and quality factor Q_p) for a chosen type of filtering function.

B. THE PROPOSED GIC PROGRAMMABLE FILTER

The basic active network considered as the heart of the GIC programmable filter is the GIC structure [31] of Fig.(3.1), whose superior performance was established in the literature [10,32]. The filter transfer function was derived using loop analysis in Chapter II.

Table (3.1), illustrates that for any of the LP, HP, BP, N and AP realizations, five resistors, two capacitors and two Op. Amps., are required. also, the transfer function of each realization is shown. The passive elements are connected to the different nodes, shown in fig.(3.2), for the different realizations. A set of MOS bilateral switches controlled by a digital binary word, are used to interchange the elements to achieve the different types of filter realization shown in Fig.(3.3). The truth table of the switch control logics is shown in Table (3.2). Fig.(3.3(a)) illustrates the CMOS logical circuit for realizing this truth table. While four of the resistors are equal and of value R each, the fifth

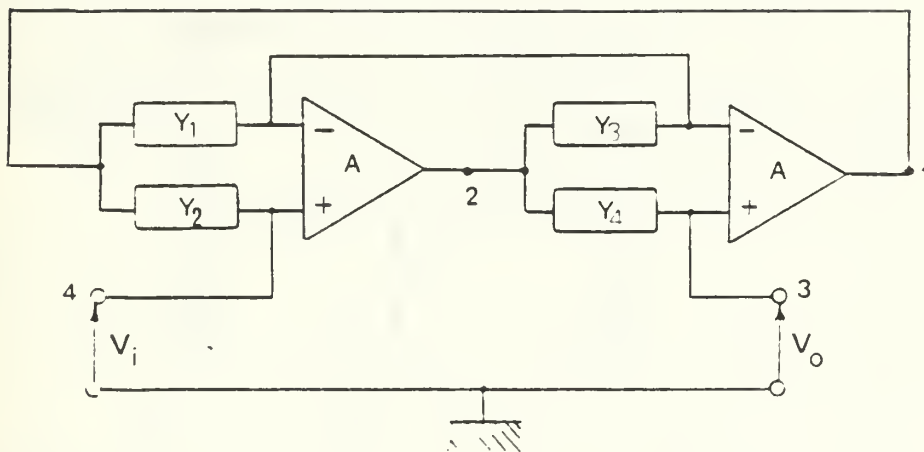


Fig. 3.1 - The Generalized Immittance Converter (GIC) Implementation Using OA's .

Filter Type	Y_1	Y_2	Y_3	Y_4	Y_5	Y_6	Y_7	Y_8	Transfer Function
LP	G	C	$C + \frac{G}{QP}$	G	G	0	0	G	$T_2 = 2Wp^2/D(s)$
HP	G	G	C	G	0	G	C	$\frac{G}{QP}$	$T_1 = 2S^2/D(s)$
BP	G	G	C	G	0	G	$\frac{G}{QP}$	C	$T_1 = 2(Wp/Qp)^S/D(s)$
N	G	G	C	G	G	0	C	$\frac{G}{QP}$	$T_2 = (S^2 + W_n^2)/D(s)$
AL	G	G	C	G	G	0	C	$\frac{G}{QP}$	$T1 = (s^2 - \frac{Wp}{QP} s + wp^2)/D(s)$

where $T(s) = N(s)/D(s)$ and $D(s) = S^2 + (Wp/Qp)S + Wp^2$

TABLE 3.1. - The Elements Identification for Different Realizations of the GIC Filter .

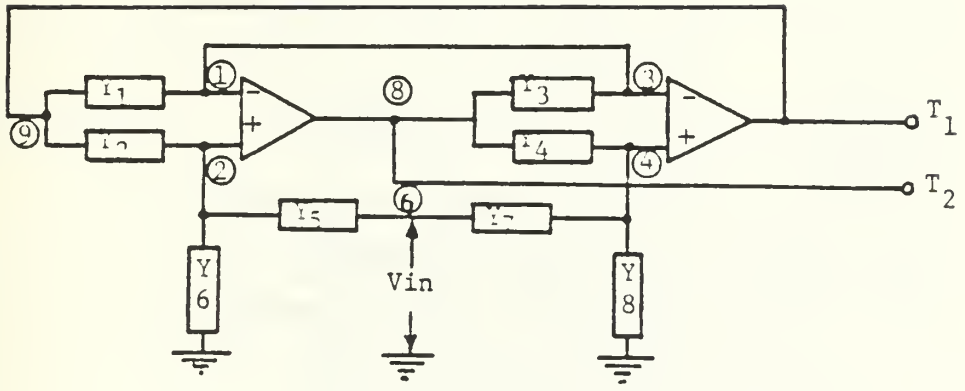


Fig. 3.2 - Schematic Diagram of the Programmable GIC Filter Showing the Controlled Nodes .

To be Connected in Case of	Component Represented Realized	Node in Fig.1	Component & Switches	Node in Fig.1	Component Represented Realized	Node in Fig.1	To be connected in case of
A, L, H, B, N	R ₂ , R ₅	②		②, ⑨, ⑩	R ₂ , R ₅	⑨, ⑩	H, B L, N, A
N, A L, H, B	R ₂ , R ₆ , R ₈	⑨		⑨, ⑩, ⑬, ⑭, ⑮, ⑯, ⑰, ⑱, ⑲, ⑳	R ₆ , R ₂ , R ₈	②, ④	H, B, N, A L
L H, B, N, A	C ₂ , C ₇ , C ₈	②, ④		②, ④, GND	C ₂ , C ₇ , C ₈	③, ⑥, GND	L H, N, A B
L H, B, N, A	RQ ₃ , RQ ₇ , RQ ₈	⑧, ④		⑧, ④, GND	RQ ₃ , RQ ₇ , RQ ₈	③, ⑥, GND	L B H, N, A
H, B, A L, N	T ₁ , T ₂	⑨, ⑧		⑨, ⑧	T ₁ , T ₂	Output	L, H, B, N, A

Fig. 3.3 1

Different Elements Realizations and the Corresponding Switches Used for Digitally Selecting the Filtering Type .

Binary Input	Switch																	
	S ₁	S ₂	S ₃	S ₄	S ₅	S ₆	S ₇	S ₈	S ₉	S ₁₀	S ₁₁	S ₁₂	S ₁₃	S ₁₄	S ₁₅	S ₁₆	S ₂₉	S ₃₀
0 0 0	0	1	0	1	1	0	0	1	0	0	1	0	1	0	0	1	0	1
0 0 1	1	0	1	0	0	1	0	0	0	1	0	1	0	1	0	1	1	0
0 1 0	1	0	1	0	0	0	1	0	1	0	0	1	0	1	0	1	1	0
0 1 1	0	1	1	0	0	1	0	0	0	1	0	1	0	1	1	0	0	1
1 0 0	0	1	1	0	0	1	0	0	0	1	0	1	0	1	1	0	1	0

TABLE 3.2 -The Truth Table of the Switches Logic Used to Select the Filtering Function .

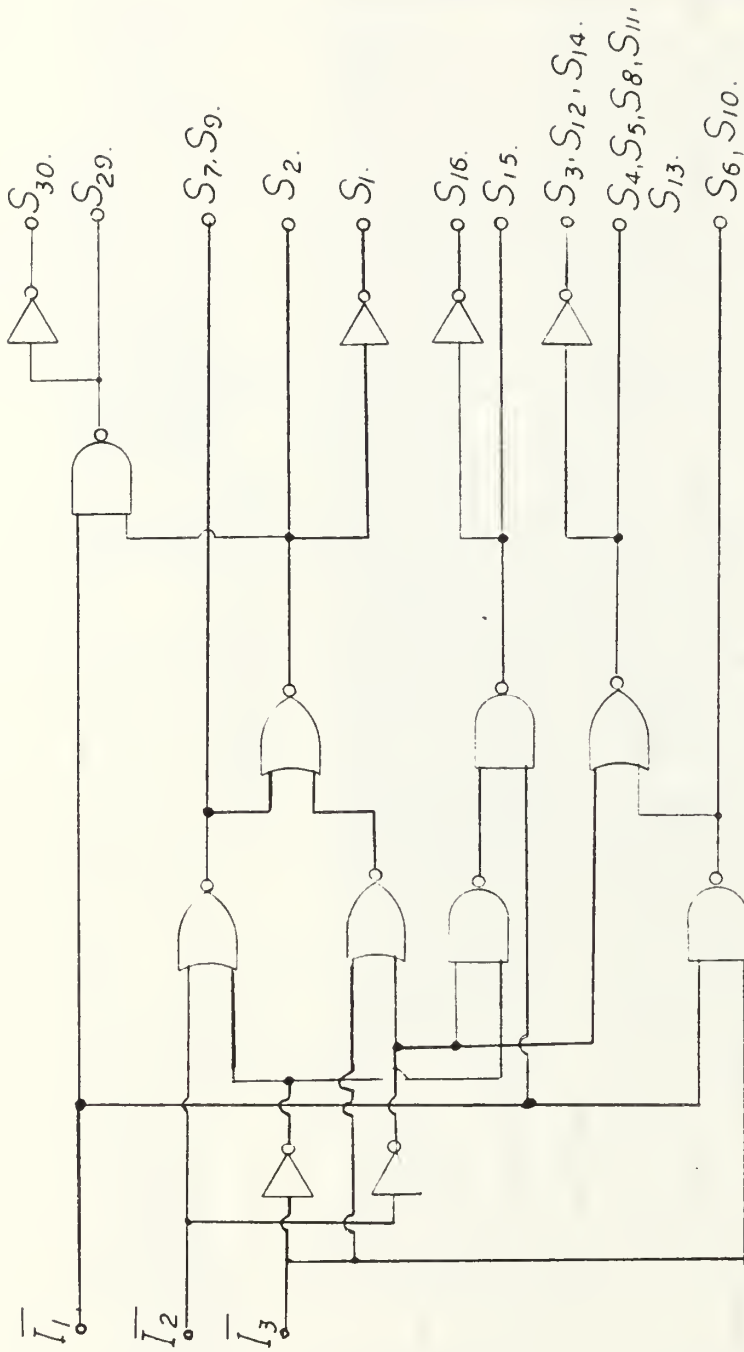


Fig. 3.3a

The CMOS Logic Diagram Used to Control the Analog CMOS Switches of Fig. and to Realize the Truth Table .

resistor is the Q_p determining resistor and of value $R_q = RQ_p$. The two capacitors are equal and of value $C = 1/W_p R$ each. The two equal banks of capacitors are used to control ω_p . Each bank contains n binary weighted capacitors connected in series through analog CMOS switches as shown in Fig.(3.5). Using a digital binary word of n bits to control W_p , 2^n different values of C will result at the 2 terminals of both capacitors banks that correspond to 2^n different values of p . Using a similar technique the value of R_q can be controlled through a bank of m binary weighted resistors in series, though analog CMOS switches as shown in Fig.(3.6). Using a digital binary word of m bits to control Q_p , 2^m different values of R_q can be achieved that correspond to 2^m different values of Q_p . Thus, full independent control of the pole pair ω_p and Q_p are achieved by programming the switches to obtain the corresponding C and R_p . It can be easily shown that with minor modifications, an additional programmable element can be added for the control of the notch frequency.

C. THE REALIZED GIC PROGRAMMABLE FILTER

A complete circuit diagram of the constructed GIC filter is shown in Fig.(3.4). The values of m and n were selected to $m=n=4$. Thus, 15 different values of ω_p (f_p) and Q_p were obtained as it is illustrated at the corresponding Table (3.3) and (3.4). the (designed) banks of the resistors for the control of Q_p and the capacitors for the control of ω_p (f_p) along with their control switches are shown correspondingly in Fig.(3.7) and Fig.(3.8).

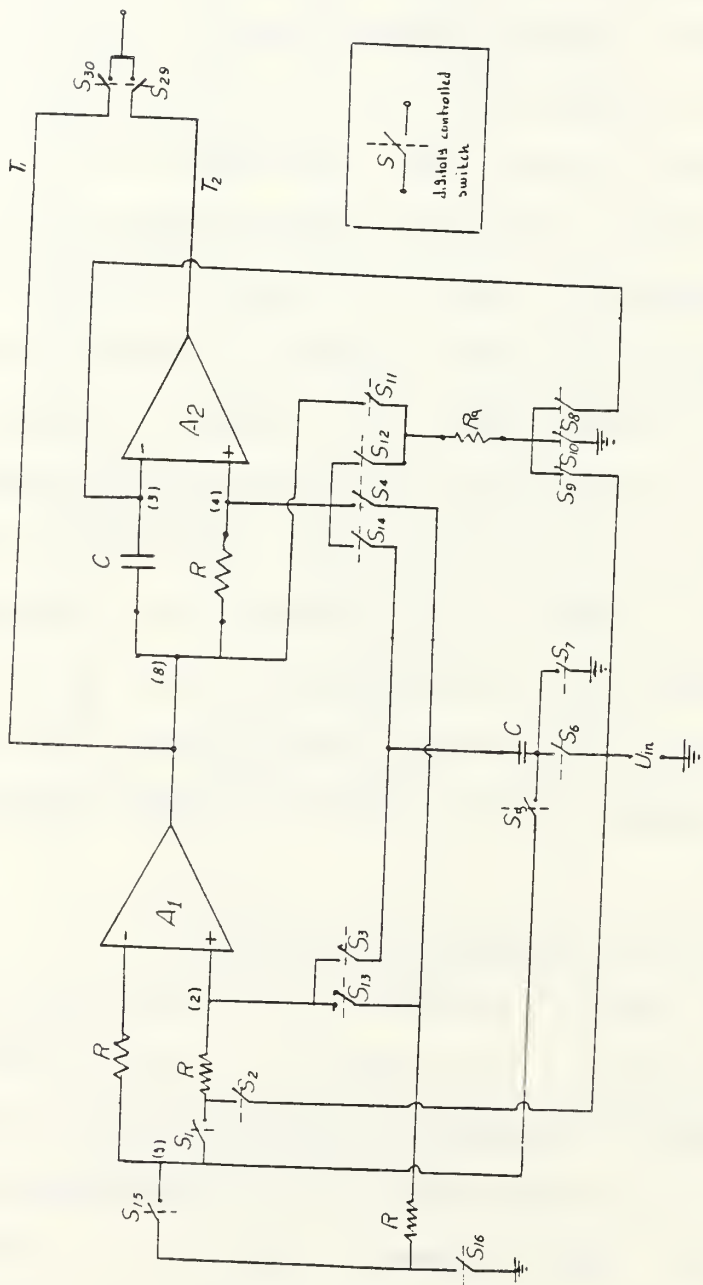


Fig. 3.4 - The Complete Circuit Diagram of the Programmable GIC Filter

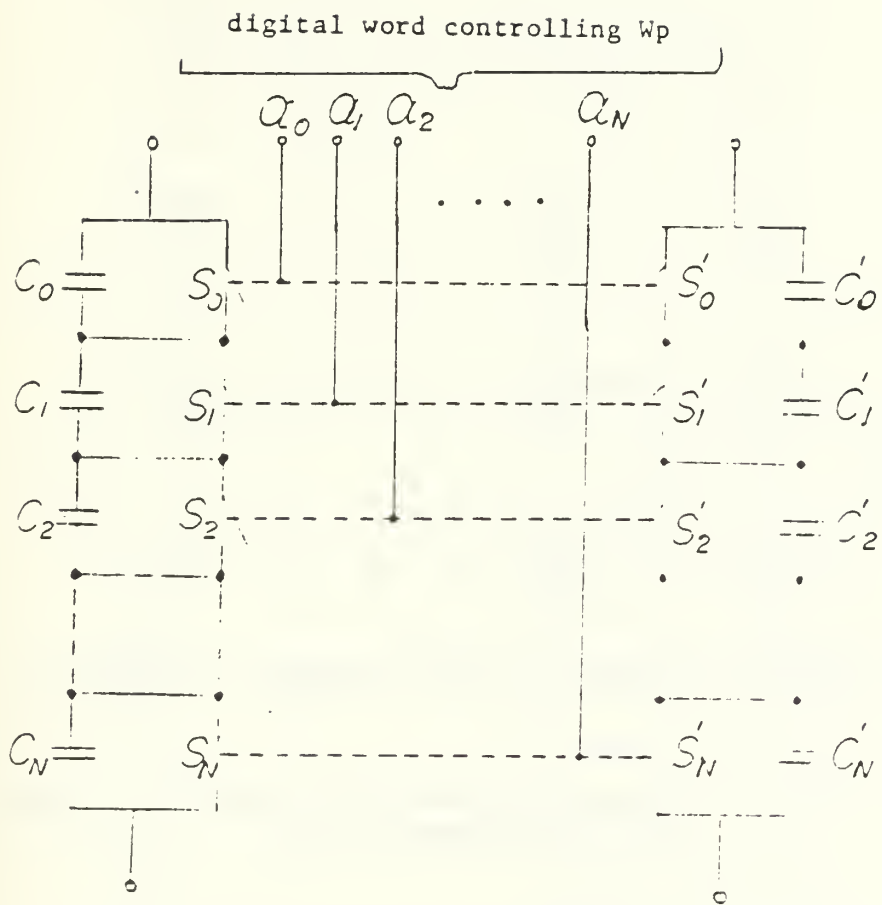
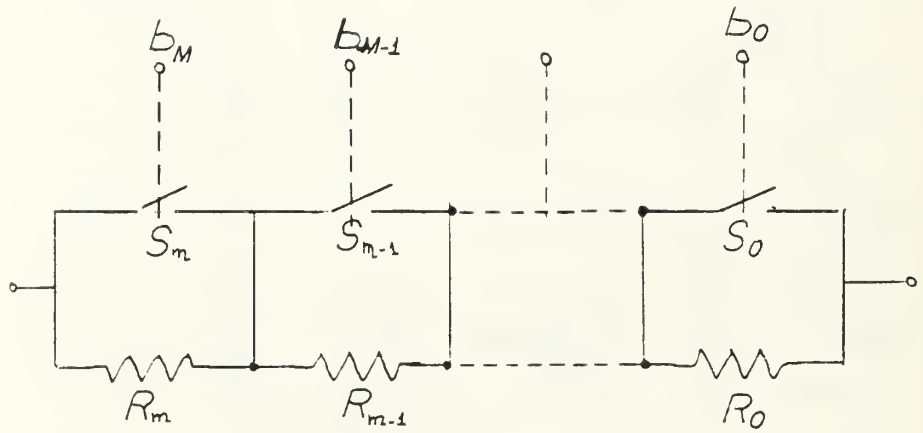


Fig. 3.5 - The Two Capacitor Banks Realizations for the Programming of ω_p .



(For linear Q_p control, $R_{j+1} = 2R_j$ resulting in $R_{Qp} = \sum_{j=0}^m R_0 b_j$)

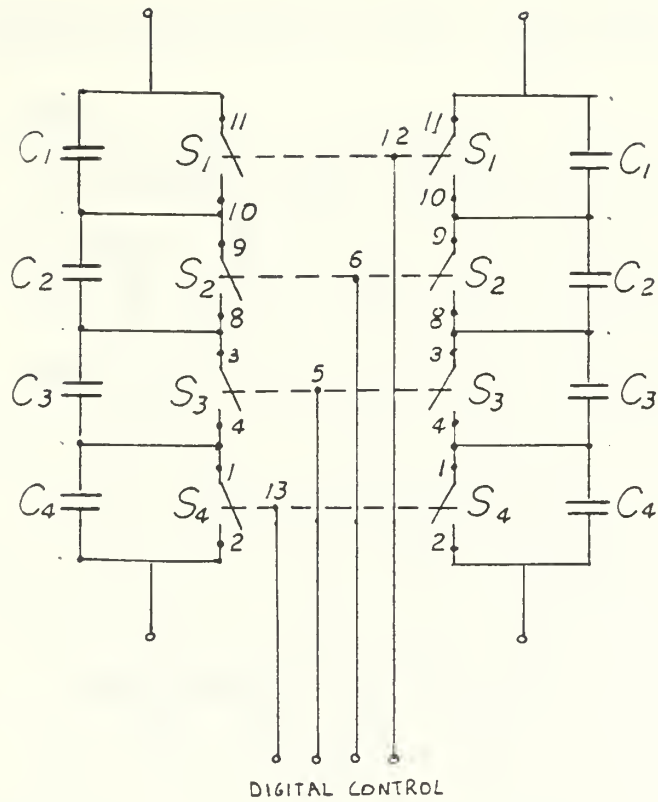
Fig. 3.6 - The Resistor Bank Used to Realize R_q Needed for the Programming of Q_p .

switch control				C	Fp
Sa	Sb	Sc	Sd	nF	Khz
0	0	0	0	5.96	16.693
0	0	0	1	6.34	15.709
0	0	1	0	7.16	13.887
0	0	1	1	7.72	12.875
0	1	0	0	8.42	11.810
0	1	0	1	9.20	10.856
0	1	1	0	10.00	10.043
0	1	1	1	11.00	9.047
1	0	0	0	15.10	6.650
1	0	0	1	17.60	5.637
1	0	1	0	20.80	4.823
1	0	1	1	26.00	3.828
1	1	0	0	35.50	2.805
1	1	0	1	55.00	1.810
1	1	1	0	100.00	.995

Table 3.3 The four - bit words that control Fp and the corresponding capacitor

switch control				Rq	Qp
Sa	Sb	Sc	Sd	K	
0	0	0	0	24.0	15
0	0	0	1	22.4	14
0	0	1	0	20.8	13
0	0	1	1	19.2	12
0	1	0	0	17.6	11
0	1	0	1	16.0	10
0	1	1	0	14.6	9
0	1	1	1	12.8	8
1	0	0	0	11.2	7
1	0	0	1	9.6	6
1	0	1	0	8.0	5
1	0	1	1	6.4	4
1	1	0	0	4.8	3
1	1	1	1	3.2	2
1	1	1	0	1.6	1

Table 3.4 The four - bit words that control Rp and Qp



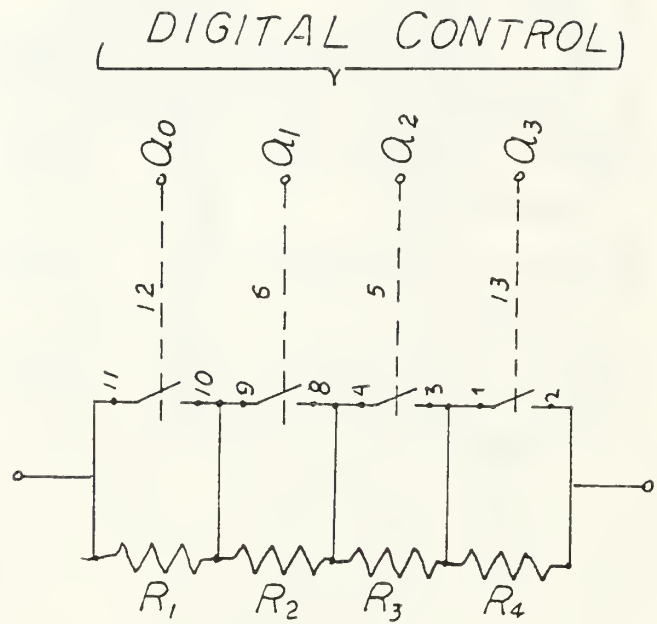
$$C_1 = 100\mu\text{f}$$

$$C_2 = 55\mu\text{f}$$

$$C_3 = 25\mu\text{F}$$

$$C_4 = 11\mu\text{F}$$

Fig. 3.7 - The Constructed Blocker Capacitor Controlling the f_p .



$$R_1 = 1.6k$$

$$R_2 = 3.2k$$

$$R_3 = 6.4K$$

$$R_4 = 12.8k$$

Fig. 3.8 - The Constructed Block of Resistance Controlling Q_p .

IV. COMPUTER SIMULATION OF THE PROGRAMMABLE FILTER

A. INTRODUCTION

In order to observe the theoretical responses of the different realizations as well as to compare them with the experimental measurements, two computer programs were written in Fortran. Those programs are shown in Appendices A and B. The first one simulates the programmable filter's responses $T_1(s)$, $T_2(s)$ and $T_3(s)$ as functions of the network's admittances Y_i , $i=1 \dots 8$, and the "constant" Op.Amps. gains A_1 and A_2 . A realistic value of $A_2=A_2=10^5$ was given to the above gains corresponding to 741 Op. Amps. used in the experiment. The second program simulates the programmable filter's responses $T_1(s)$, $T_2(s)$ and $T_3(s)$ as functions of the network's admittances Y_i , $i=1 \dots 8$ and the frequency dependent Op. Amps. gains A_1 and A_2 . In this second case a single pole approximation value of w_{i1s} was assigned for $A_i(i=1, 2)$. Where, W_i is the GBWP of the Op. Amps. used, a value of $W_1=W_2=2\pi \times 10^6$ was given to the above $W_i(i=1, 2)$ corresponding to 741 Op. Amps. used throughout the research.

To be able to compare the computer simulation results with the experimental ones obtained, the same values of admittances were used as input data. That means that the same values of R , R_q and C according to Chapters III and V were used. With the value of R selected to be 1.6k Table

(4.1) illustrates the different values of R_q s used in the simulation to realize the different values of Q_p and Table (4.2) illustrates the different values of capacitors used in the simulation to realize the different frequencies ω_p s.

The "DO CASE I" command of Fortran simulated the digital logic (including the control switches) used to realize the different responses of the programmable filter that is LP, HP, BP, N and AP. The frequency's (ω_p) translations and the different Q_p values were simulated by changing the values of R_q and C_s at every run of the program.

The above programs also simulated the transfer function of two cascaded GIC programmable filters as it will be discussed later in Chapter VI. Each of the filters could have been at different realization (as well as at different p and Q_p) relative to the other one. The 25 possible combinations of transfer function realizations are shown in Table 4.3.

B. SIMULATION RESPONSE(S)

1. Low Pass (LP) Realization

Using the elements values prescribed in Table (3.1) yields the following L.P. transfer function:

$$T_2(s) = \frac{2\omega_p^2}{s^2 + \frac{\omega_p}{Q_p}s + \omega_p^2} \quad (4.1)$$

For R=1.6k Φ	
Rq k Φ	Qp
1.1	0.7
1.6	1.0
3.2	2.0
6.4	4.0
11.2	7.0
16.0	10.0
32.0	20.0

Where Qp = Rq

Table 4.1 - The Resulting Qp Values for the Different Introduced Rq Values in the Computer Simulation.

For R-1.6k Ω

C nf	f _p khz
100.00	.099
50.00	1.99
26.00	3.83
12.5	7.96
6.6	15.10
3.3	30.16
0.85	117.09
0.42	236.67

$$f_p = \frac{1}{2 \pi \cdot R \cdot C}$$

Table 4.2 - The Resulting ω_p Values for the Different Introduced C Value (R constant 1.6k Ω)

FILTER 1	FILTER 2	J	I
LP	LP	2	2
HP	HP	1	1
BP	BP	4	4
N	N	3	3
AP	AP	3	3
LP	HP	2	1
LP	BP	2	4
LP	N	2	3
LP	AP	2	3
HP	LP	1	2
HP	BP	1	4
HP	N	1	3
HP	AP	1	3
BP	LP	4	2
BP	HP	4	1
BP	N	4	3
BP	AP	4	3
N	LP	3	2
N	BP	3	1
N	HP	3	4
N	AP	3	3
AP	LP	3	2
AP	HP	3	1
AP	BP	3	4
AP	N	3	3

Table 4.3 - The 25 Possible Combinations of Transfer Function Realizations

This transfer function assumes the following complex value

$$T_2(j\omega_p) = -2jQ_p \quad (4.2)$$

with magnitude of

$$|T_2(j\omega_p)| = 2Q_p = 20 \log |2Q_p|, \text{ db} \quad (4.3)$$

Fig. 4.1 illustrates the theoretical "ideal" LPF magnitude response for $f_p=3.8\text{Khz}$ and for 3 different values of Q_p . The simulation results match the equations of (4.2).

Fig. 4.2 illustrates the theoretical "ideal" LPF magnitude response for $Q_p=2$ and for 3 different values of ω_p . the Op. Amps. gains A_i , ($i=1, 2$) are frequency depended. This dependance affects the magnitude of the filter and causes a frequency shift from the theoretical value of the ideal's case. Figs.(4.3) and (4.4) illustrates the ideal vs. nonideal theoretical LPF amplitude responses.

Data extracted from Figs.(4.3) and (4.4) are illustrated in Tables (4.4(a)) and (4.4(b)) simultaneously.

L.P.F AMPL RESPONSE (F=3.828KH)

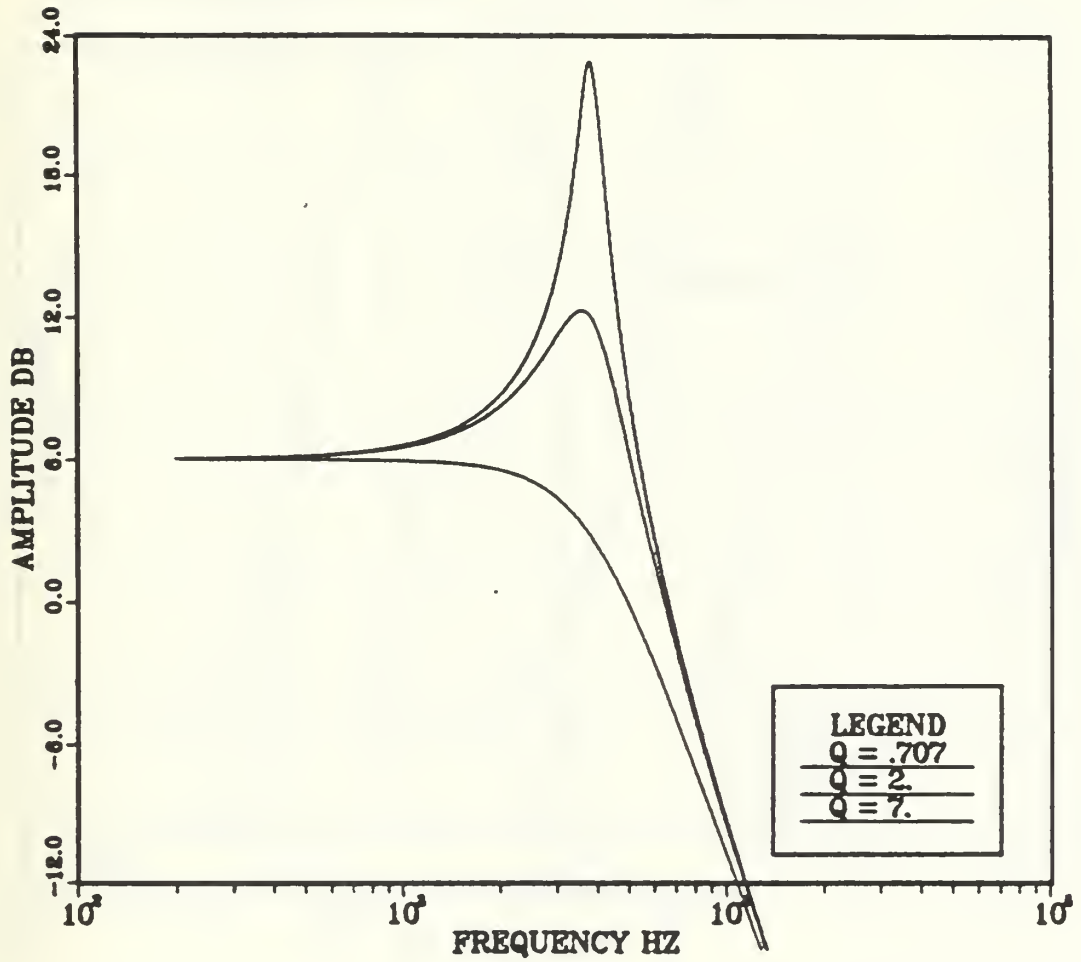


Fig. 4.1 - "Ideal" LPF Amplitude Response

L.P.F AMPL RESPONSE (Q=2)

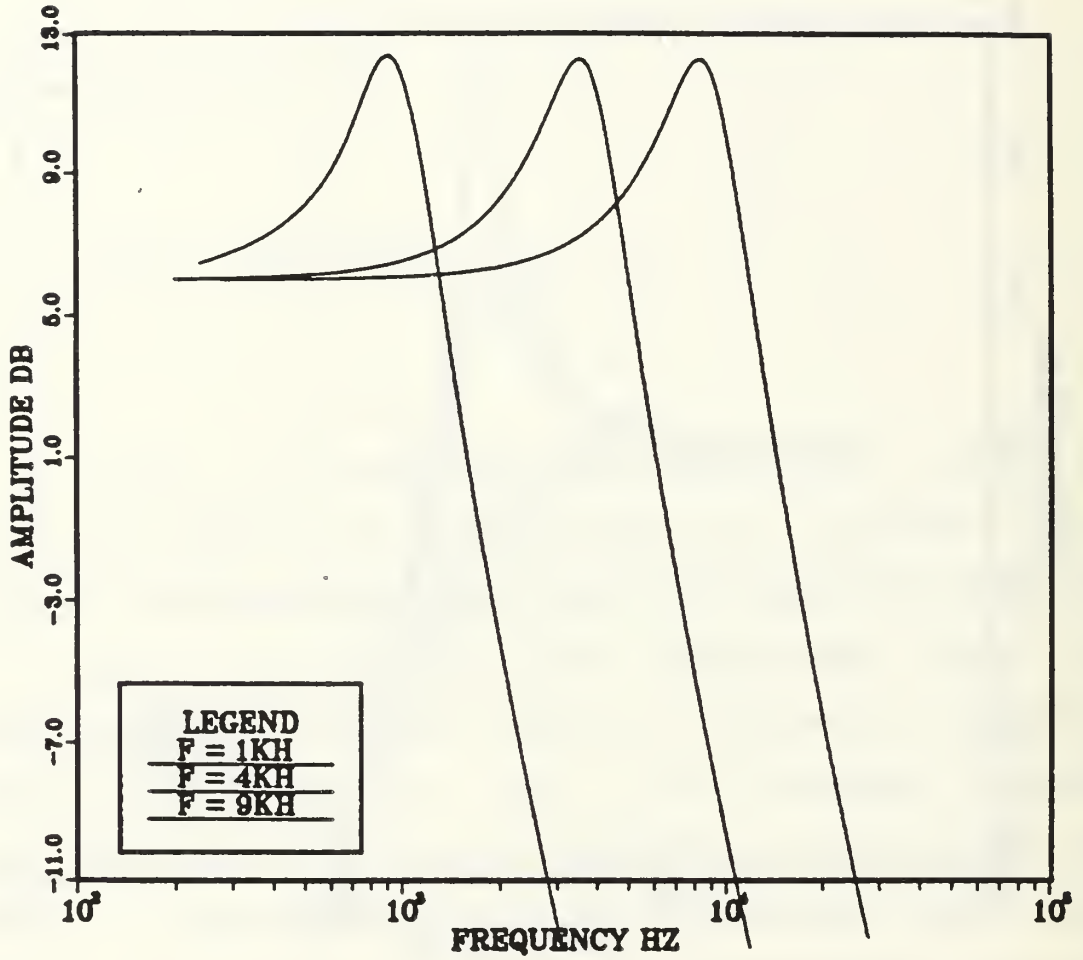
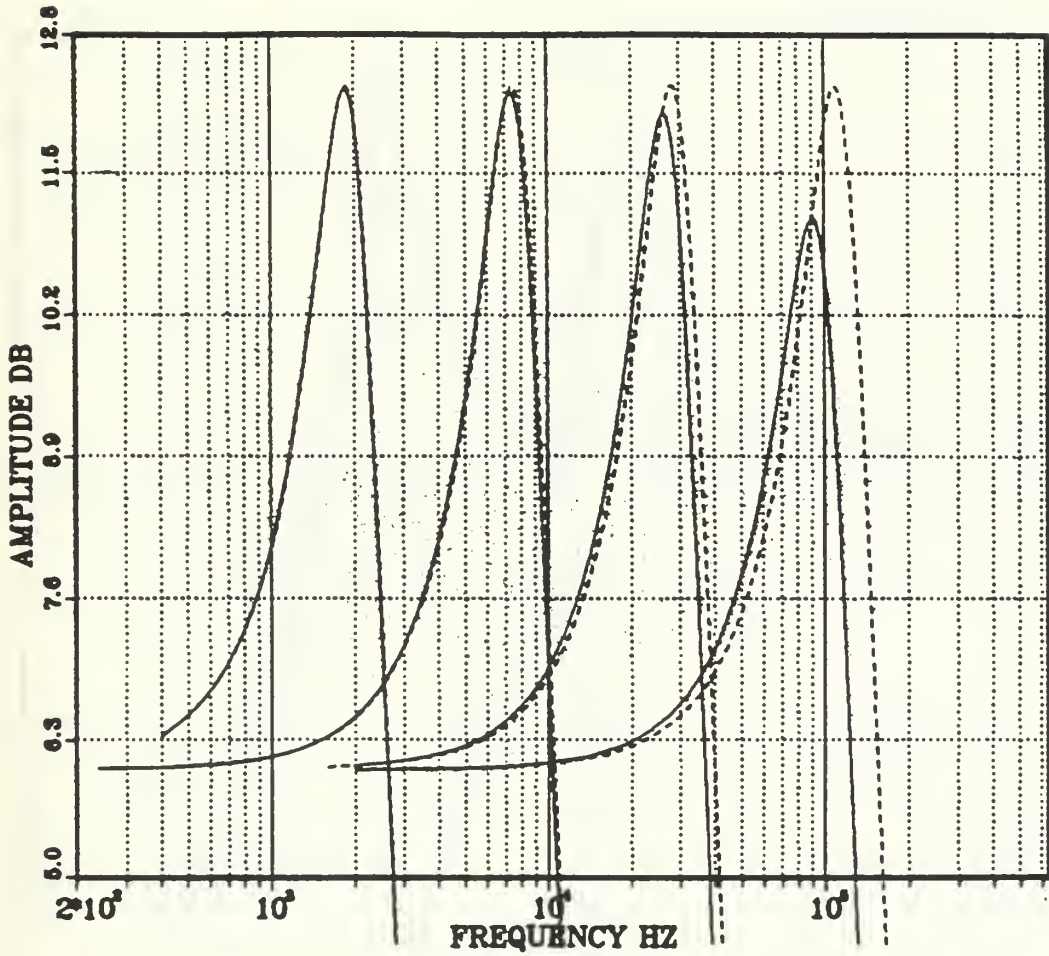


Fig. 4.2 - "Ideal" LPF Amplitude Response

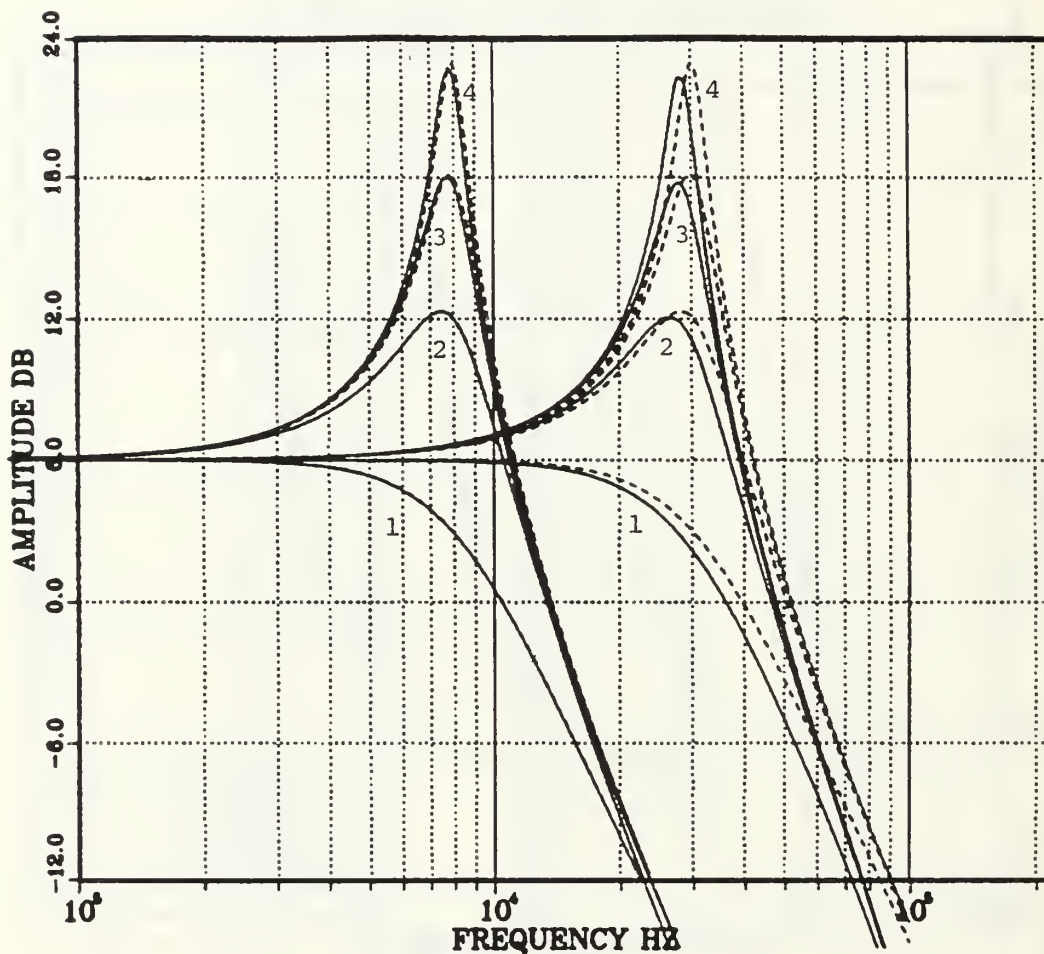
L.P.F AMPL RESPONSE (Q=2)



----- ideal
 _____ nonideal

Fig. 4.3 Ideal .vs. nonideal L.P.F. amplitude response for $Q=2$ and frequencies (1.99K, 7.96K, 30.16K and 117.1K)Hz

L.P.F AMPLITUDE RESPONSE



- 1. $Q = 0.7$
- 2. $Q = 2.0$
- 3. $Q = 4.0$
- 4. $Q = 7.0$

Fig. 4.4 Ideal .vs. nonideal L.P.F. amplitude response for frequencies $(7.96K, 30.1K)_{Hz}$ and variety of Q_s .

Data From Fig. (4.4) LPF Characteristic

Ideal			Nonideal	
Qp	$ T_2(s) $ at pick value	Rq ke	Qp	$ T_2(s) $ at pick value
.07	3.0	1.1	6.7	3.0
2.0	12.0	3.2	2.0	12.0
4.0	18.1	6.4	4.0	18.1
7.0	22.9	17.2	7.0	22.7
The pick values obtained at fpick = 7.9k			The pick values obtained at fpick = 7.9k	

(b)

Ideal		C	Nonideal	
Fp khz	Amp. Response dB	nf	fp khz	Amp. Response dB
1990.45	12.04	50	1990.45	12.72
7165.60	12.24	12.5	8359.87	12.113
28662.42	12.31	6.6	25875.80	12.04
109745.50	12.31	0.085	90565.00	11.08

Table 4.4 - Data from Figs. (4.3) and (4.4) indicating the Affect of Frequency Dependency of A_i , $i=1, 2$

2. High Pass (HP) Realization

Using the elements value shown in Table (3.1) yields the following HP transfer function:

$$T_1(s) = \frac{2s^2}{s^2 + \frac{\omega_p}{Q_p} s + \omega_p^2} \quad (4.4)$$

takes the following complex value at ω_p .

$$T_1(j\omega_p) = 2jQ_p \quad (4.5)$$

which magnitude is

$$|T_1(j\omega_p)| = 2Q_p = 20 \log(2Q_p), \text{ db} \quad (4.6)$$

Fig. (4.5) illustrates the theoretical "ideal" HPF amplitude response for $f_p=3.8\text{KHZ}$ and for 3 different values of Q_p . The computer simulation results match that of the (4.6) relation.

Fig. (4.6) illustrates the theoretical "ideal" HPF amplitude response for $Q=2$ and for 3 different frequencies.

Fig. (4.7) illustrates how this dependency effects the amplitude of the HP filter. (The amplitude decreases as

H.P.F AMPL. RESPONSE(F=3.828KH)

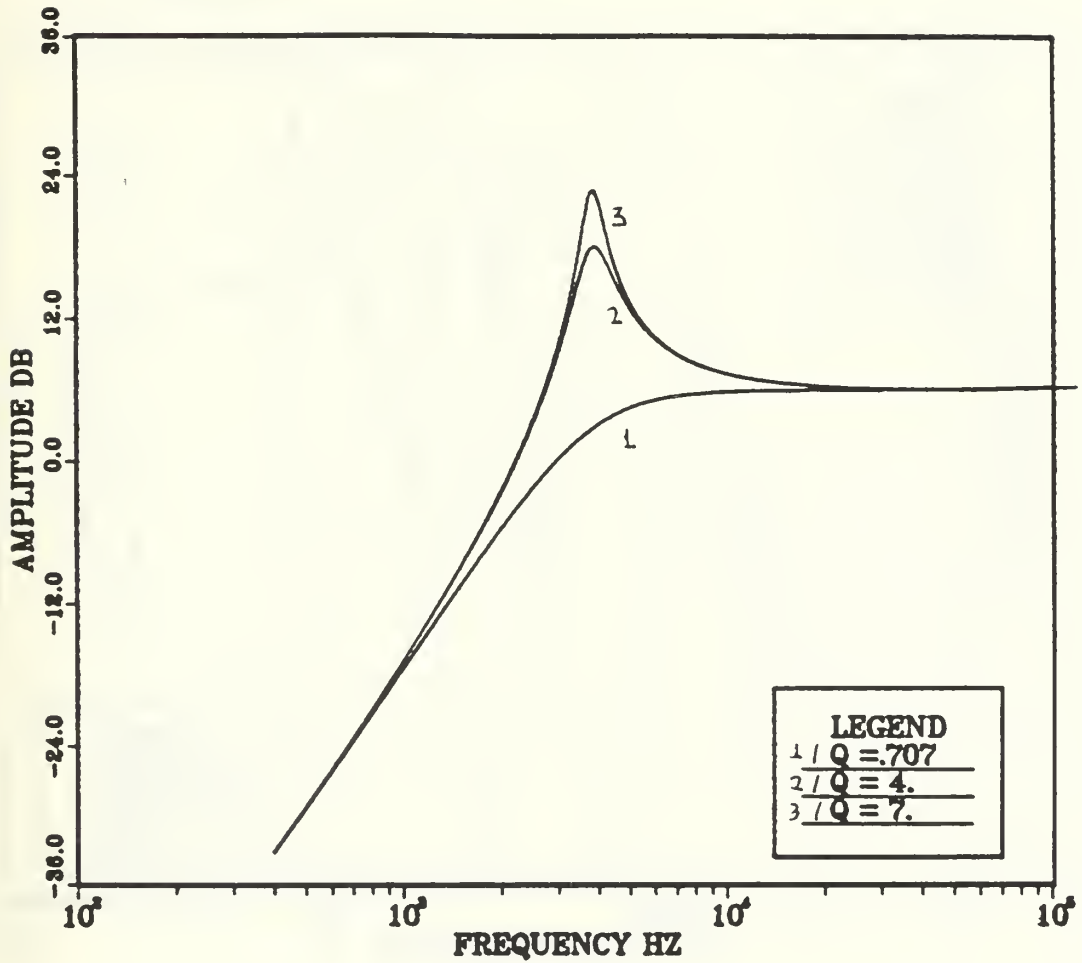


Fig. 4.5 - "Ideal" HPF Amplitude Response for a Variation of Qs.

H.P.F AMPLITUDE RESPONSE(Q=2)

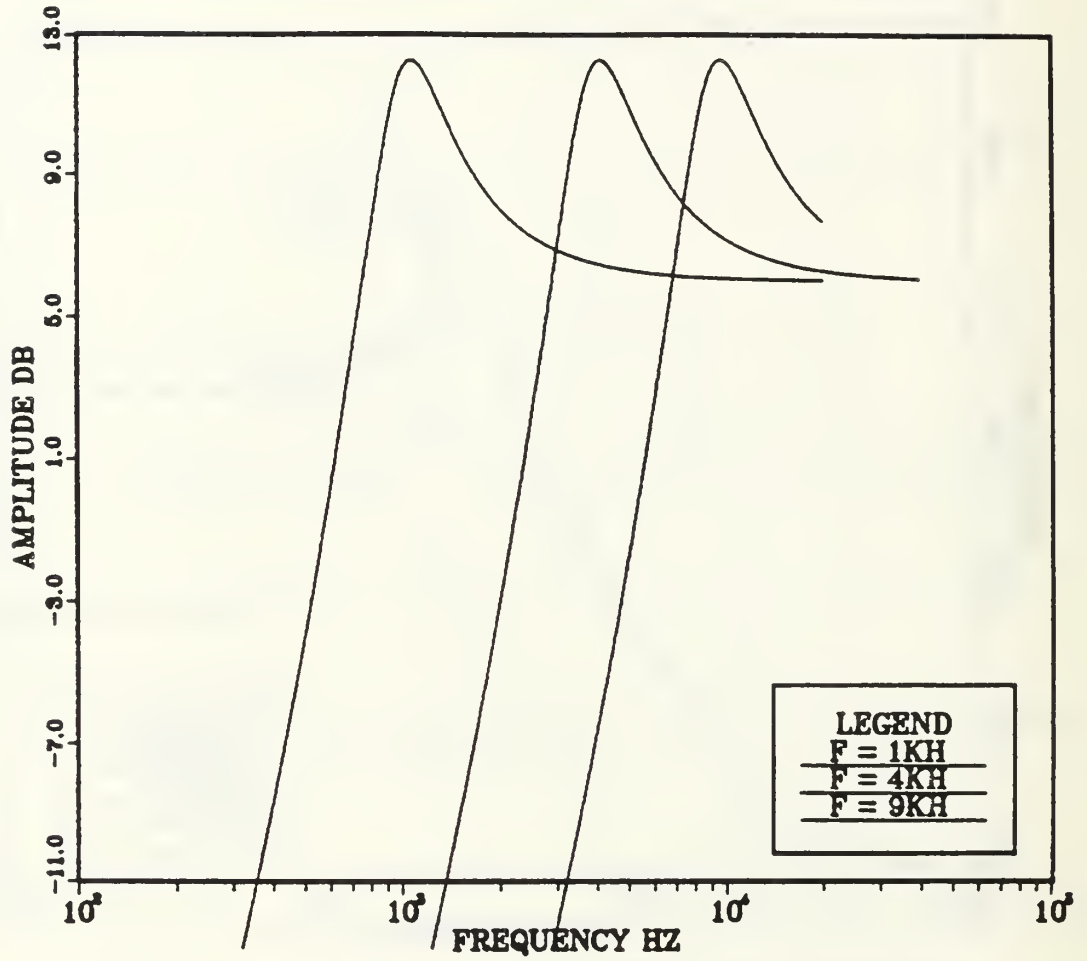


Fig. 4.6 - "Ideal" HPF Amplitude Response.

H.P.F AMPLITUDE RESPONSE(Q=2)

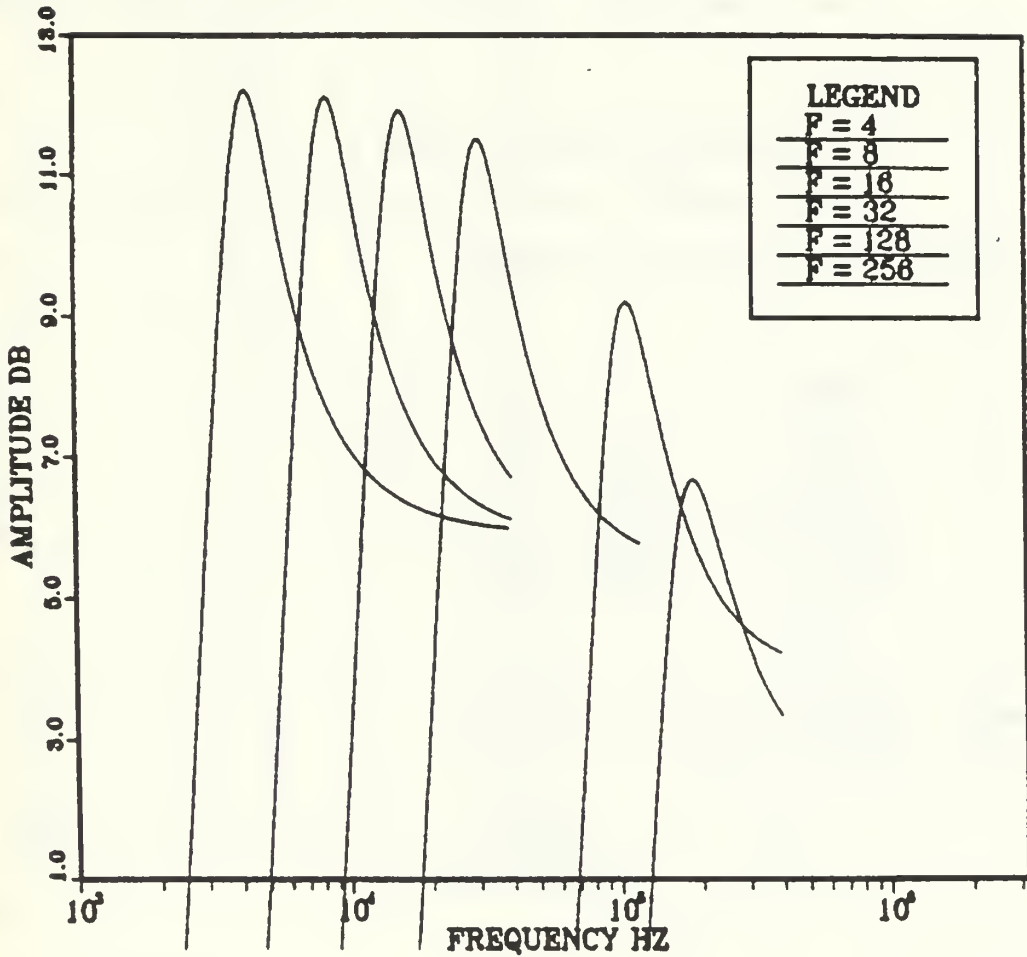


Fig. 4.7 - Nonideal HPF Amplitude Response.

the frequency increases) while Figs. (4.8) and (4.9) illustrate the frequency shift of the amplitude response due to that dependency.

From the data of Fig. (4.8), Table (4.5) were constructed.

3. Band Pass (BP) Realization

Using element values from Table 3.1 the following BP transfer function is achieved:

$$T_1(s) = \frac{2\left(\frac{\omega_p}{Q_p}\right)s}{s^2 + \frac{\omega_p}{Q_p}s + \omega_p^2} \quad (4.7)$$

takes the following value at ω_p .

$$T_1(j\omega_p) = 2 \quad (4.8)$$

which has constant magnitude of 6dB

$$|T_1(j\omega_p)| = 2 = 20 \log 2 = 6 \text{ dB} \quad (4.9)$$

H.P.F AMPLITUDE RESPONSE(Q=2)

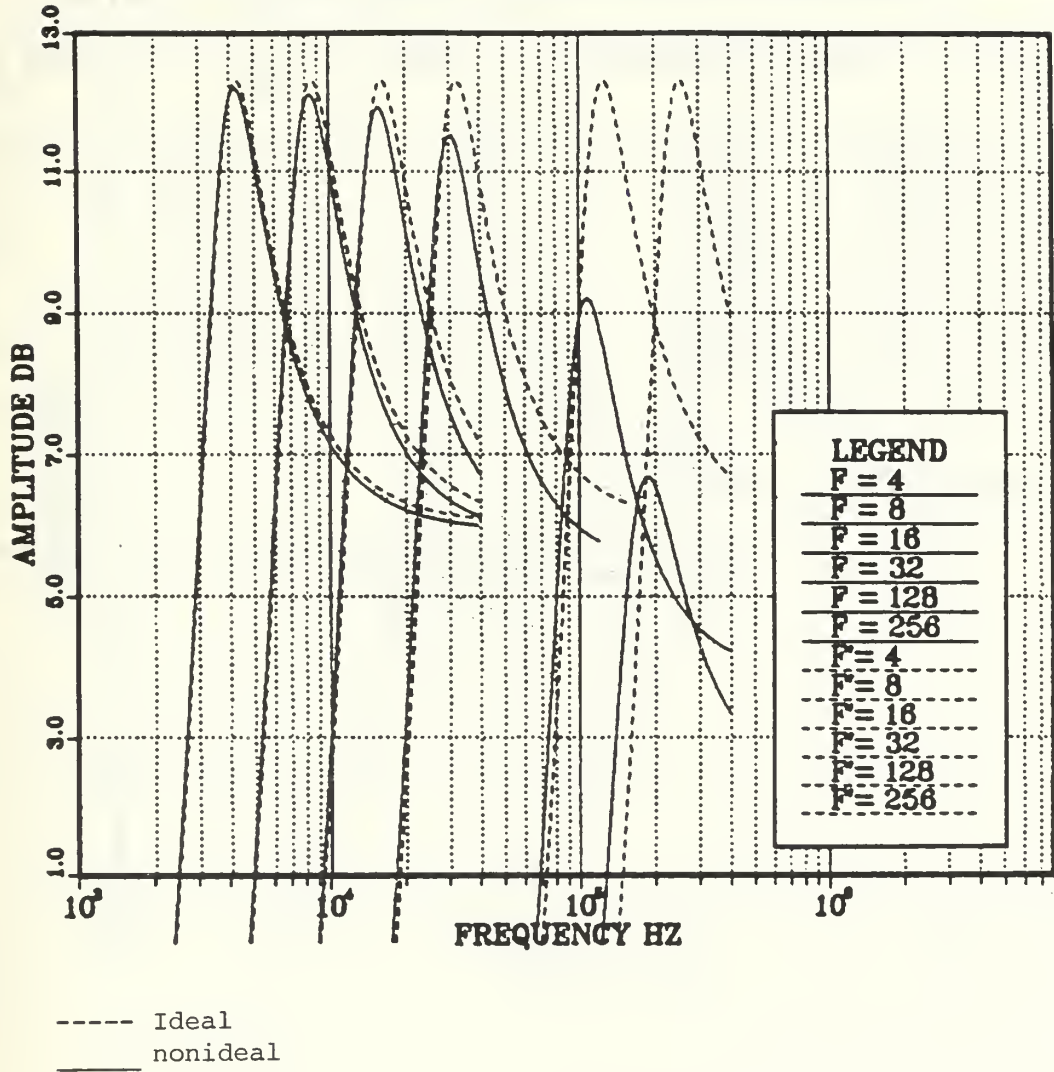
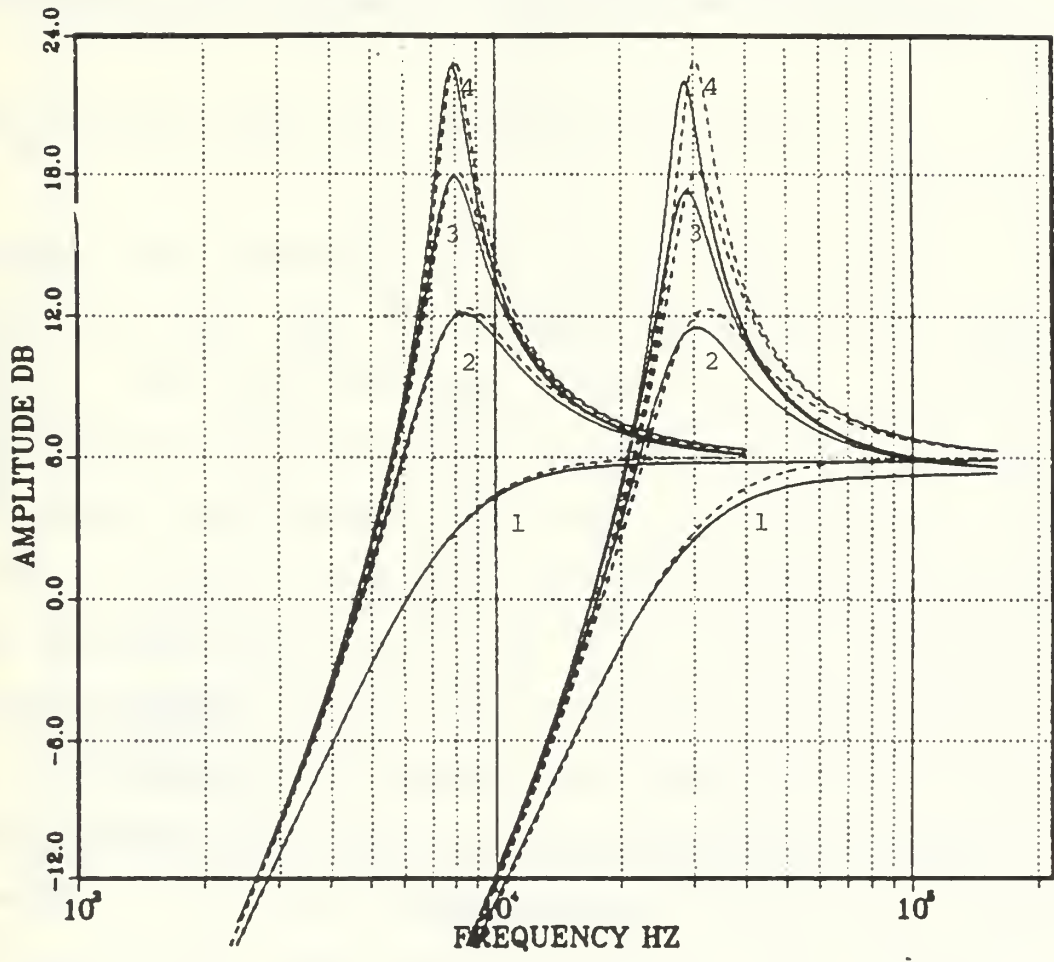


Fig. 4.8 - "Ideal" vs. Nonideal HPF Amplitude Response.

Ideal		c	Nonideal	
fp Hz	Amp Response dB	nf	fp Hz	Amp Response Db
4,378.98	12.28	26	4,378.98	12.148
8,359.87	12.30	12.5	8,359.87	12.11
15,923.57	12.31	6.6	15,923.57	12.02
31,847.13	12.31	3.3	31,847.73	11.41
123,407.00	12.31	0.85	107,484.00	9.21
252,781.05	12.31	0.43	187,101.80	9.21
242,781.05	12.32	0.43	187,101.80	6.69

Table 4.5 - Data Illustrating the Ideal vs. the Nonideal Responses of the HPF

H.P.F AMPL. RESPONSE(F=8K/16K)



- 1. Q = 0.7
- 2. Q = 2.0
- 3. Q = 4.0
- 4. Q = 7.0

Fig. 4.9 - "Ideal" vs. Nonideal HPF Amplitude Response.

Fig. (4.10) illustrates the theoretical BPF magnitude response for $f_p=3.83$ KHZ for different values of Q_p . These agree with the (4.9) equation since as it is indicated by the simulation plot the amplitude is constant and independent of Q_p .

Fig. (4.11) illustrates the above concept but at $f_p=15.1$ KHZ.

Fig. (4.12) and (4.13) illustrate the theoretical "ideal" BPF amplitude response for $Q_p=2$ and for different values of p . As it is indicated from Fig. (4.13) the amplitude remain constant even at very high frequencies (10 HZ). But with A_i , ($i=1, 2$) depending on frequency the amplitude decreases as the frequency increases. This is indicated in Figs. (4.14) and (4.15) which describe the BPF amplitude response plots for $Q=4$ and $Q=1$ respectively and for different frequencies. The frequency dependence of A_i , ($i=1, 2$) creates a frequency shift from the ideal theoretical value which is indicated in Figs. (4.16) and (4.17). Table (4.6) illustrates the data extracted from figs. (4.16) and (4.17).

4. Notch (N) Realization

Using the admittances value of Table (3.1), the following Notch transfer function can be achieved:

(4.10)

B.P.F AMPL. RESPONSE(F=3.828KH)

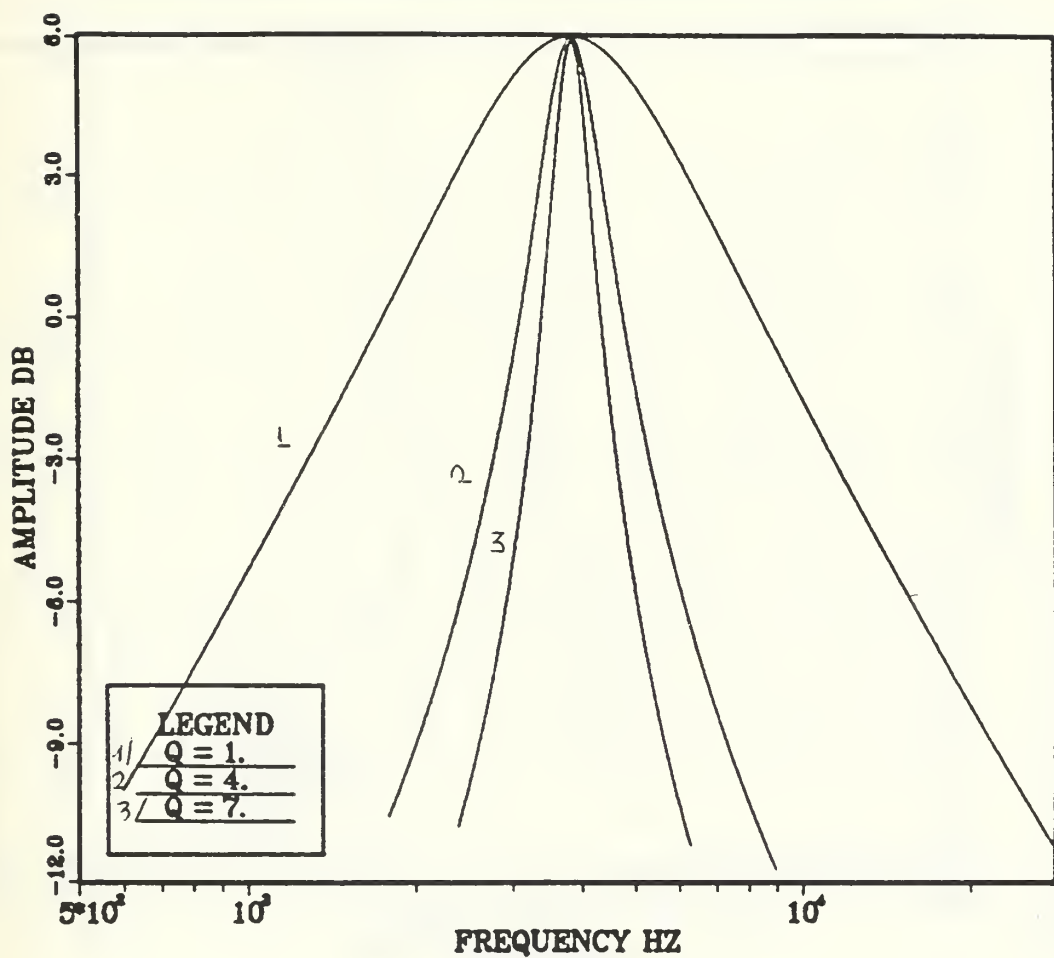


Fig. 4.10 - "Ideal" BPF Amplitude Response.

B.P.F AMPLITUDE RESPONSE(F=16K)

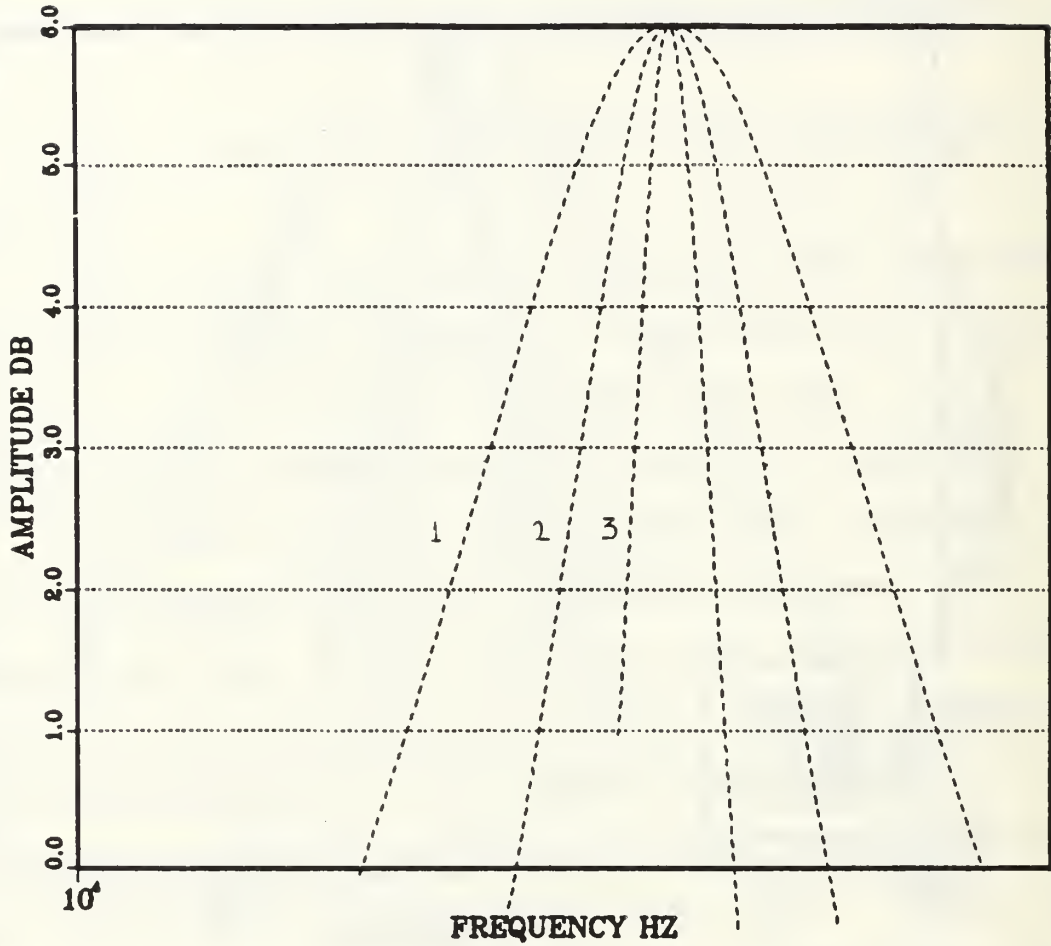


Fig. 4.11 - "Ideal" BPF Amplitude Response.

B.P.F AMPLITUDE RESPONSE(Q=4)

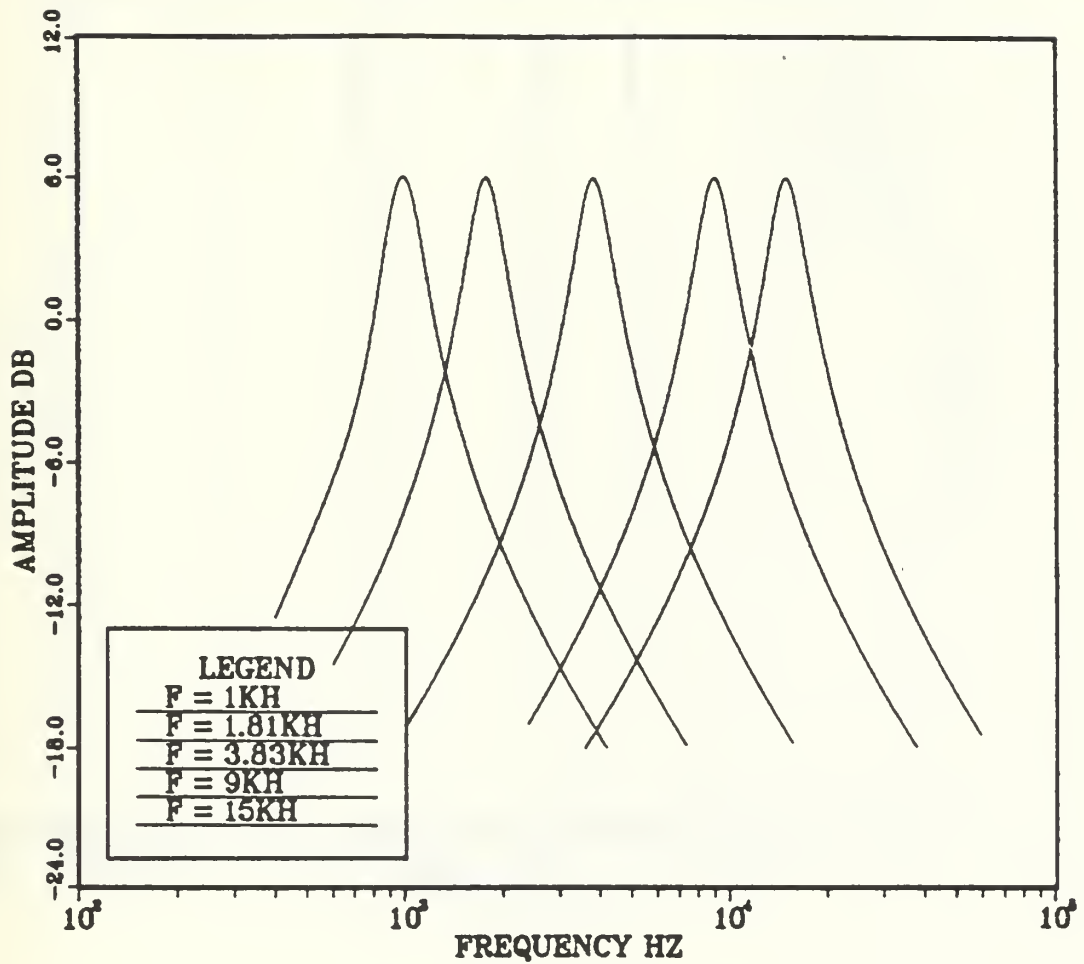


Fig. 4.12 - "Ideal" BPF Amplitude Response.

B.P.F AMPLITUDE RESPONSE(Q=4)

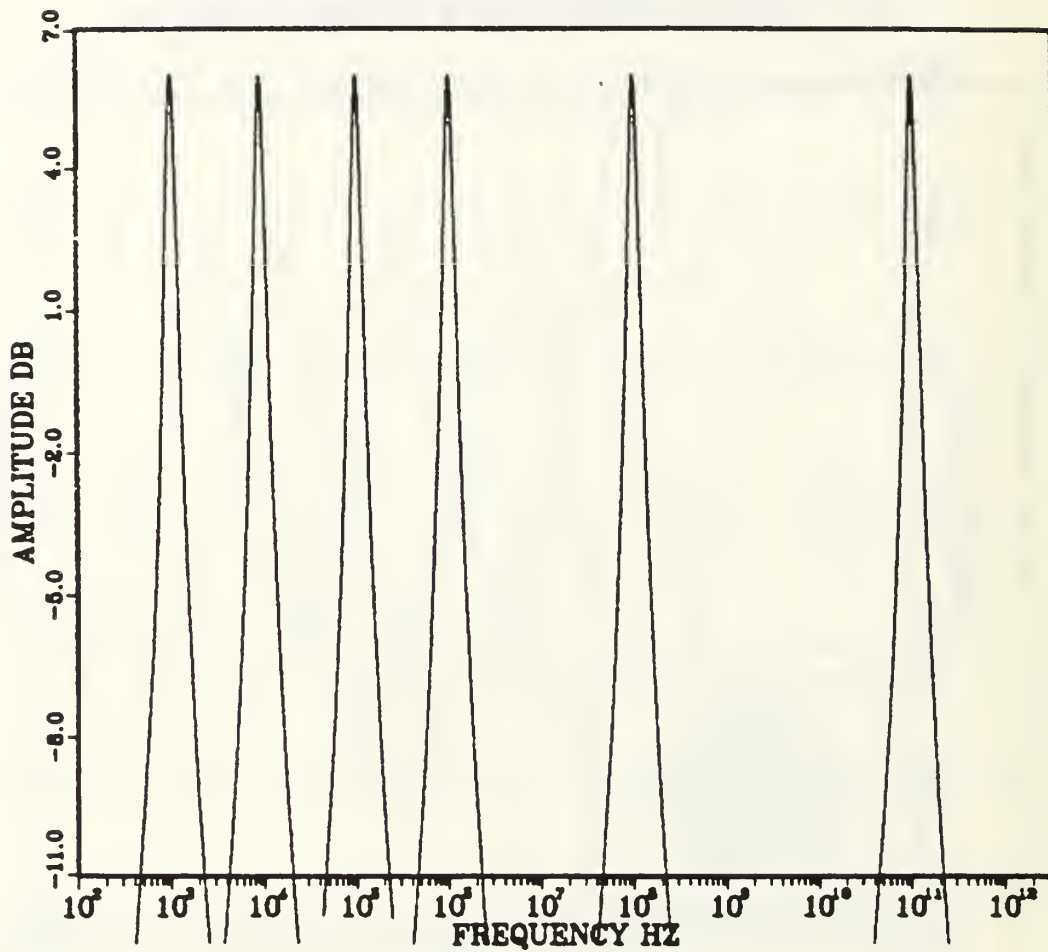


Fig. 4.13 - "Ideal" BPF Amplitude Response.

B.P.F AMPLITUDE RESPONSE(Q=4)

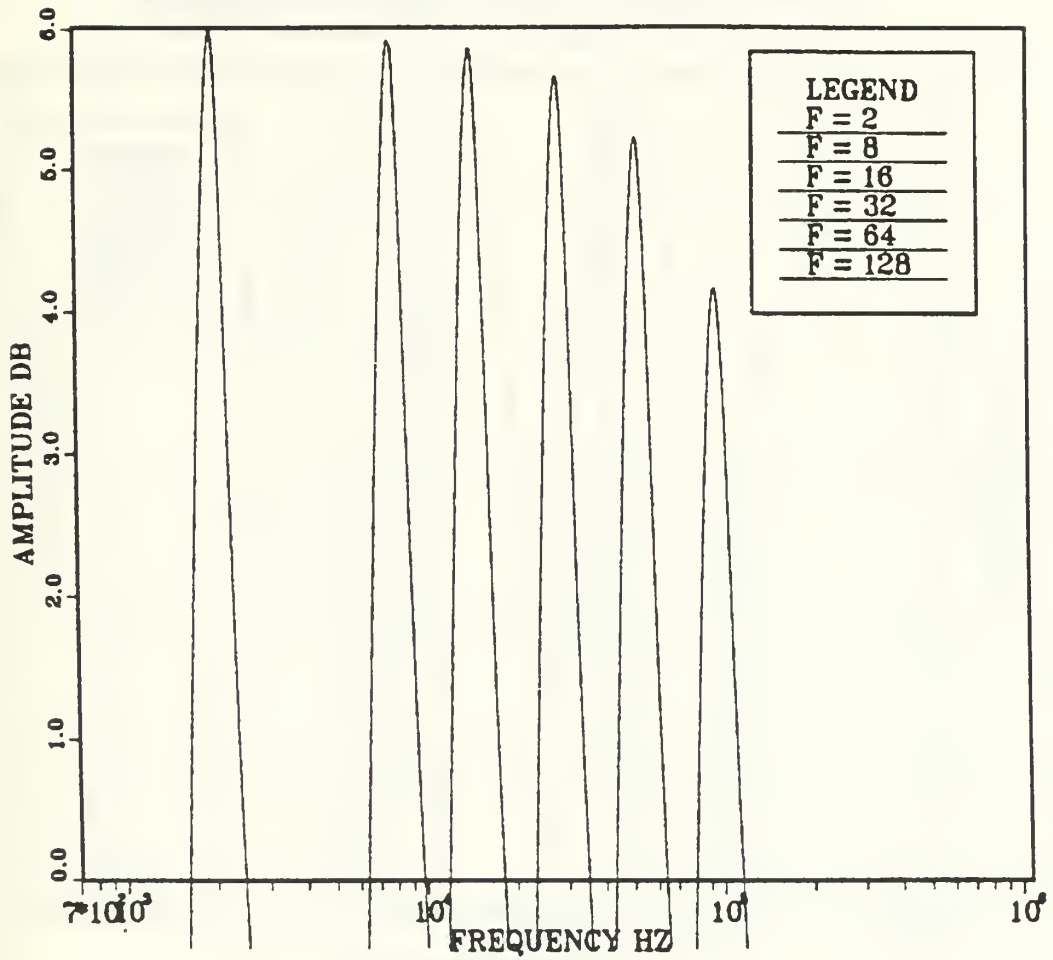


Fig. 4.14 - Nonideal PBF Amplitude Response.

B.P.F AMPLITUDE RESPONSE(Q=1)

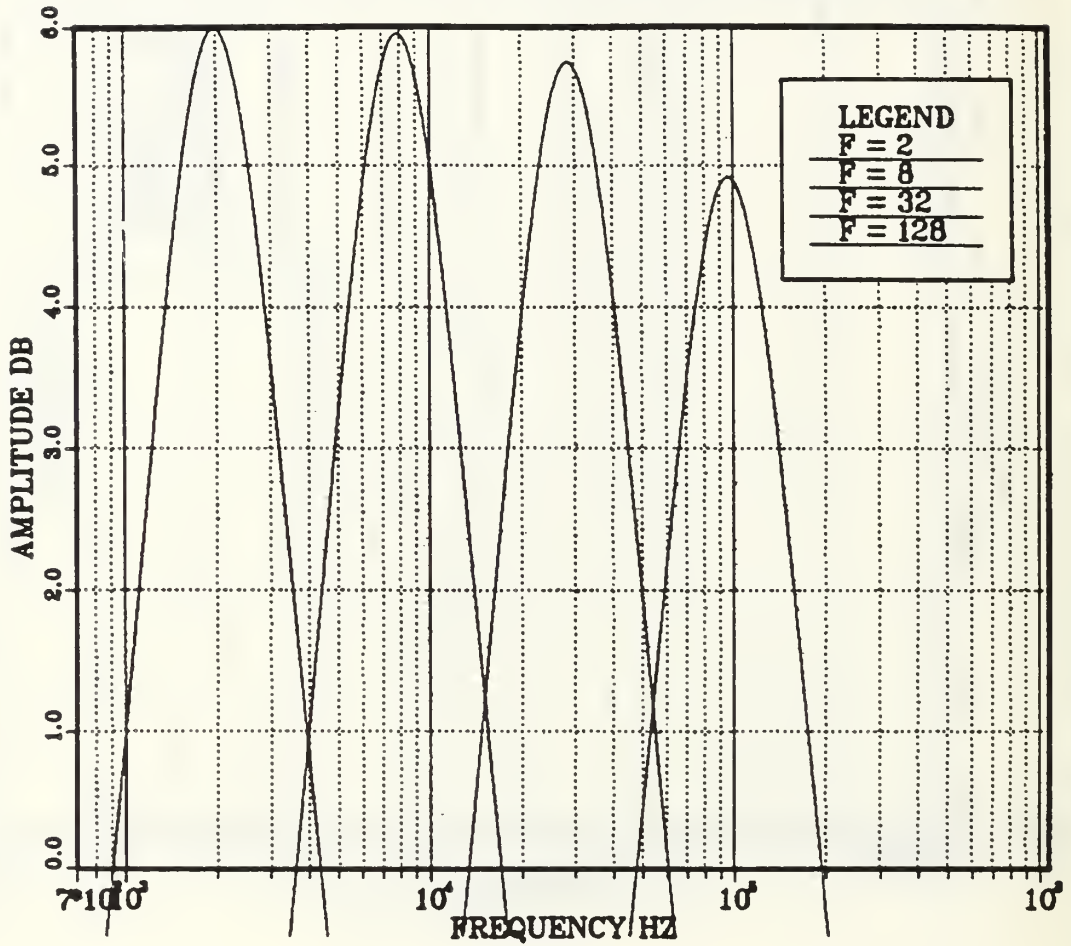


Fig. 4.15 - Nonideal BPF Amplitude Response.

B.P.F AMPLITUDE RESPONSE(Q=4)

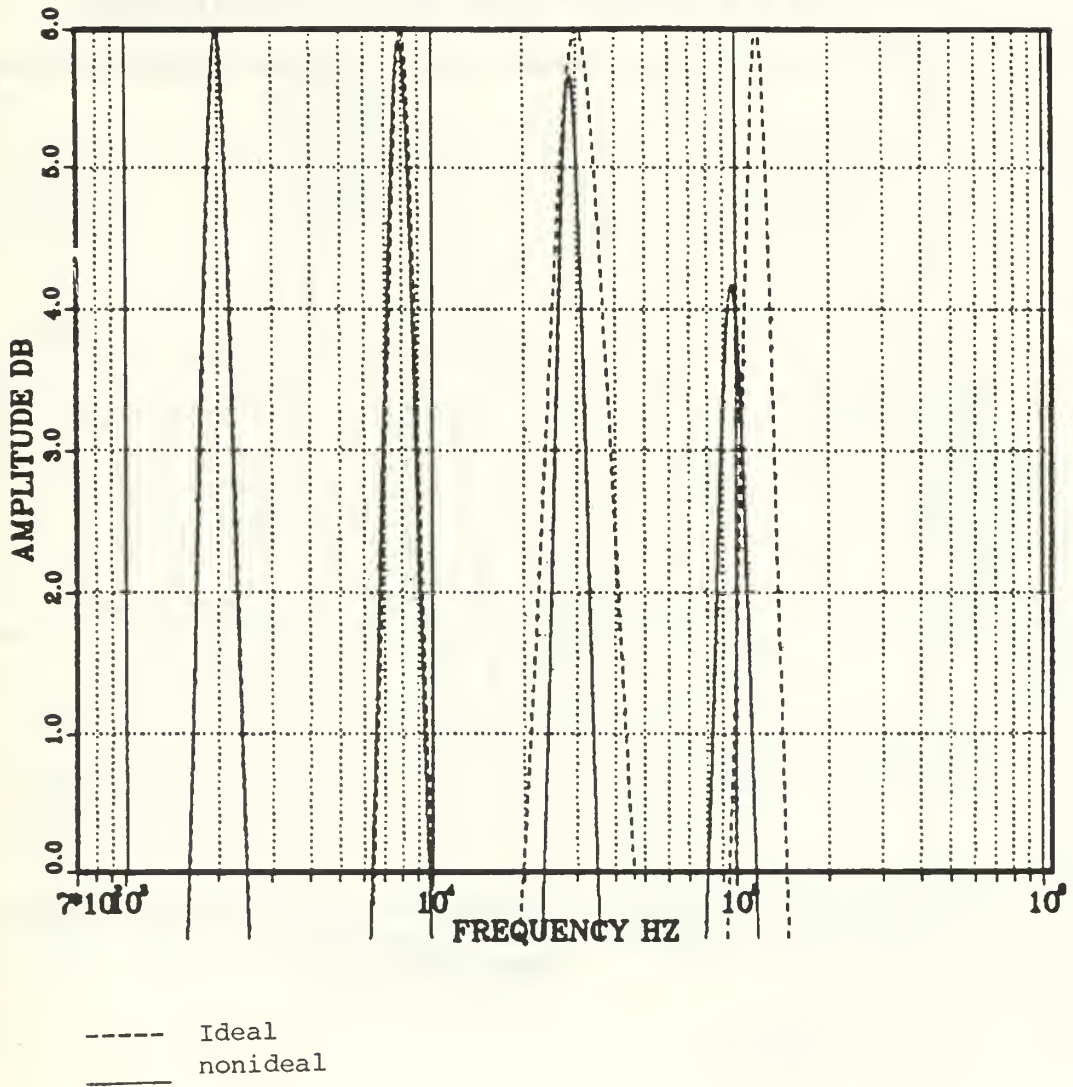


Fig. 4.16 - Ideal vs. Nonideal BPF Amplitude Response.

B.P.F AMPLITUDE RESPONSE(F=16K)

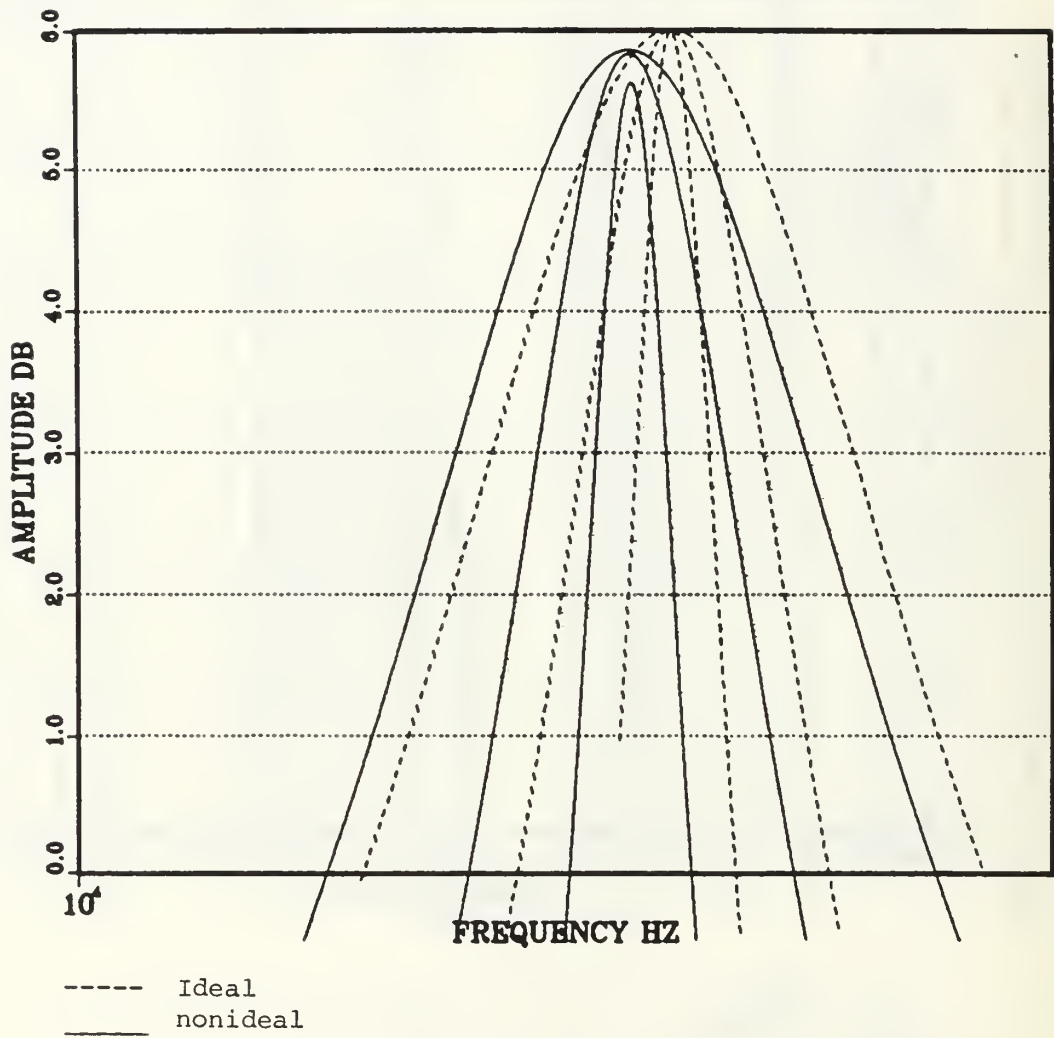


Fig. 4.17 - Ideal vs. Nonideal BPF Amplitude Response.

Ideal		C nf	Nonideal	
fp khz	Amp. Response dB		fp khz	Amp. Response dB
7,961.78	6.02	12.5	7,969.738	5.958
30,254.78	6.02	3.3	28,662.42	5.75
115,445.80	5.97	0.85	95,541.38	4.92

and

Ideal		Rq k	Nonideal	
Qp	Max. Amp. Response dB		Qp	Max. Amp. Response dB
4	6.01	6.4	4	5.902
8	6.01	12.8	8	5.728
20	5.95	32.0	20	5.528
fp ₁ = 15,127.33Hz			fp ₁ = 14,739.29Hz	

Table 4.6 - Data Indicating the Ideal vs. the Nonideal Responses of the BPF Realization

N.F AMPLITUDE RESPONSE(Q=2.)

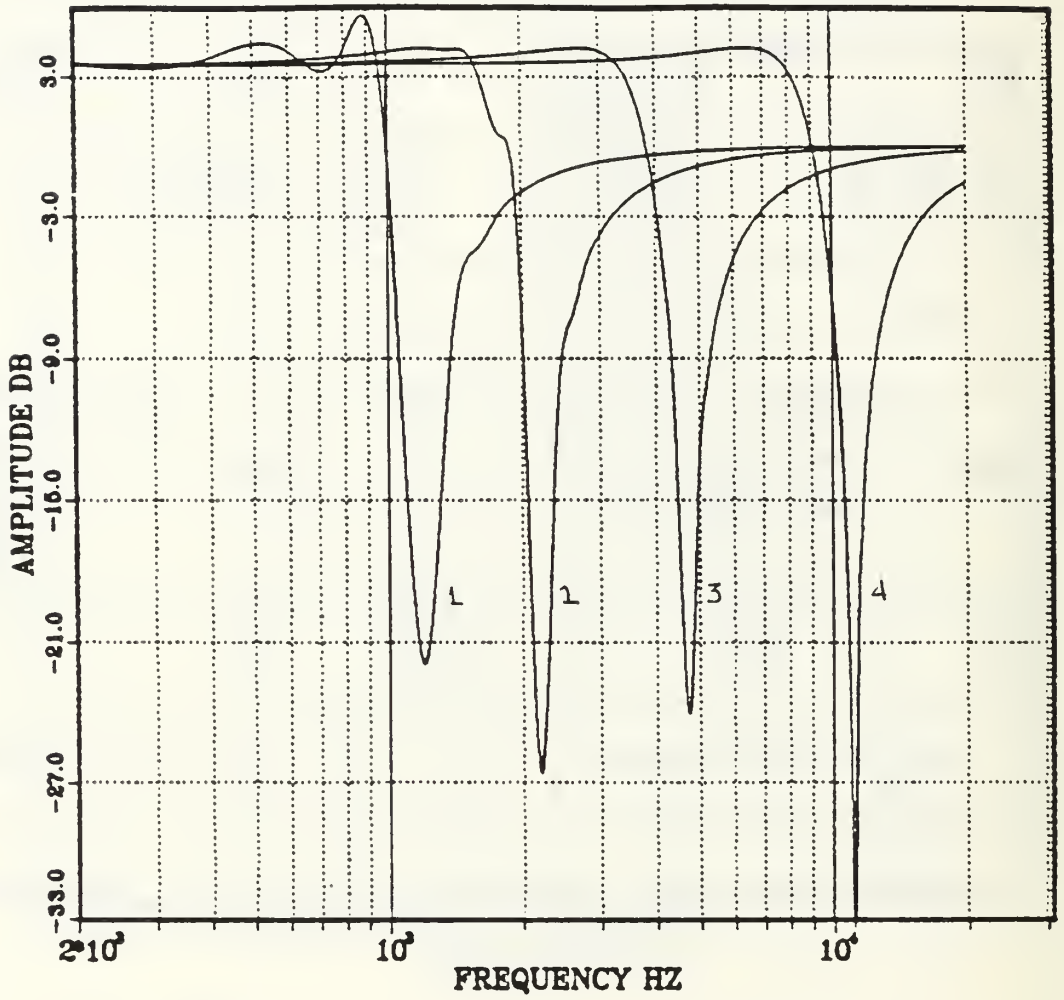


Fig. 4.18 - Ideal Notch Amplitude Response.

NOTCH AMPL RESPONSE(F=3.83KH)

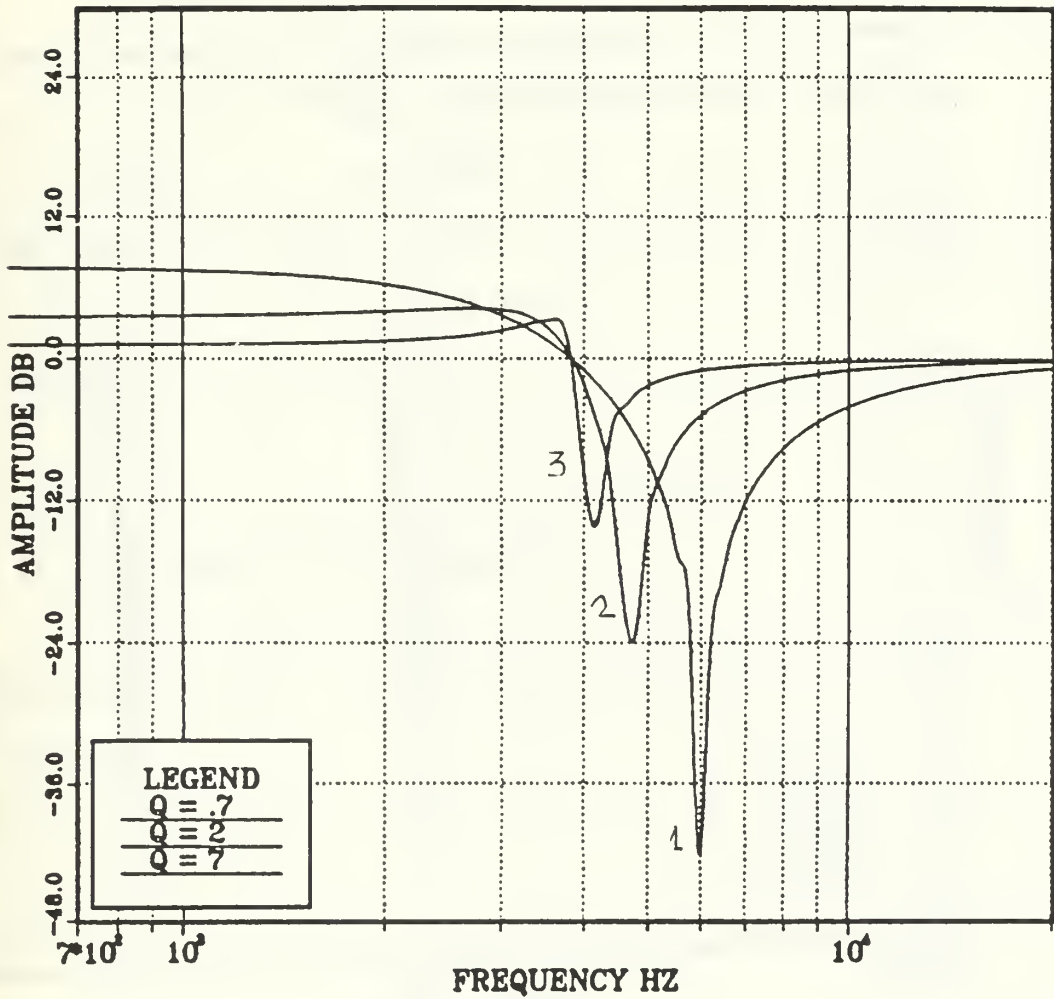


Fig. 4.19 - Ideal Notch Amplitude Response.

N.F AMPLITUDE RESPONSE(Q=2.)

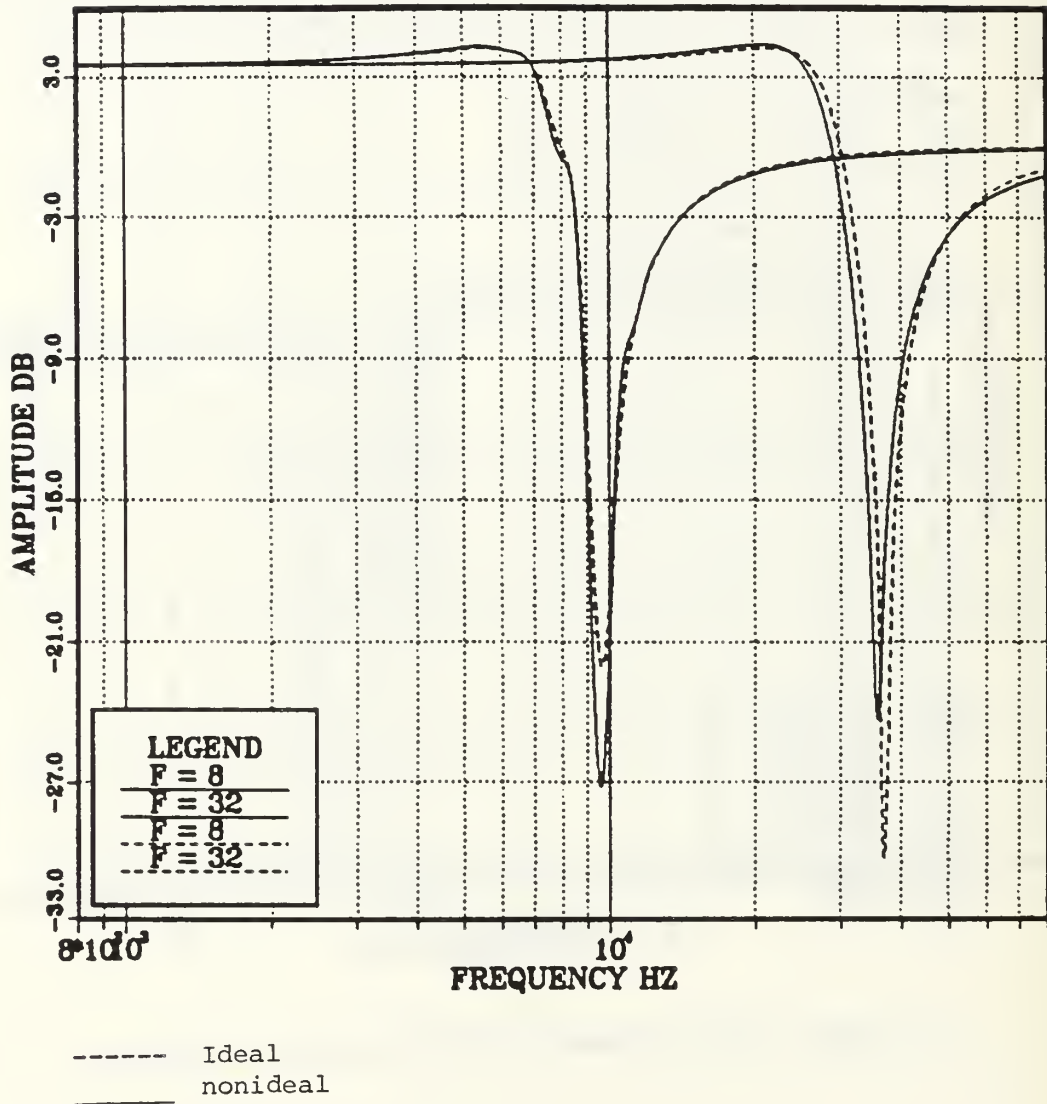


Fig. 4.20 - Ideal vs. Nonideal Amplitude Response.

where ω_n is the Notch frequency.

At ω_p the transfer function takes the value

$$T_2(j\omega_p) = \frac{\omega_p^2 + \omega_n^2}{j \frac{\omega_p^2}{Q_p}} \quad (4.11)$$

Fig.(4.18) illustrates the "ideal" theoretical Notch filter amplitude response for a variety of frequencies and constant $Q_p(Q=2)$, while Fig.(4.19) for a variety of Q_p s and for constant ω_p ($\omega_p=3.83\text{KHZ}$).

Fig. (4.20) illustrates the effect of the frequency dependency of A_i , ($i=1, 2$) on the response.

5. All Pass (AP) Realization

As proposed in Table (3.1) using the same admittances values as Notch. An All Pass transfer function can be derived as

$$T_1(s) = \frac{s^2 - \frac{\omega_p}{Q_p} s + \omega_p^2}{s^2 + \frac{\omega_p}{Q_p} s + \omega_p^2} \quad (4.12)$$

which takes the following values

$$\text{at } \omega \rightarrow 0, |T_1(j\omega)| \rightarrow 1 = 0 \text{ db}, \angle T_1(j\omega) \rightarrow 360^\circ$$

$$\omega \rightarrow \infty, |T_1(j\omega)| \rightarrow 2 = 6 \text{ db}, \angle T_1(j\omega) \rightarrow 0^\circ$$

(4.13)

The above agree with the computer simulation results of Figs. (4.21) and (4.22).

A.P AMPLITUDE RESPONSE(Q=2)

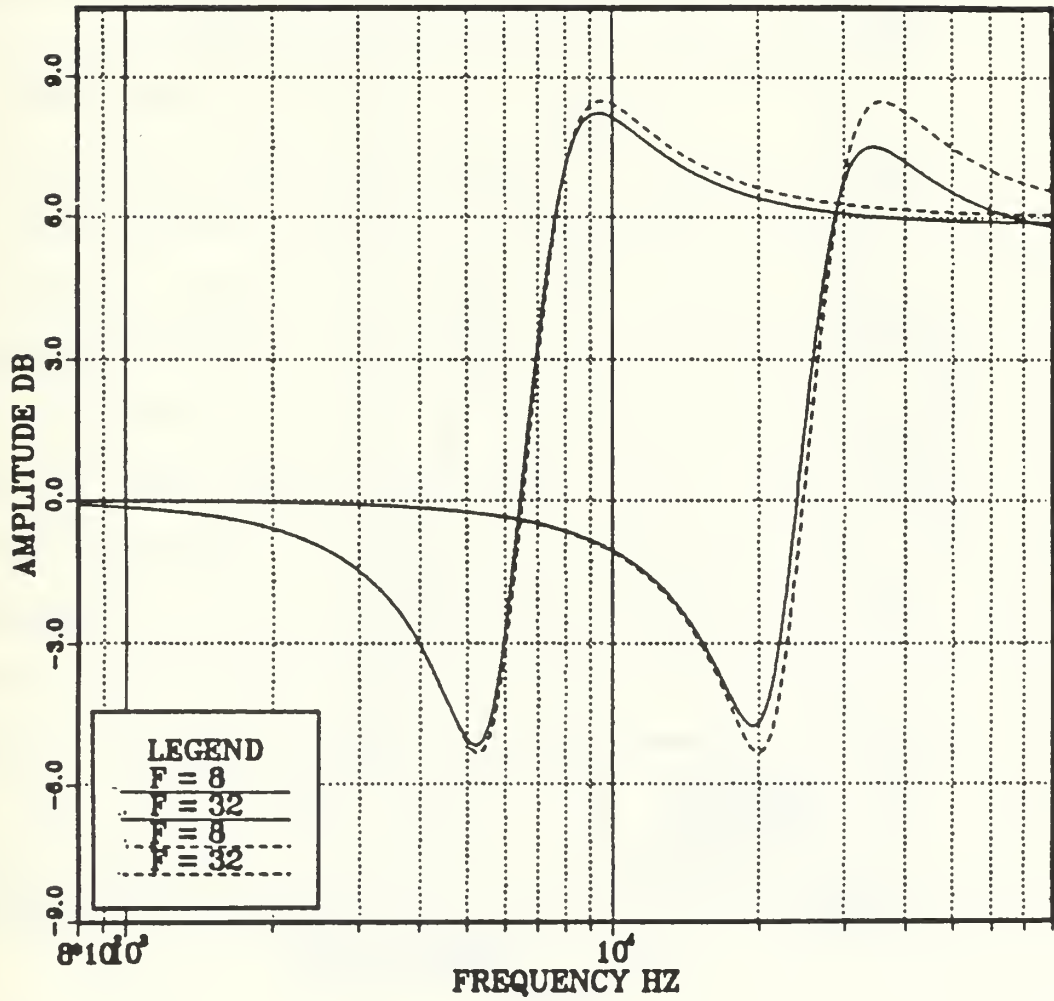


Fig. 4.21 - Ideal vs. Nonideal APF Amplitude Response.

A.P PHASE RESPONSE(Q=2/F=8K)

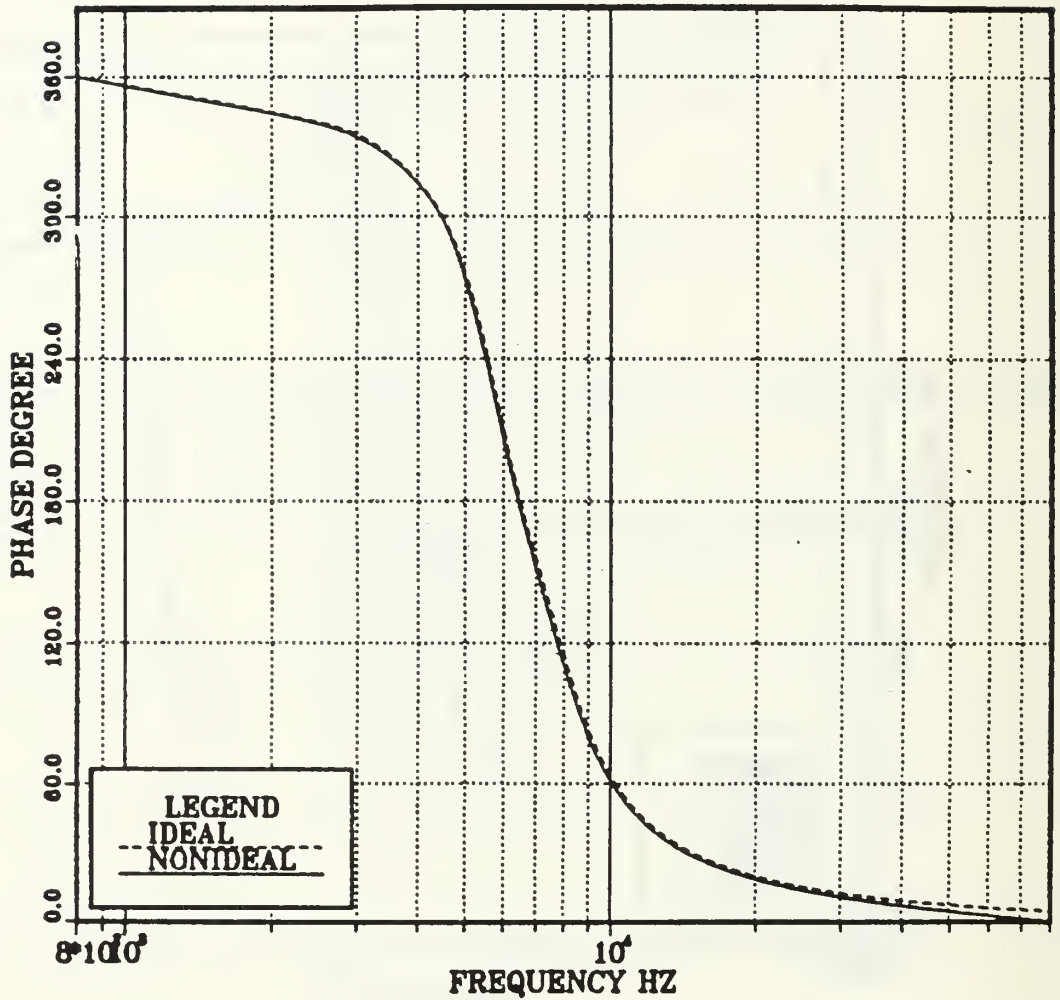


Fig. 4.22 - Ideal vs. Nonideal Phase Response.

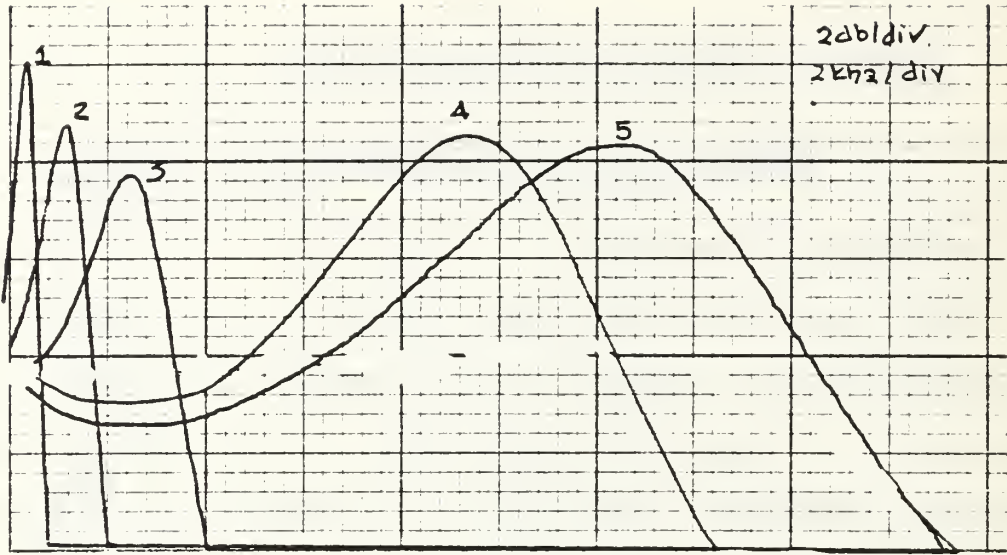
V. REALIZATION OF PROGRAMMABLE GIC FILTER

A. EXPERIMENTAL RESULTS

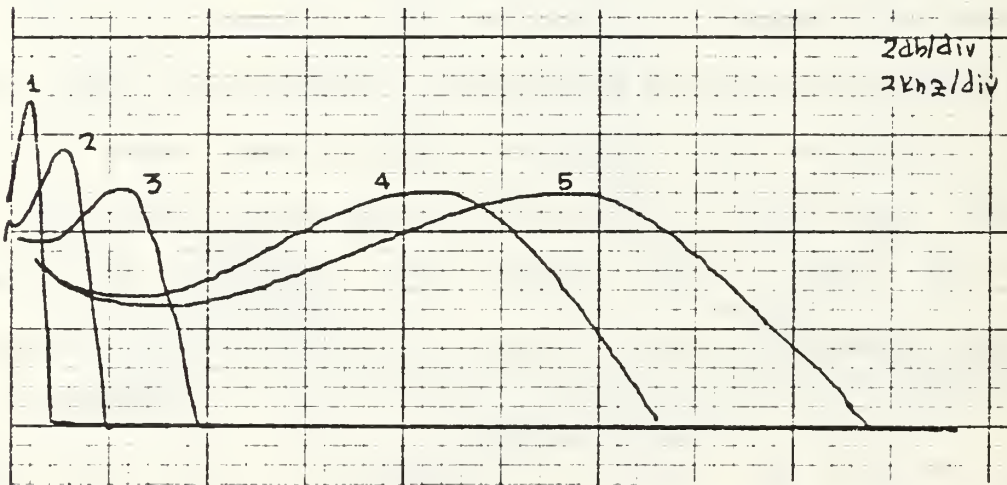
After the circuit of Figs. (3.10), (3.9), (3.8), (3.7), was constructed a variety of measurements were taken in order to study the response of the network to the different inputs (control bitwords). To observe the affect of the control switches which introduce a resistance of 80 each at CLOSED position, two values of R_s , R_q , and C_s were used with one decade difference in magnitude. That means that R was given the values of 1.6K (as discussed in Chapter III) and 16K, the four resistors that consisted the R_q bank were of values (1.6K, 3.2K, 6.4K, 12.8K) in the first case and (16K, 32K, 64K and 128K) in the second one, and that the capacitor bank's capacitors were chosen of values (100nF, 50nF, 12, 5nF, 11nF) and (10nF, 5nF, 1.2nF, 0.1nF) accordingly, to be able to keep the range of frequencies as much the same as possible for both cases.

1. Low Pass Filter

With the topology-control bit word 000 the network realized a LPF response. Fig. 5.1(a) illustrates the LP response for $R=1.6K\Omega$ to a variety of frequencies for $Q=5$ while 5.1(b) illustrates the same but for $Q=2$. It can be observed from 5.1(a) ($Q=5$) that the amplitude response



(a)



(b)

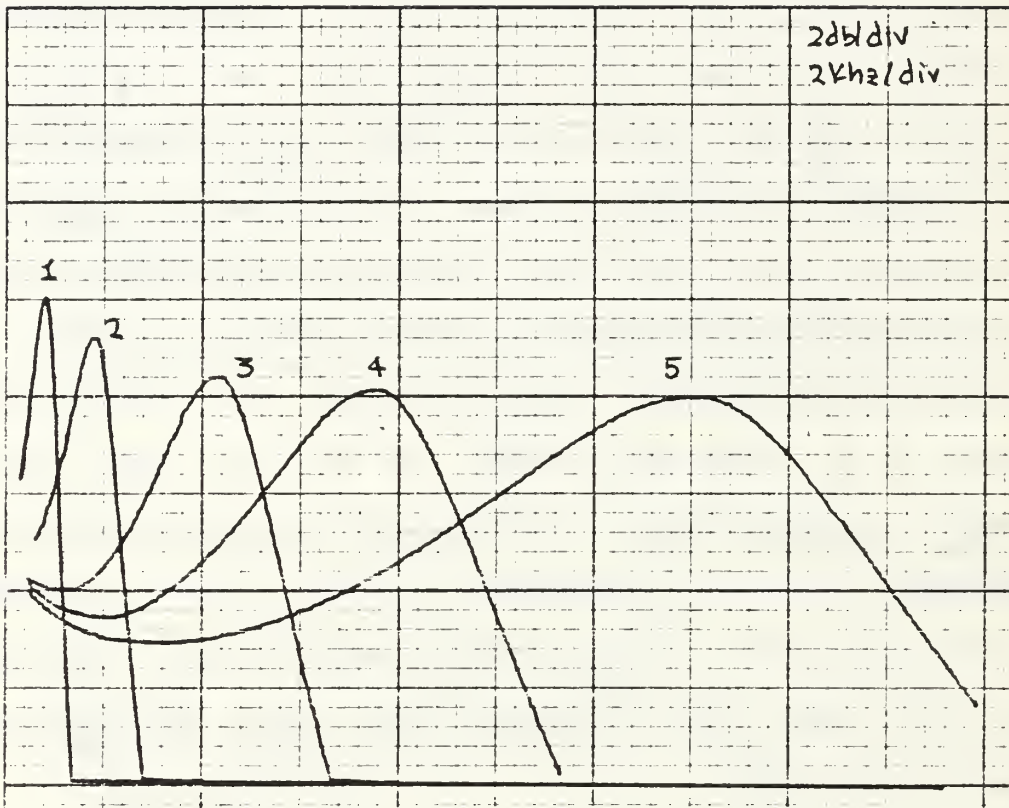
- 1 - $f = 0.99\text{kHz}$
- 2 - $f = 1.98\text{kHz}$
- 3 - $f = 3.83\text{kHz}$
- 4 - $f = 7.96\text{kHz}$
- 5 - $f = 12.0\text{kHz}$

Fig. 5.1 - (a) LPF Response for $R=1.6\text{k}$ ($Q=5$, $R_q=8.0\text{k}$)
 (b) LPF Response for $R=1.6\text{k}$ ($Q=2$, $R_q=3.2\text{k}$)

decreases while the frequency increases as it was expected from computer simulation. This is occurred up to the frequency of 6KHZ; then it started increasing with the frequency, while at Fig. (5.1(b)) ($Q=2$) it remained constant. Fig. (5.2) illustrates (for $R=16KHZ$) that the observation in Fig (5.1) is not any more the case (for that frequency range) and the network responses the same as in computer simulation while in Fig. (5.3) ($Q=5$) the above can be noticed again. this is due to the interference of the control switches as it was discussed previously. Figs. (5.4) and (5.5) illustrate a variation of Q values for $f=9KHZ$ for the two cases ($R=1.6k$ and $R=16K$) respectively. A difference in magnitude can be observed due to the interference of the control switches. Figs. (5.6) and (5.7) illustrate the same but for $F=12.8KHZ$. Figs. (5.8) and (5.9) illustrate the phase and amplitude response of the LPf.

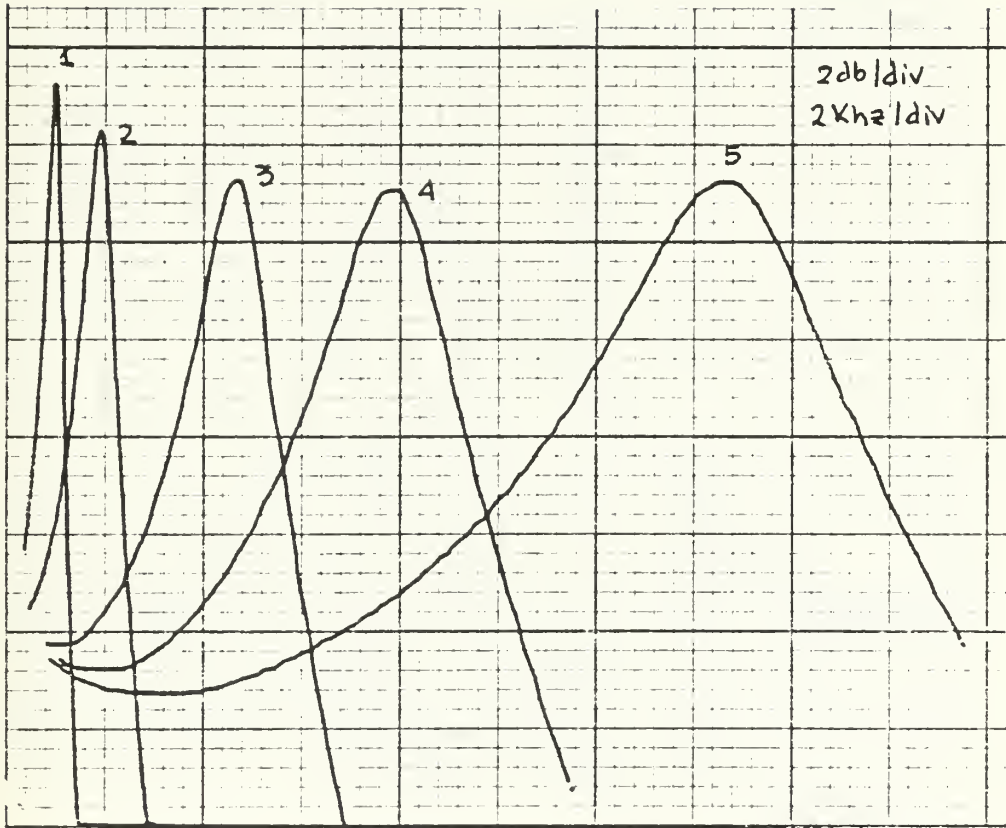
2. High Pass (HP) Realization

With the topology-control bitword 001, the network realized a high pass filter. Figs. (5.10) and (5.11) illustrate the HPF amplitude response for a variety of frequencies and ($Q=2$). It can be observed (as in LPF realization) that for this frequency range and for $R=1.6K\Omega$ the amplitude starts increasing as the frequency increases, decreases then again while for $R=16K\Omega$ this does not occur. the same observation submerges comparing Fig.(5.14) and (5.15). Figs. (5.12) and (5.13) are the plots obtained for



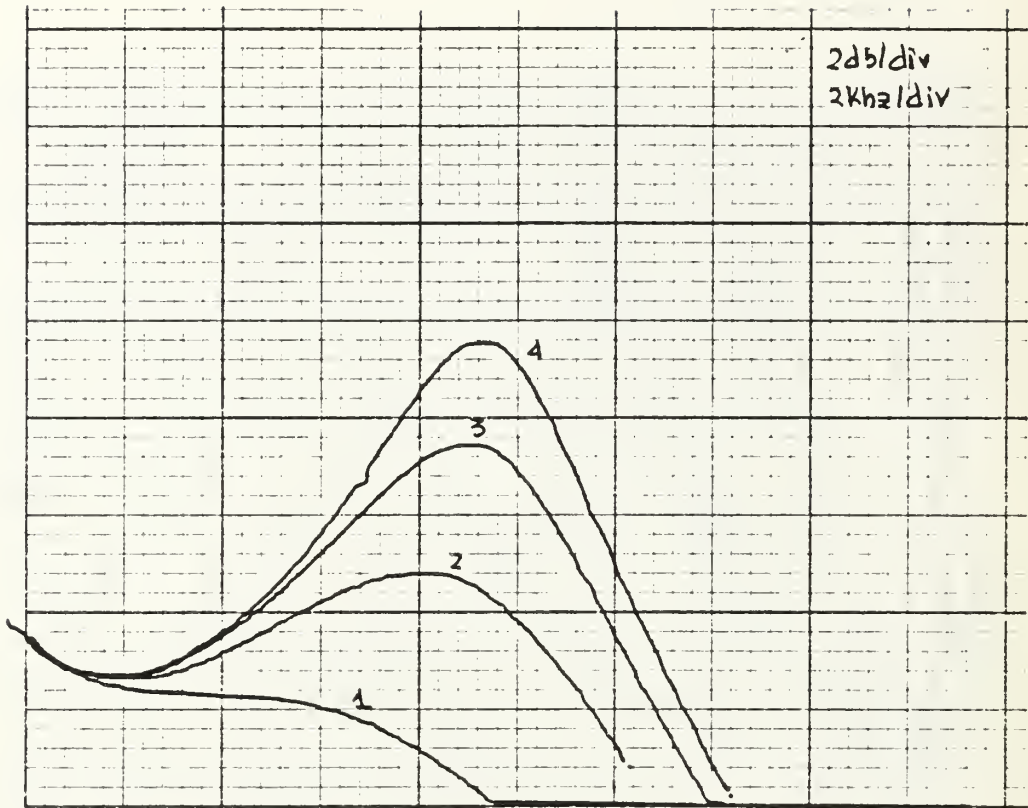
- 1 - $f = 0.99\text{kHz}$
- 2 - $f = 1.99\text{kHz}$
- 3 - $f = 3.83\text{kHz}$
- 4 - $f = 7.90\text{kHz}$
- 5 - $f = 12.8\text{kHz}$

Fig. 5.2 - LPF Amplitude Response
 $R=1.6\text{k}$ ($Q=2$, $R_q=32\text{k}$)



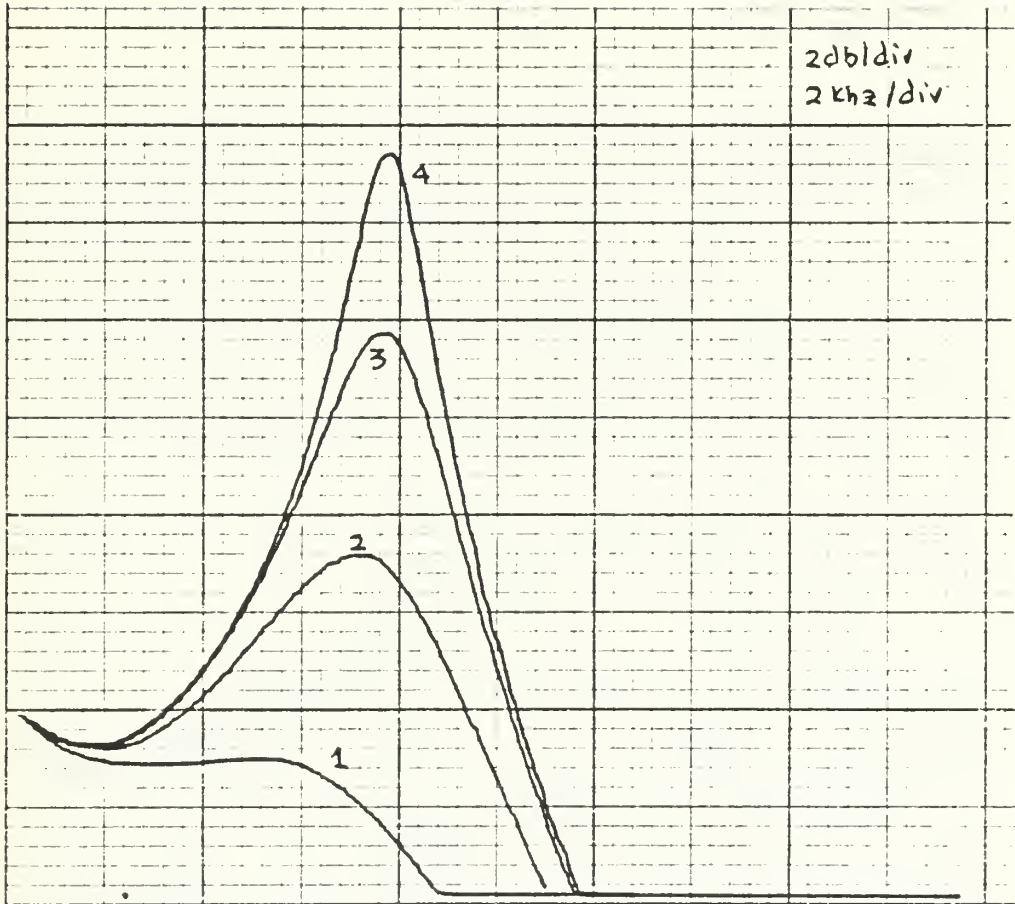
- 1 - $f = 0.99\text{kHz}$
- 2 - $f = 1.99\text{kHz}$
- 3 - $f = 9.20\text{kHz}$
- 4 - $f = 7.96\text{kHz}$
- 5 - $f = 15.0\text{kHz}$

Fig. 5.3 - LPF Amplitude Response
 $R=16\text{k}$ ($Q=5$, $R_q=50\text{k}$)



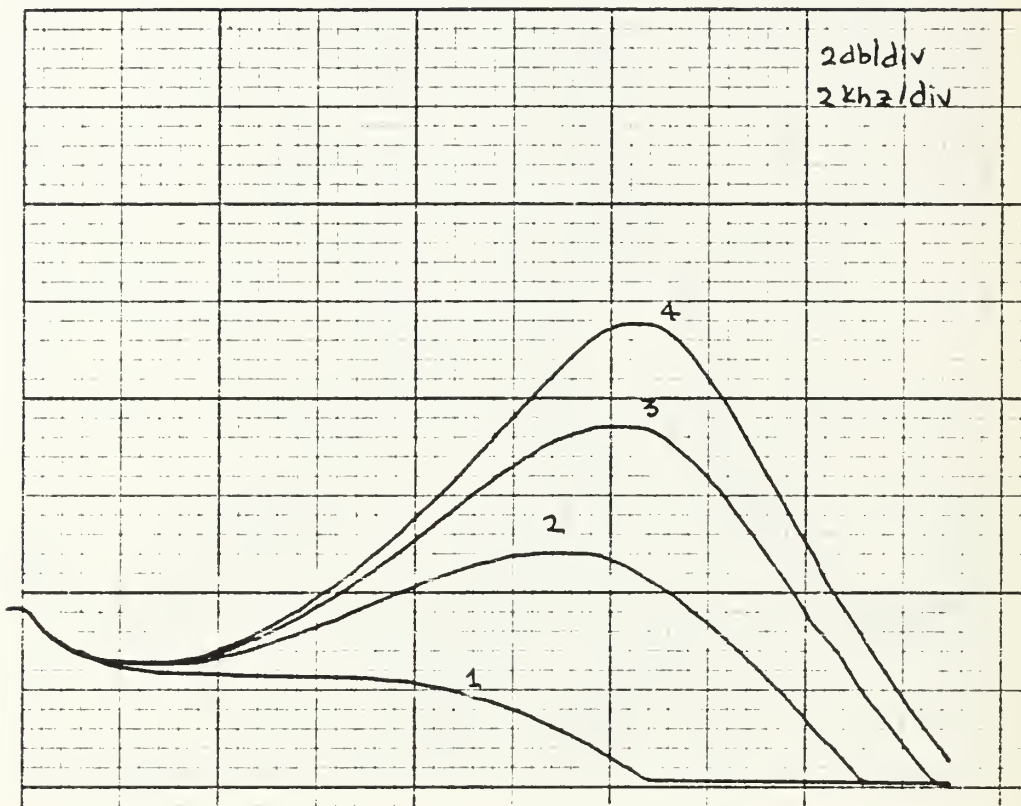
- 1 - $Q = 1$
- 2 - $Q = 2$
- 3 - $Q = 4$
- 4 - $Q = 7$

Fig. 5.4 - LPF Amplitude Response ($R=1.6k$),
 $f=7.96kHz$



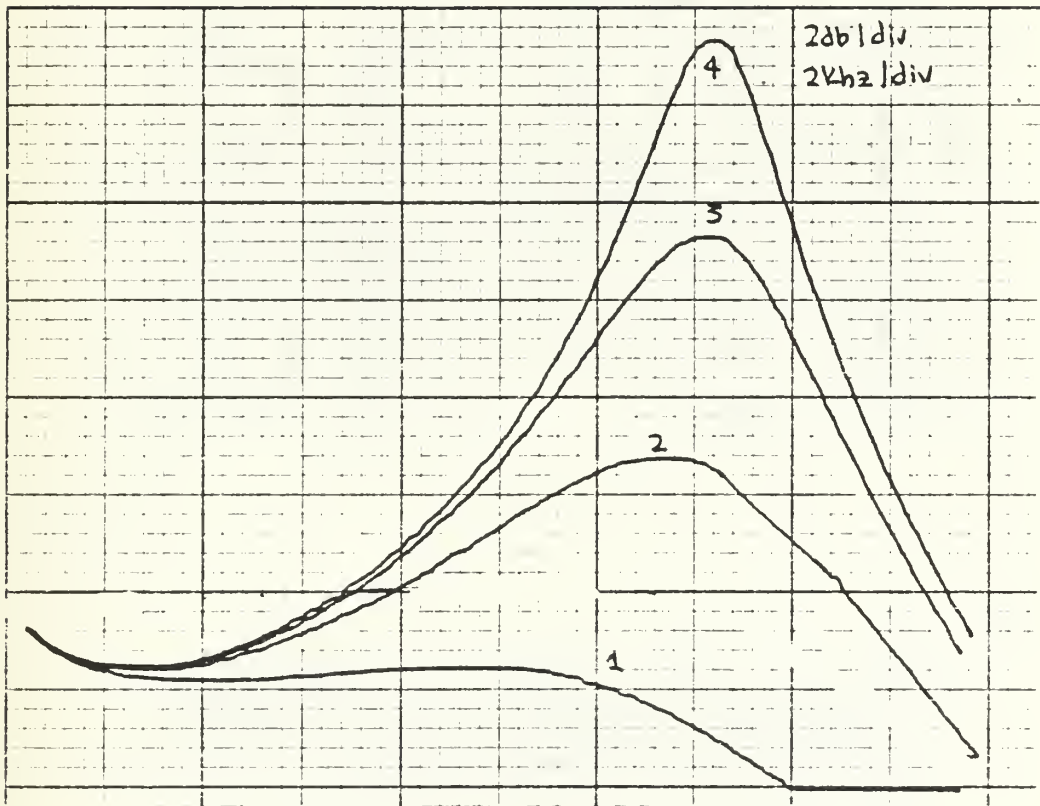
- 1 - Q = 1
- 2 - Q = 2
- 3 - Q = 4
- 4 - Q = 7

Fig. 5.5 - LPF Amplitude Response (R=10k),
f=7.96kHz



- 1 - $Q = 1$
- 2 - $Q = 2$
- 3 - $Q = 4$
- 4 - $Q = 7$

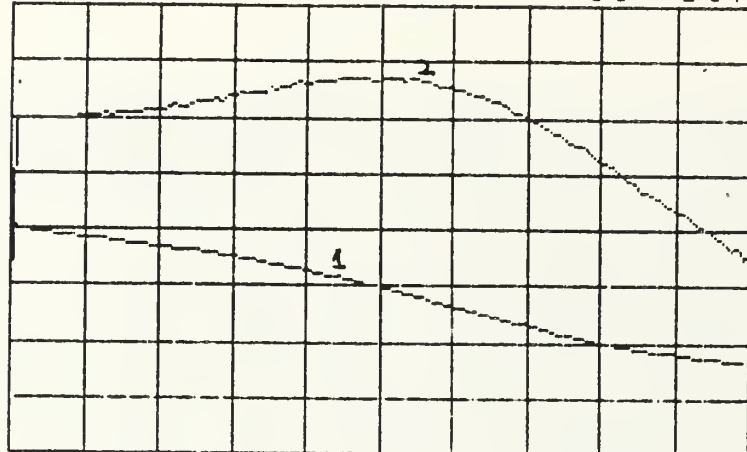
Fig. 5.6 LPF Amplitude Response ($R=1.6k$) and $f=12.8kHz$



- 1 - Q = 1
- 2 - Q = 2
- 3 - Q = 4
- 4 - Q = 7

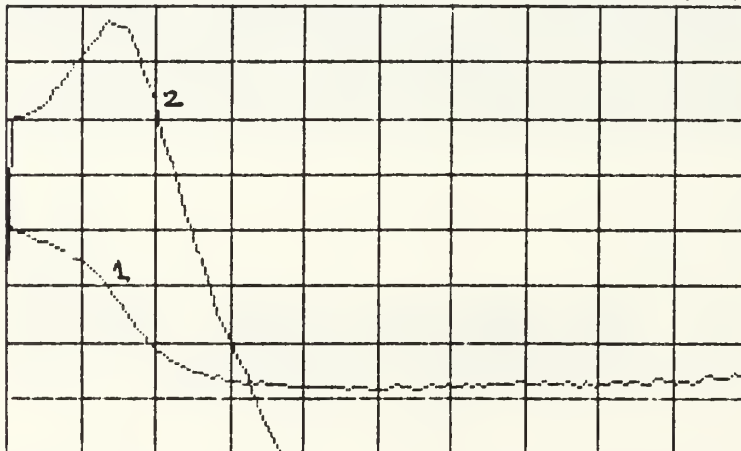
Fig. 5.7 - LPF Amplitude Response ($R=1.6k$),
 $f=12.8kHz$

XFR FCTN MKR: 2.9dB 2 dB/DIV
XFR FCTN: 0° CENTER 500°/DIV



0 Hz 10 KHz /
MKR: 8 800 Hz BW: 80.0 Hz

XFR FCTN MKR: 2.7dB 2 dB/DIV
XFR FCTN: 0° CENTER 500°/DIV

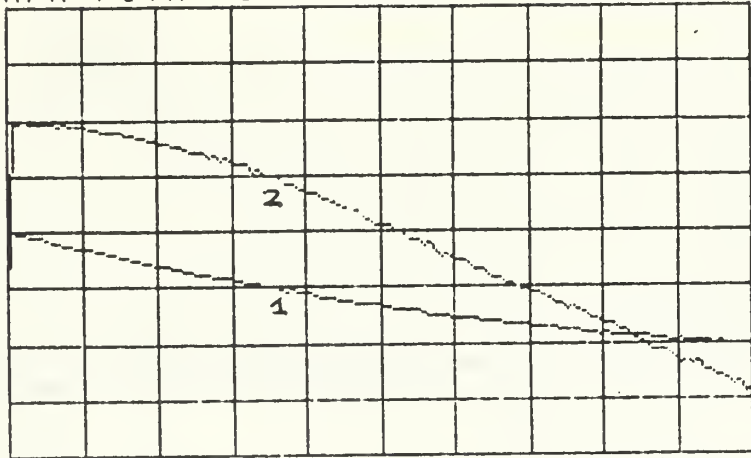


0 Hz 10 KHz /
MKR: 2 400 Hz BW: 80.0 Hz

1. Phase Response.
2. Amplitude Response.

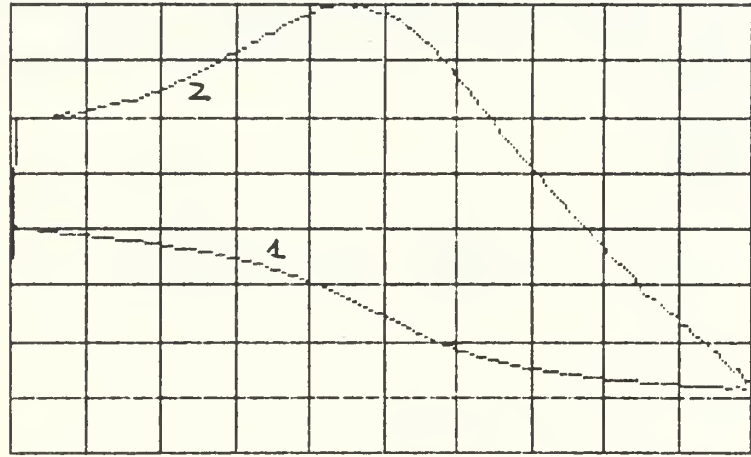
Fig. 5.8 - LPF Amplitude/Phase Response.

XFR FCTN MKR: 3.0dB 2 dB/DIV
XFR FCTN: 0° CENTER 500/DIV



0 Hz 10 kHz
MKR: 4 400 Hz BW: 80.0 Hz

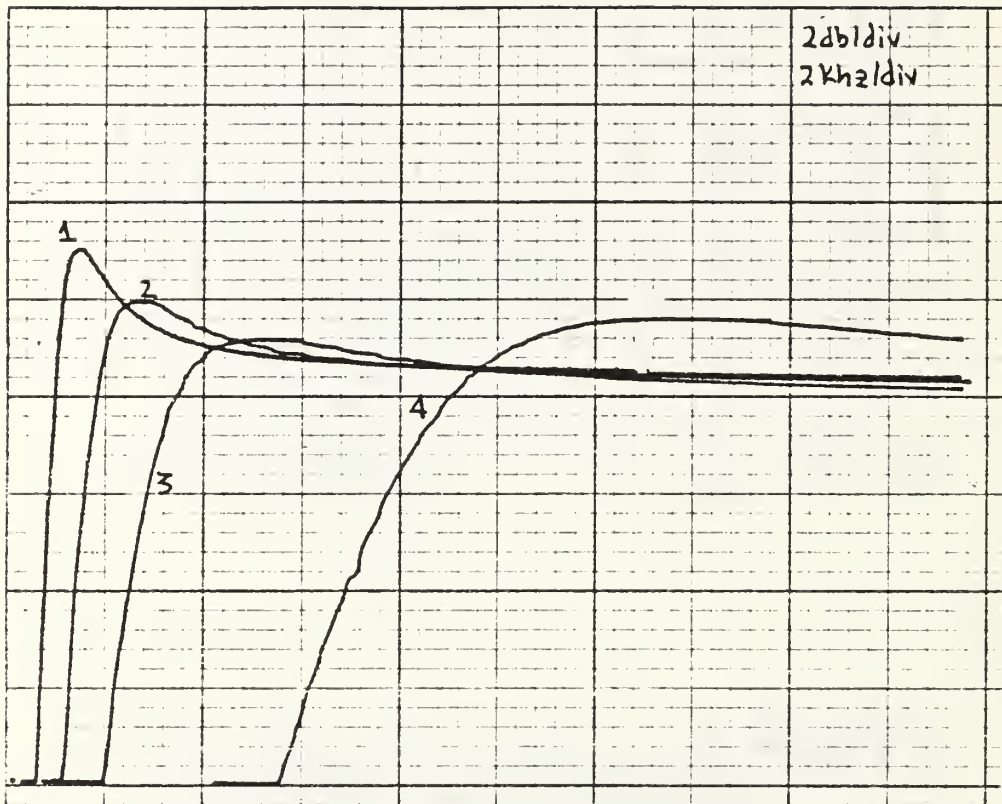
XFR FCTN MKR: 2.9dB 2 dB/DIV
XFR FCTN: 0° CENTER 500/DIV



0 Hz 10 kHz
MKR: 7 440 Hz BW: 80.0 Hz

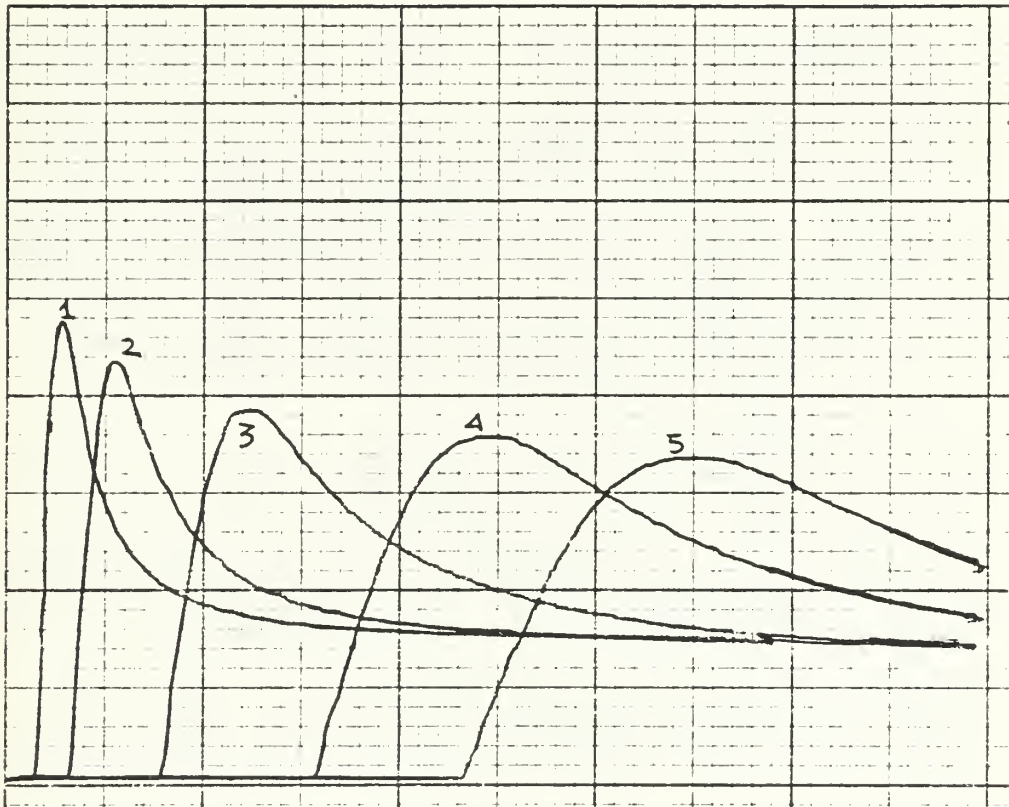
- 1. Phase
- 2. Amplitude

Fig. 5.9 - LPI Phase/Amplitude Response.



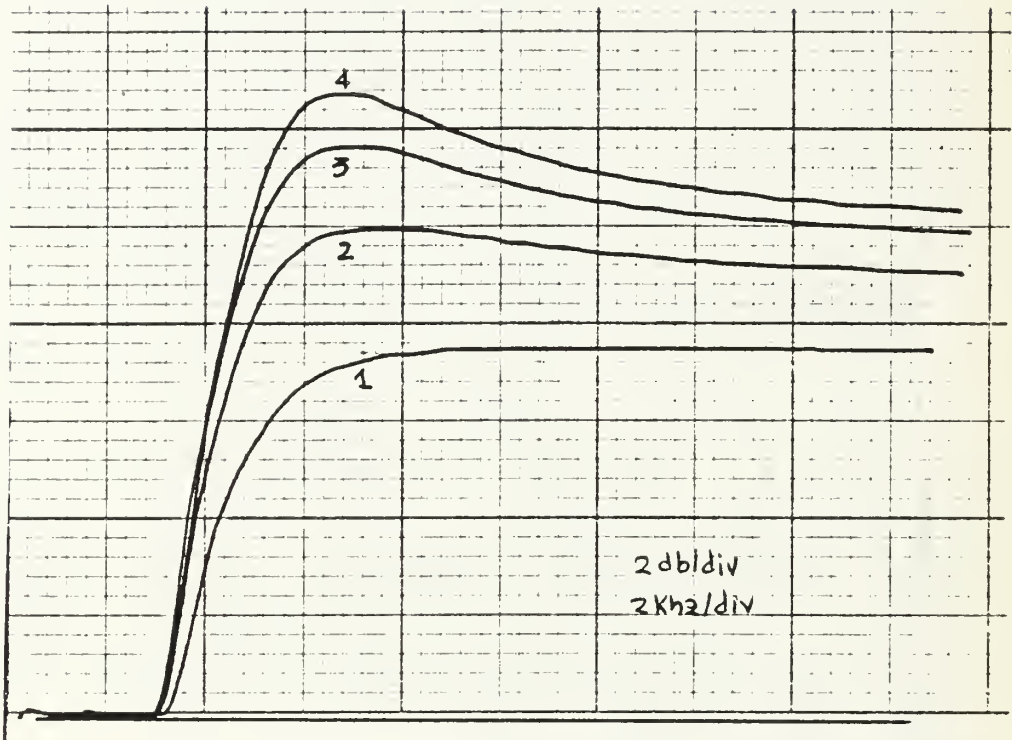
- 1 - $f = 0.99\text{kHz}$
- 2 - $f = 1.99\text{kHz}$
- 3 - $f = 3.83\text{kHz}$
- 4 - $f = 7.96\text{kHz}$

Fig. 5.10 - HPF Amplitude Response
($R=1.6\text{k}$), $Q=2$



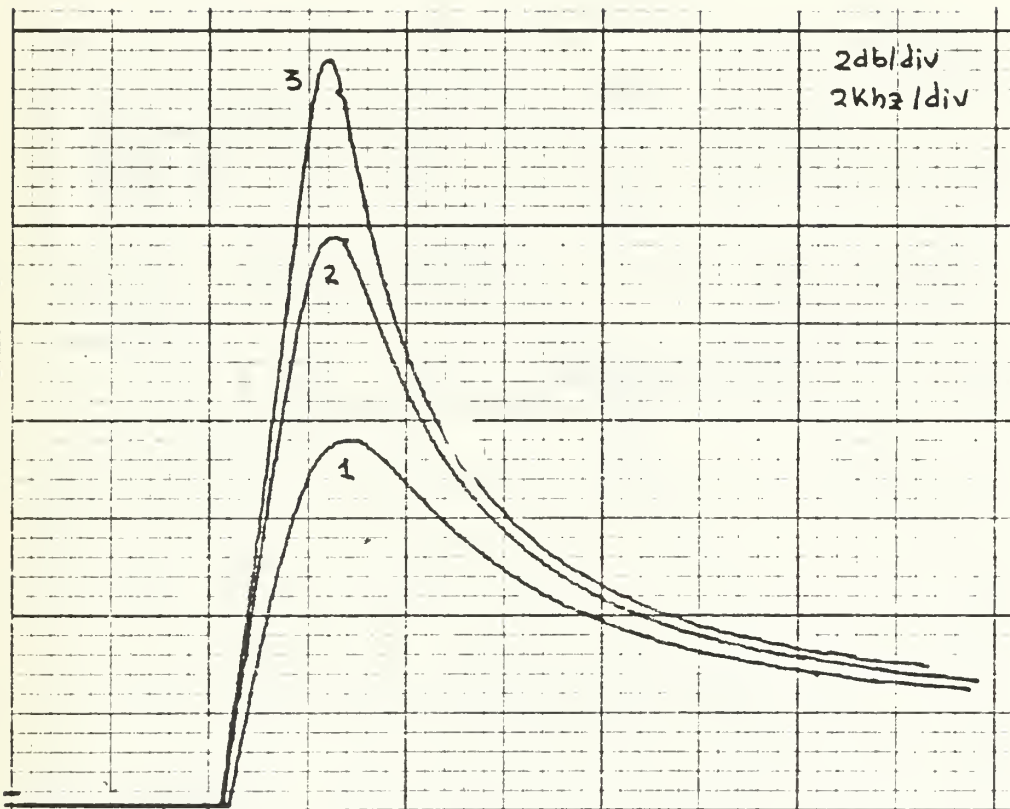
- 1 - $f = 0.99\text{kHz}$
- 2 - $f = 1.9\text{ kHz}$
- 3 - $f = 5.0\text{ kHz}$
- 4 - $f = 8.0\text{ kHz}$
- 5 - $f = 13.8\text{ kHz}$

Fig. 5.11 - HPF Amplitude Response
 ($R=1.6k$), $Q=2$



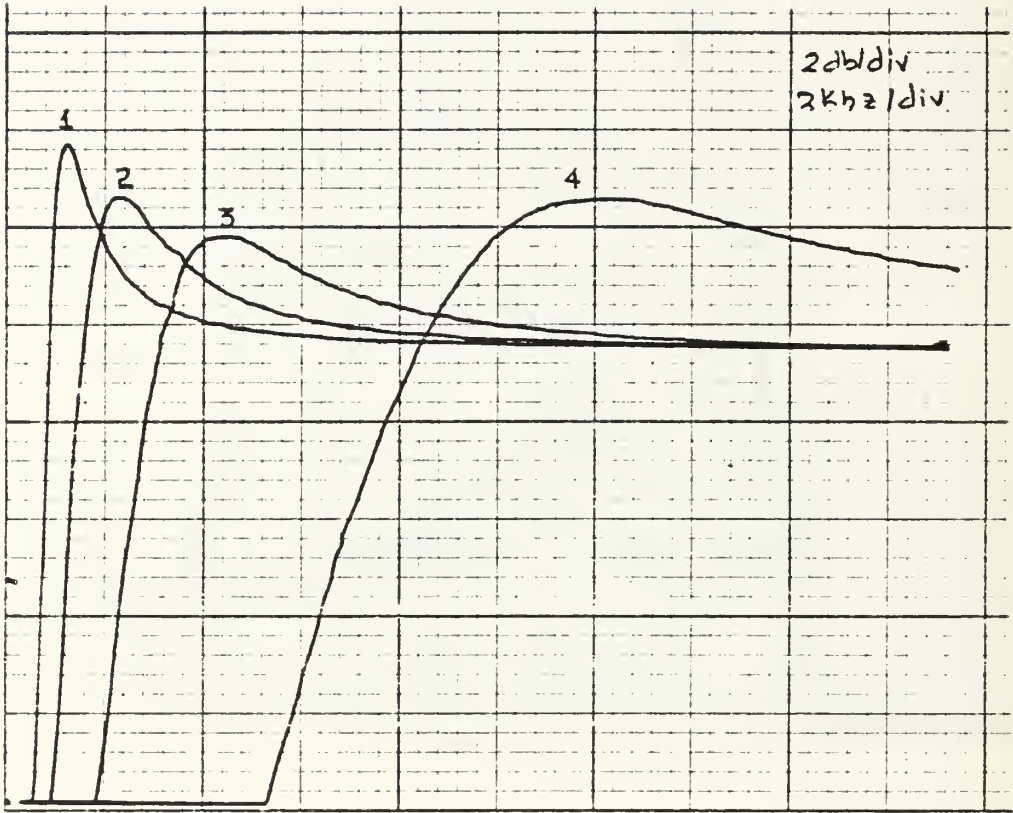
- 1 - $Q = 0.7$
- 2 - $Q = 2.0$
- 3 - $Q = 4.0$
- 4 - $Q = 7.0$

Fig. 5.12 - HPF Response ($R=1.6k$),
 $f=6.65kHz$



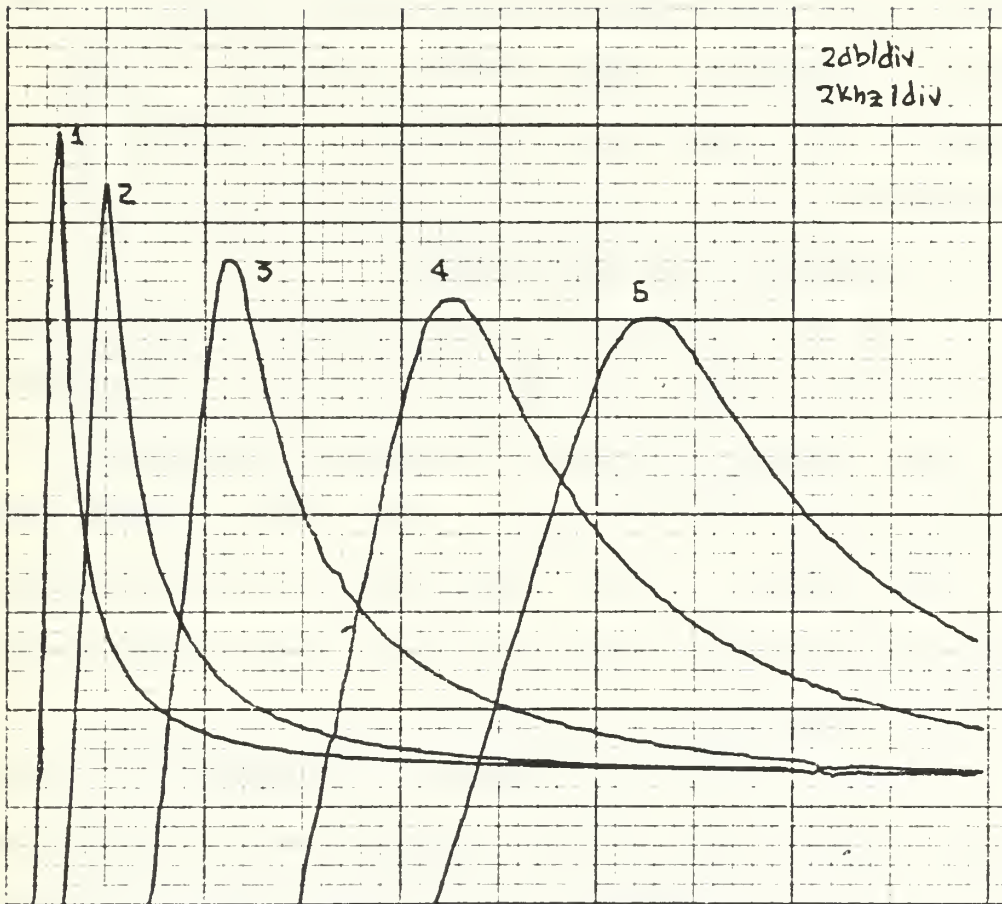
- 1 - $Q = 2.0$
- 2 - $Q = 4.0$
- 3 - $Q = 7.0$

Fig. 5.13 - HPF Amplitude Response
($R=1.6k$), $f=6.65kHz$



- 1 - $f = 0.99\text{kHz}$
- 2 - $f = 1.99\text{kHz}$
- 3 - $f = 3.83\text{kHz}$
- 4 - $f = 7.96\text{kHz}$

Fig. 5.14 - HPB Amplitude Response
($R=1.6\text{k}$), $Q=5$



- 1 - $f = 0.99\text{kHz}$
- 2 - $f = 1.99\text{kHz}$
- 3 - $f = 3.83\text{kHz}$
- 4 - $f = 7.96\text{kHz}$
- 5 - $f = 12.8\text{kHz}$

Fig. 5.15 - HPB Amplitude Response
($R=1.6\text{k}$), $Q=5$

$f=6.65\text{KHZ}$ and a variety of Q_s for $R=1.6\text{K}\Omega$ and $R=16\text{K}\Omega$, respectively. a difference of about 12dB in amplitude appears. Finally, figs (5.16), (5.17), (5.18), (5.19) illustrate the phase and amplitude responses of the HP realization.

3. Band Pass (BP) Realization

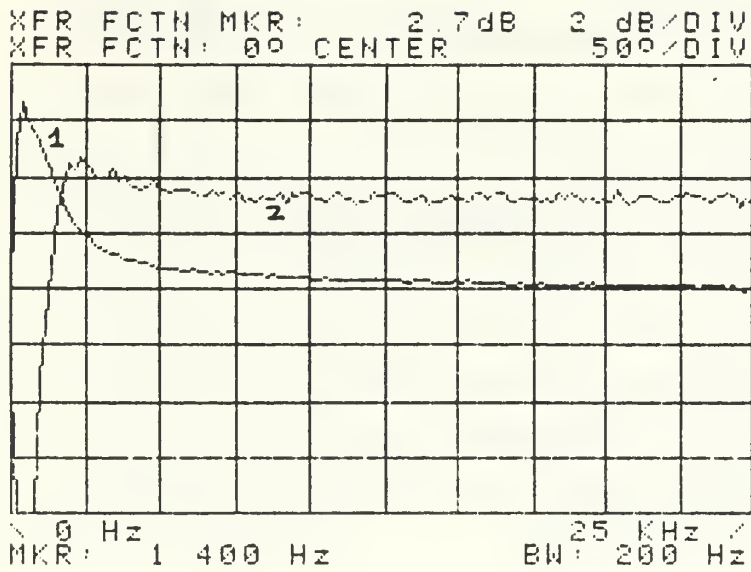
The 010 topology-control bitword realizes the Band Pass Filter. Figs. (5.20) and (5.21) illustrates the amplitude response for set of frequencies and $Q=10$. At both cases the amplitude decreases while the frequency increases until the value of 9KHZ. Then starts increasing again. It can be also observed that for $R=1.6\text{K}$ the frequency deviation from the theoretical f_p is larger.

Figs. (5.22) and (5.23) illustrate the amplitude response again, but for $Q=1$. This time the deviations from the theoretical response (both of amplitude fluctuations and frequency shift) are less.

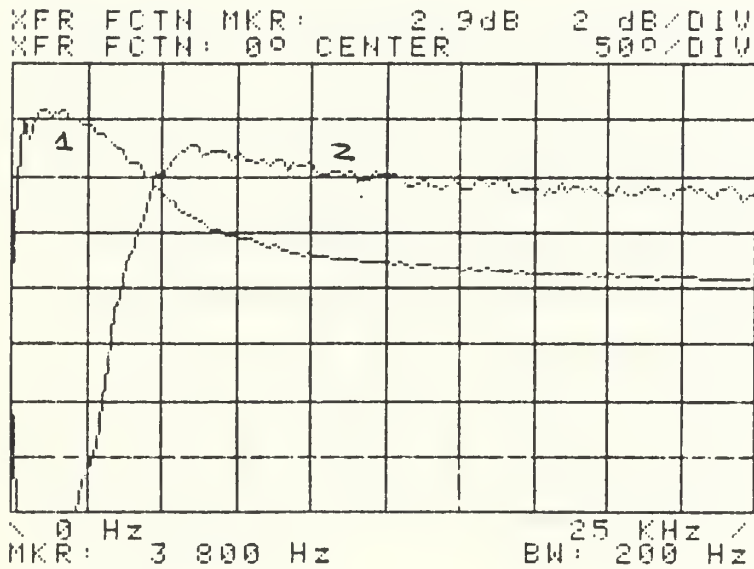
Figs. (5.24), (5.25), (5.26), and (5.27) are also plots of the amplitude response but for variation of Q . A difference of approximately 1dB appears for the lowest frequency (3.8KHZ) and of 0.5dB for the higher (9KHZ), Finally, Figs. (5.28)-(5.32) illustrate the phase and amplitude of the BPF response.

4. Notch (N) Filter Realization

With the topology-control bitword 011, a Notch filter realization can be achieved. Figs. (5.33) and (5.34)



(a)

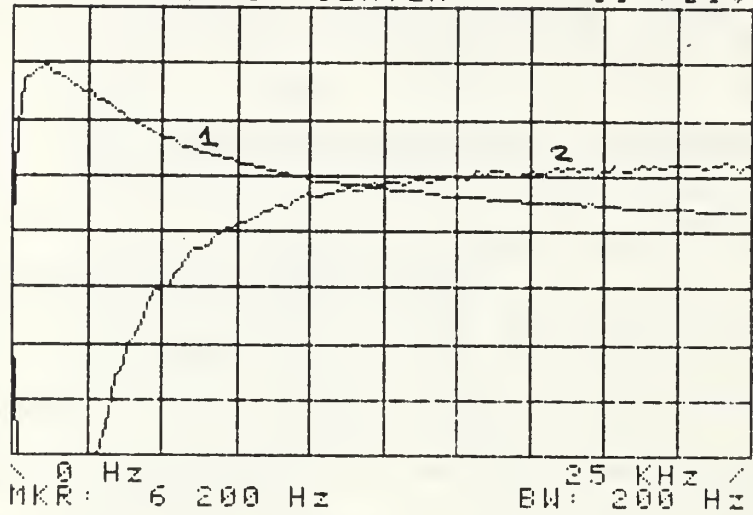


(b)

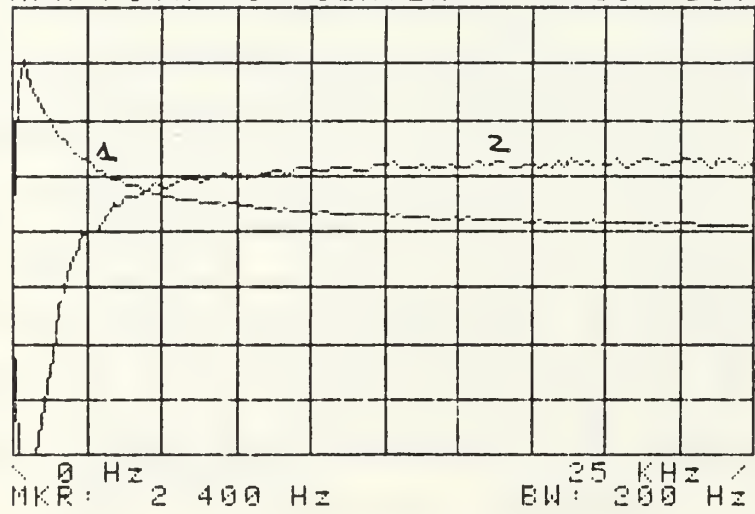
1. Phase
2. Amplitude

Fig. 5.16 - HPF Amplitude/Phase Response (Q=1)

XFR FCTN MKR: 1.4dB 2 dB/DIV
XFR FCTN: 0° CENTER 50°/DIV



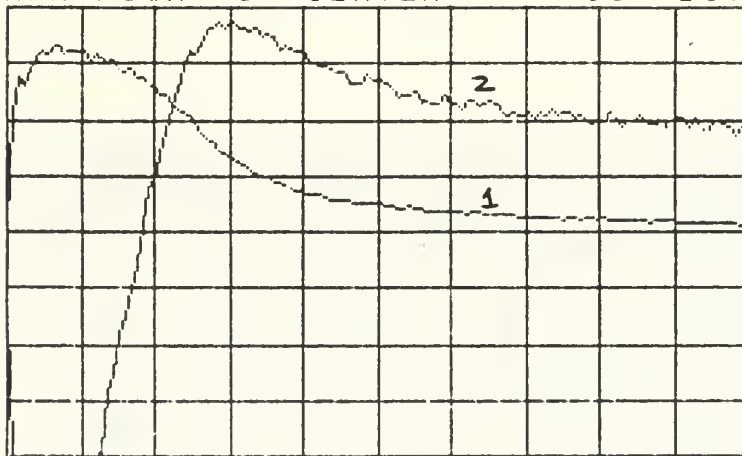
XFR FCTN MKR: 2.0dB 2 dB/DIV
XFR FCTN: 0° CENTER 50°/DIV



- 1. Phase
- 2. Amplitude

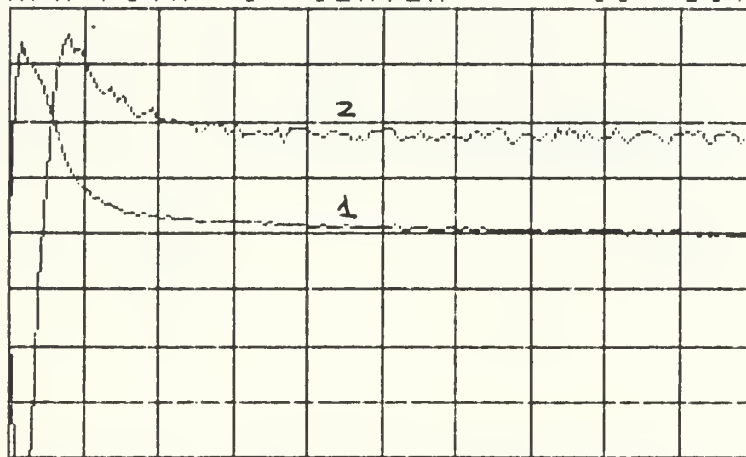
Fig. 5.17 - HBF Amplitude/Phase Response (Q=0.5)

XFR FCTN MKR: 3.6dB 2 dB/DIV
XFR FCTN: 0° CENTER 50°/DIV



0 Hz 25 kHz /
MKR: 4 000 Hz BW: 200 Hz

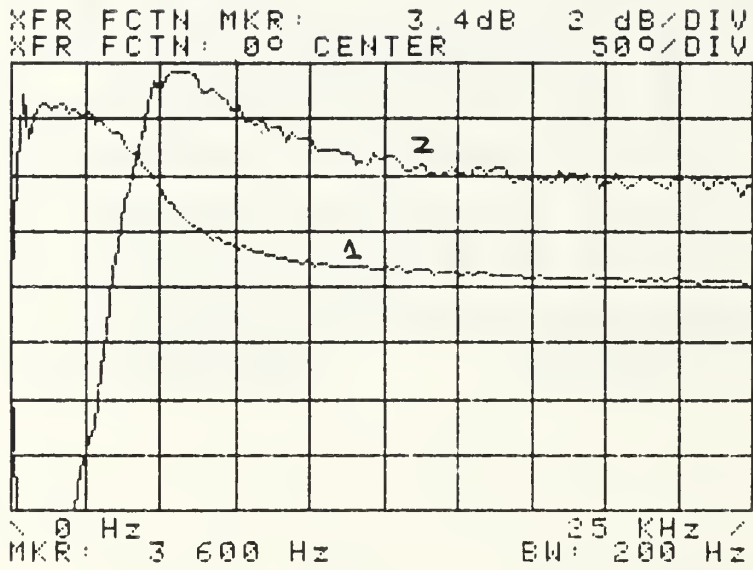
XFR FCTN MKR: 2.6dB 2 dB/DIV
XFR FCTN: 0° CENTER 50°/DIV



0 Hz 25 kHz /
MKR: 1 000 Hz BW: 200 Hz

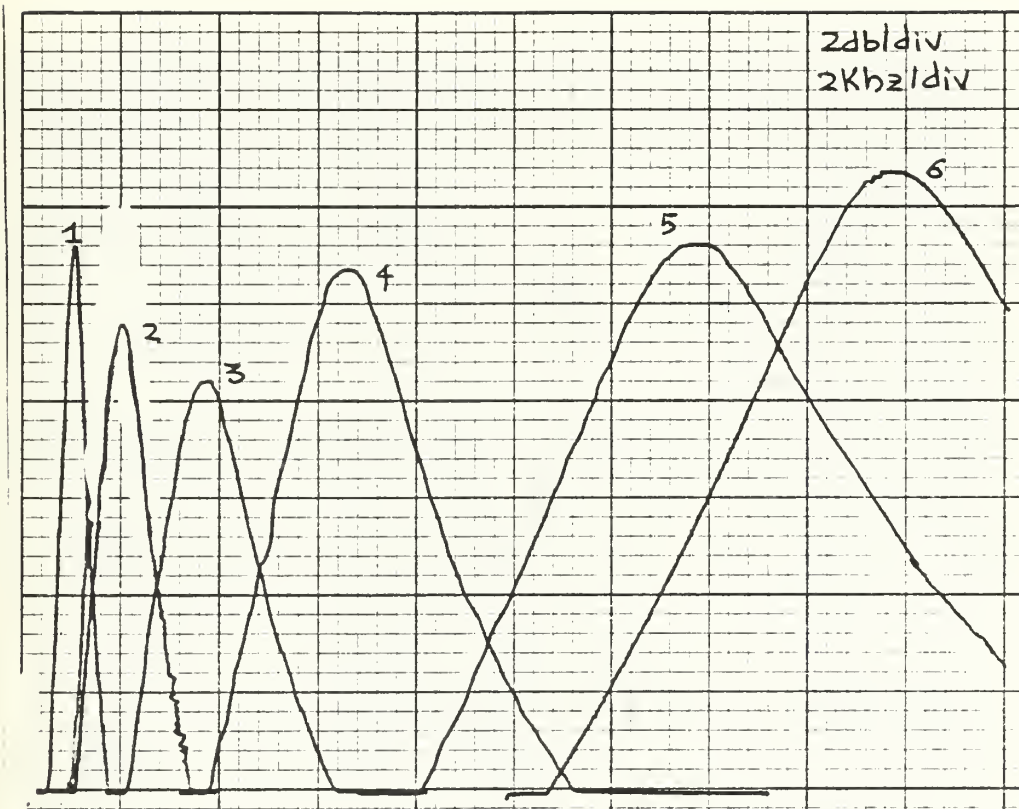
1. Phase
2. Amplitude

Fig. 5.18 - HPF Phase/Amplitude Response
($Q=2$)



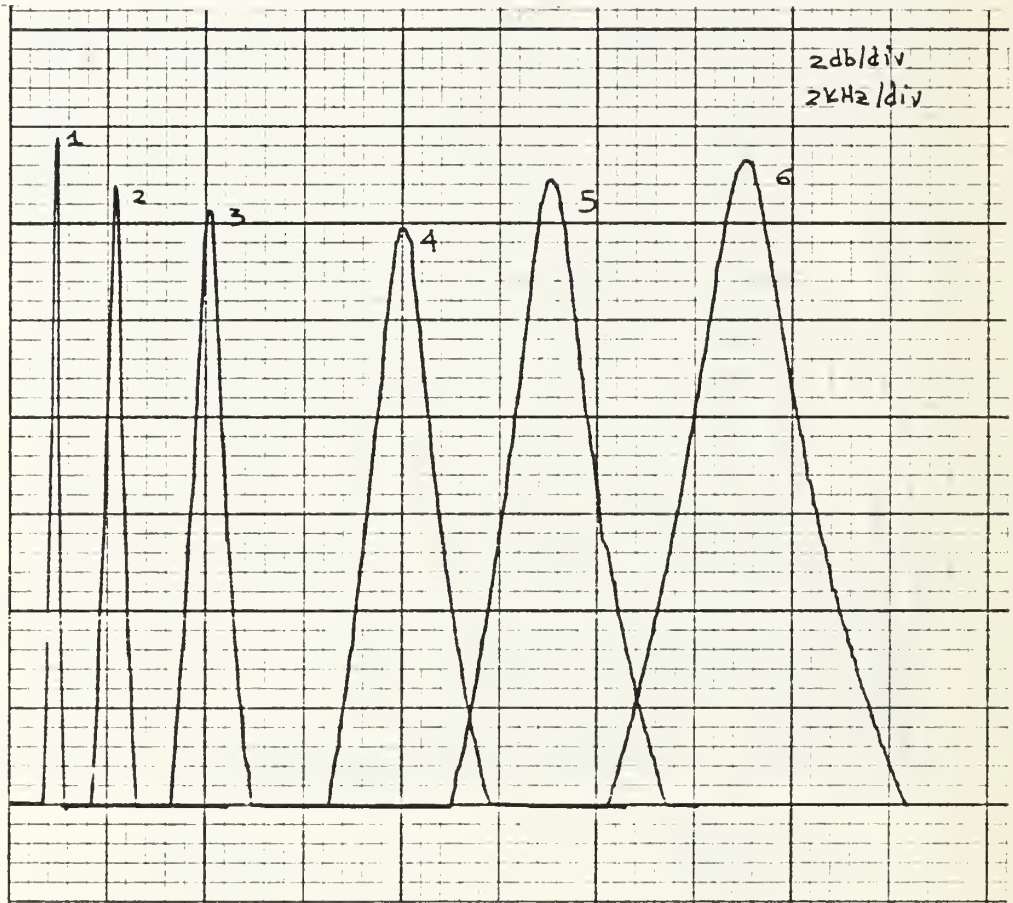
1. Phase
2. Amplitude

Fig. 5.19 - HPF Amplitude Response (Q=2)



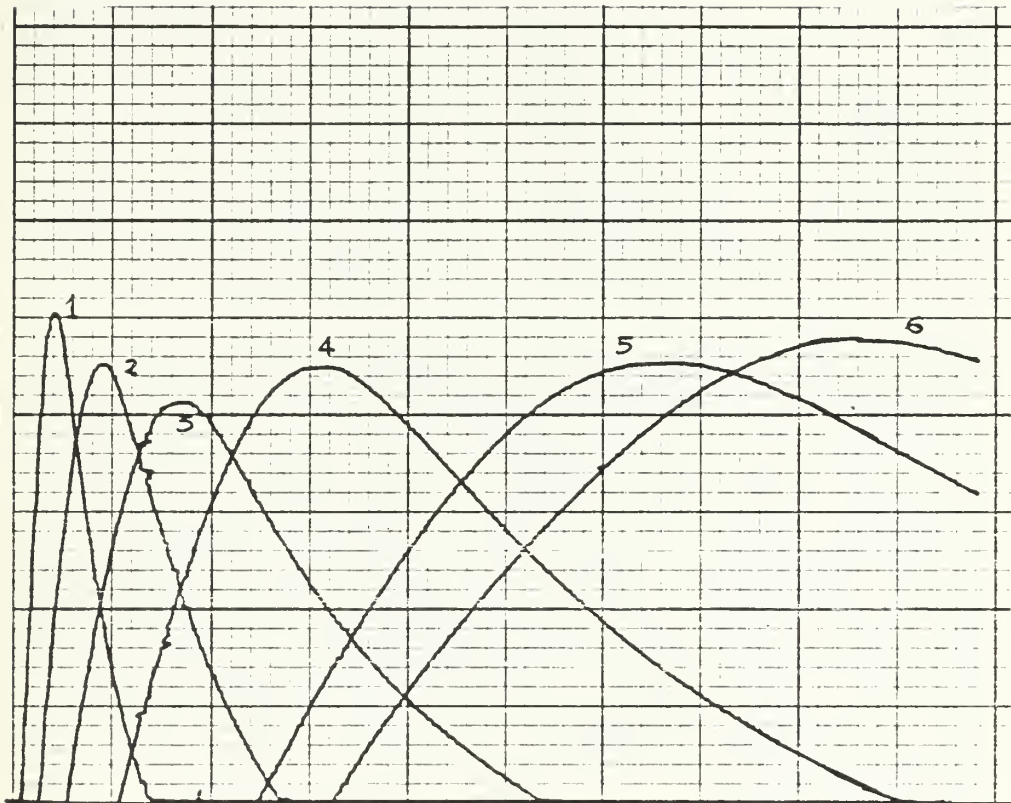
- | | |
|--------------------------|--------------------------|
| 1 - $f = 0.99\text{kHz}$ | 4 - $f = 6.65\text{kHz}$ |
| 2 - $f = 1.99\text{kHz}$ | 5 - $f = 10.5\text{kHz}$ |
| 3 - $f = 3.8\text{kHz}$ | 6 - $f = 15.1\text{kHz}$ |

Fig. 5.20 - BPF Amplitude Response
($R=1.6k$), $Q=10$



- | | |
|----------------|-----------------|
| 1. $f = 0.99K$ | 4. $f = 7.96K$ |
| 2. $f = 1.99K$ | 5. $f = 11.2 K$ |
| 3. $f = 3.8K$ | 6. $f = 15.1 K$ |

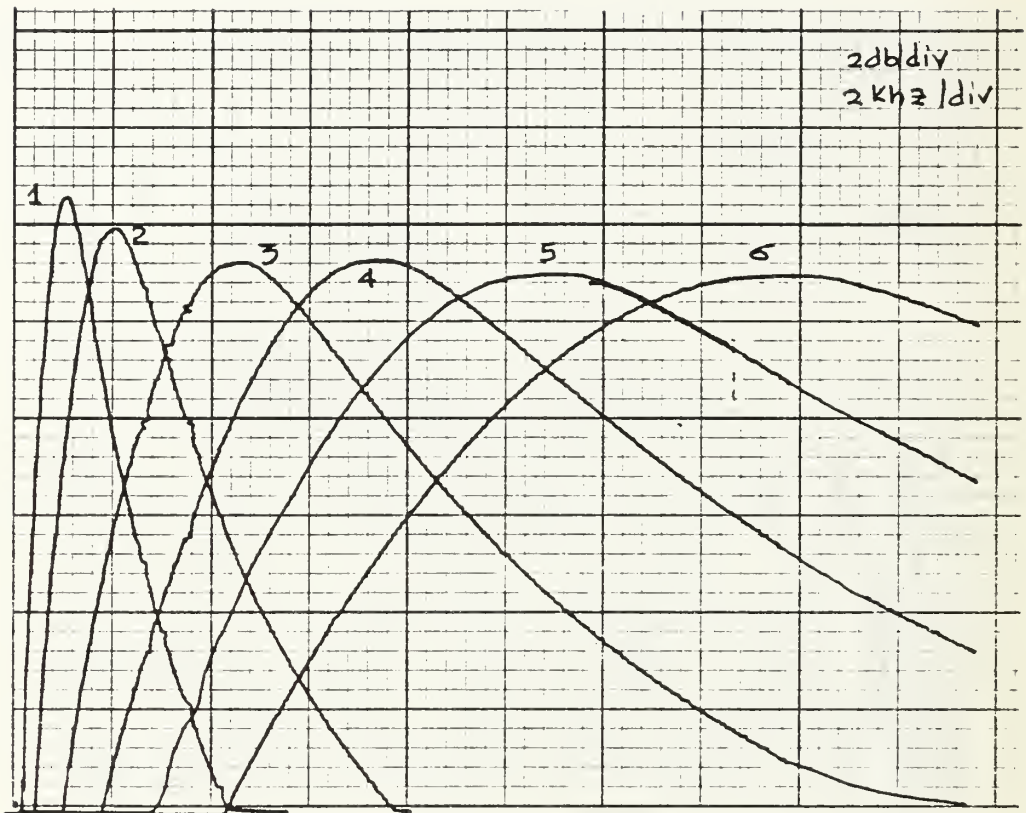
Fig. 5.21 - BPF Amplitude Response
($R=1.6k$), $Q=10$



- 1. 0.99khz
- 2. 1.99khz
- 3. 3.8 khz

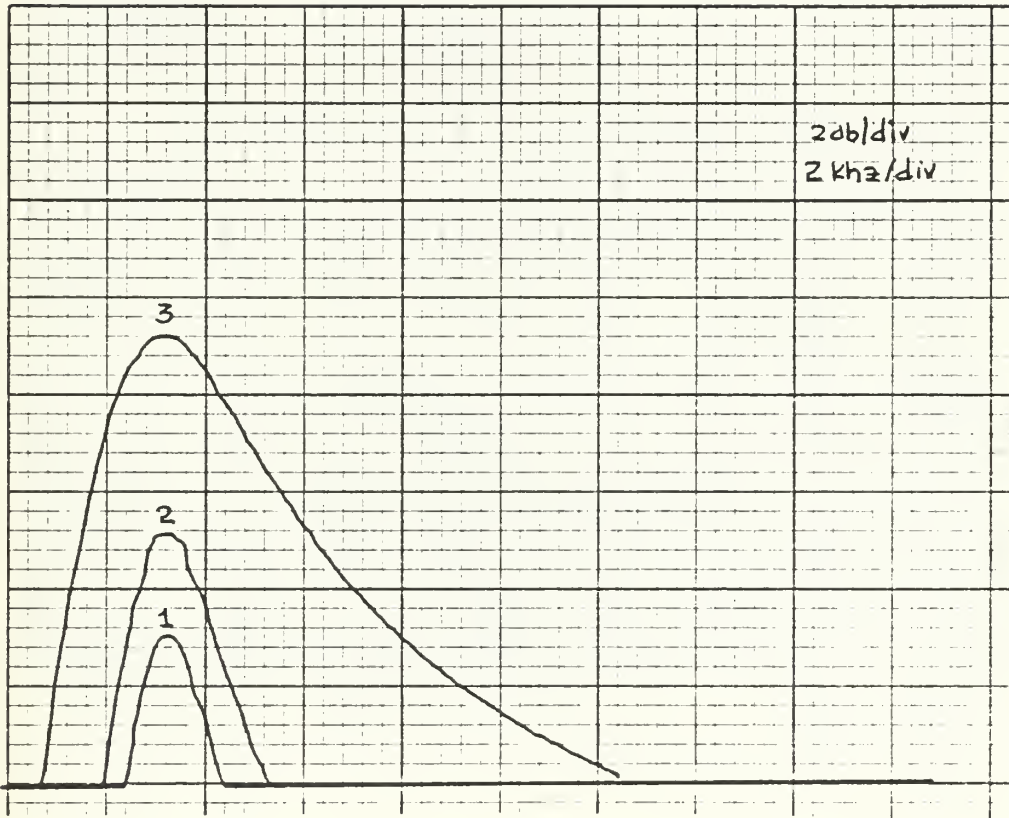
- 4. 6.65khz
- 5. 12.8khz
- 6. 15.1khz

Fig. 5.22 - BPF Amplitude Response
 (R=1.6k), Q=7



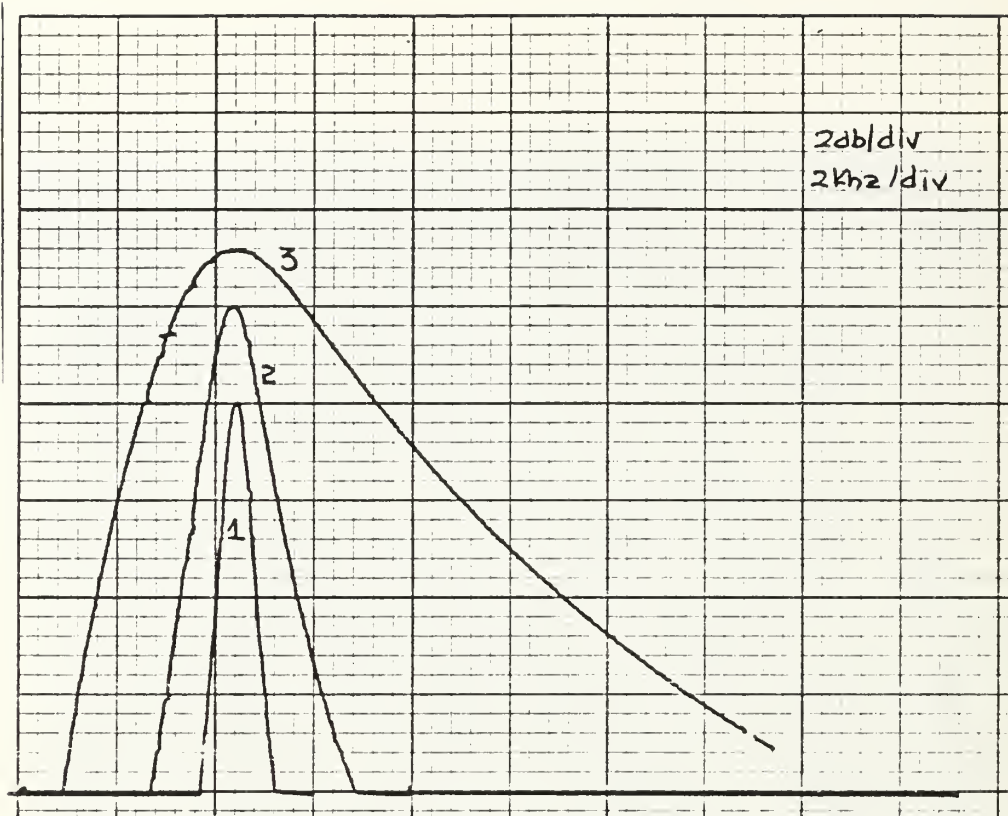
- | | |
|------------|------------|
| 1. 0.99khz | 4. 7.96khz |
| 2. 1.99khz | 5. 12.8khz |
| 3. 3.83khz | 6. 15. khz |

Fig. 5.23 - BPF Amplitude Response
($R=1.6k$), $Q=1$



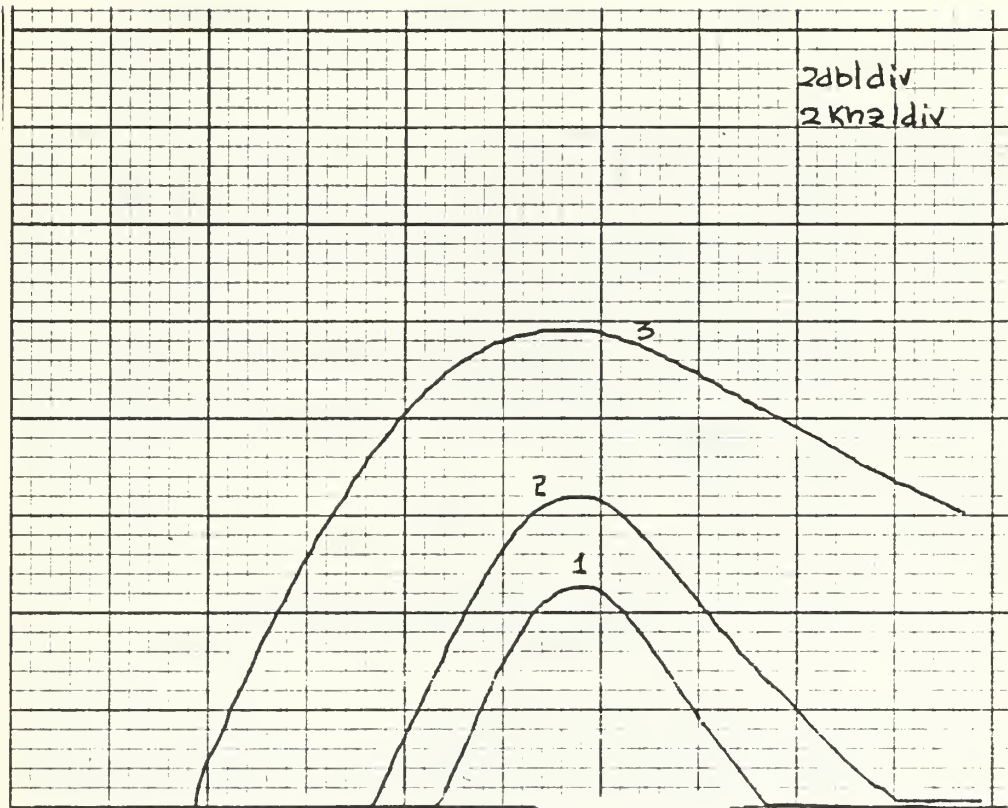
- 1 - $Q = 10.0$
- 2 - $Q = 4.0$
- 3 - $Q = 1.0$

Fig. 5.24 - BPI Amplitude Response
($R=1.6k$), $f=3.83kHz$



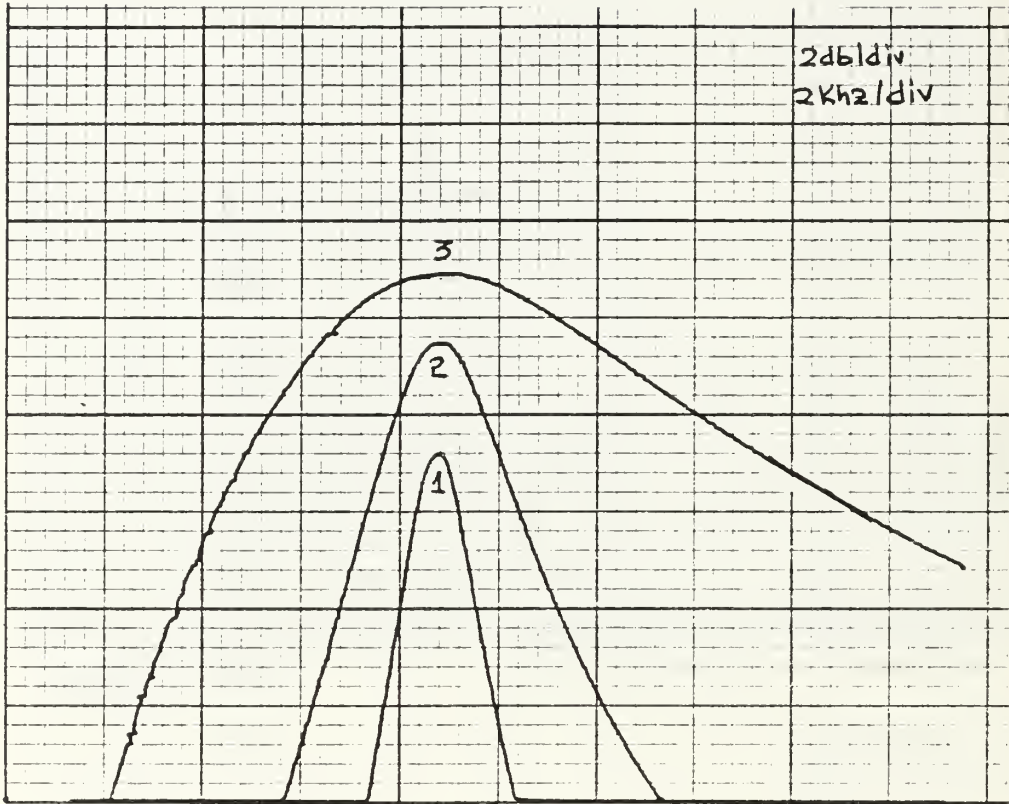
- 1 - $Q = 10.0$
- 2 - $Q = 4.0$
- 3 - $Q = 1.0$

Fig. 5.25 - BPI Amplitude Variation
($R=1.6k$), $f=3.83kHz$



- 1 - $Q = 10.0$
- 2 - $Q = 4.0$
- 3 - $Q = 1.0$

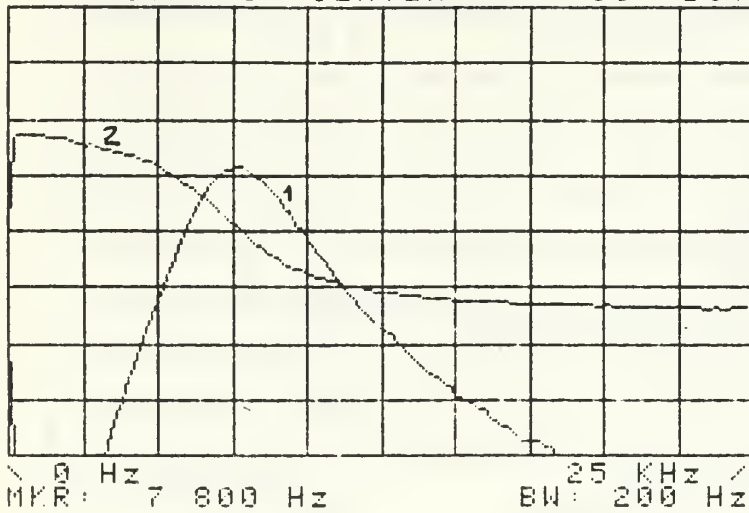
Fig. 5.26 - BPF Amplitude Response
($R=1.6k$)



- 1 - $Q = 10$
- 2 - $Q = 4$
- 3 - $Q = 1$

Fig. 5.27 - BPF Amplitude Response
($R=1.6k$), $f=9.khz$

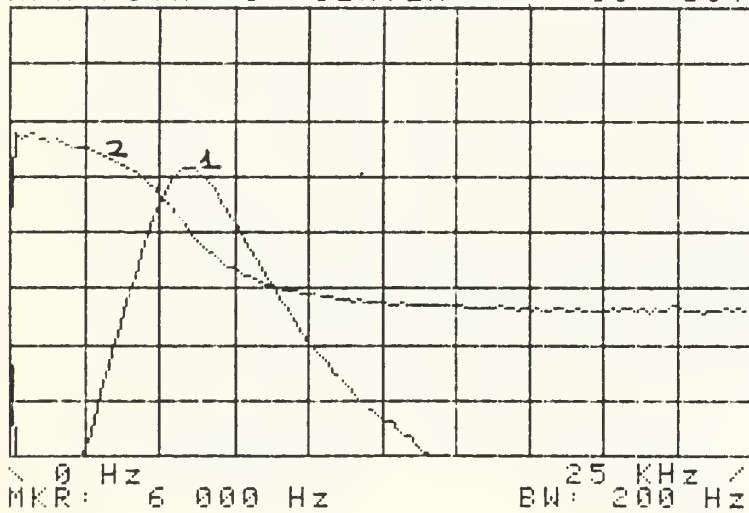
XFR FCTN MKR: 4.3dB 2 dB/DIV
XFR FCTN: 0° CENTER 50°/DIV



(a)

1. Phase Response
2. Amplitude Response

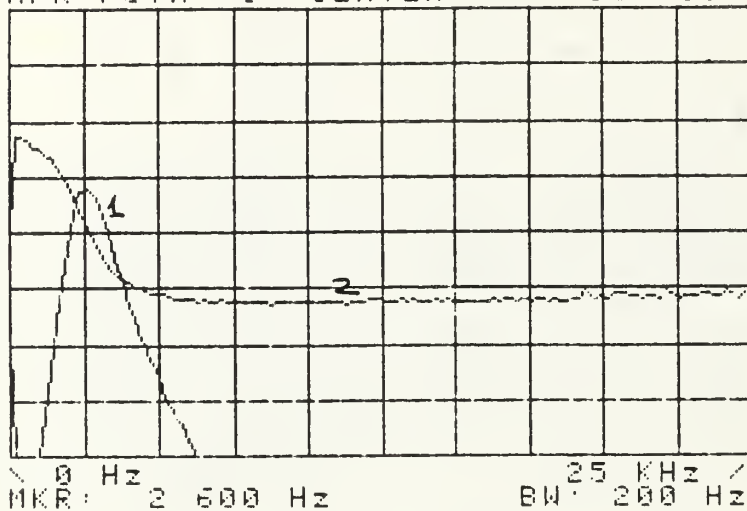
XFR FCTN MKR: 4.3dB 2 dB/DIV
XFR FCTN: 0° CENTER 50°/DIV



(b)

Fig. 5.8 - BPF Phase/Amplitude Response

XFR FCTN MKR: 3.6dB 2 dB/DIV
XFR FCTN: 00 CENTER 500/DIV



1. Phase Response.
2. Amplitude Response.

XFR FCTN MKR: 1.8dB 2 dB/DIV
XFR FCTN: 00 CENTER 500/DIV

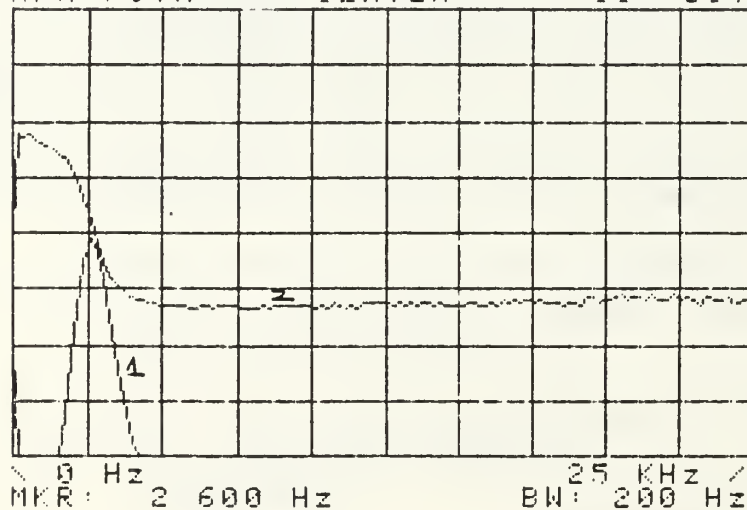
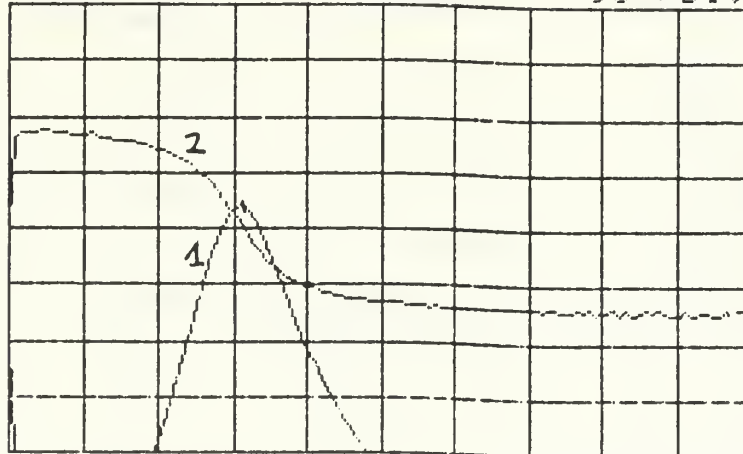


Fig. 5.29 - BPI Phase/Amplitude Response

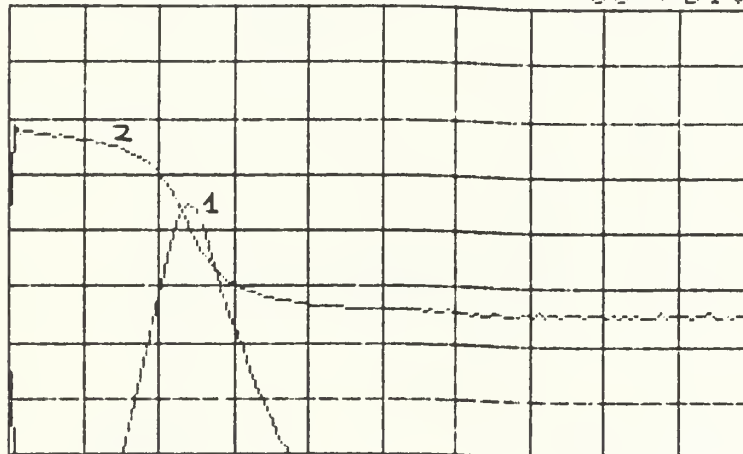
XFR FCTN MKR: 2.0dB 2 dB/DIV
XFR FCTN: 00 CENTER 500/DIV



0 Hz 25 KHz /
MKR: 7 000 Hz BW: 200 Hz

1. Phase Response.
2. Amplitude Response.

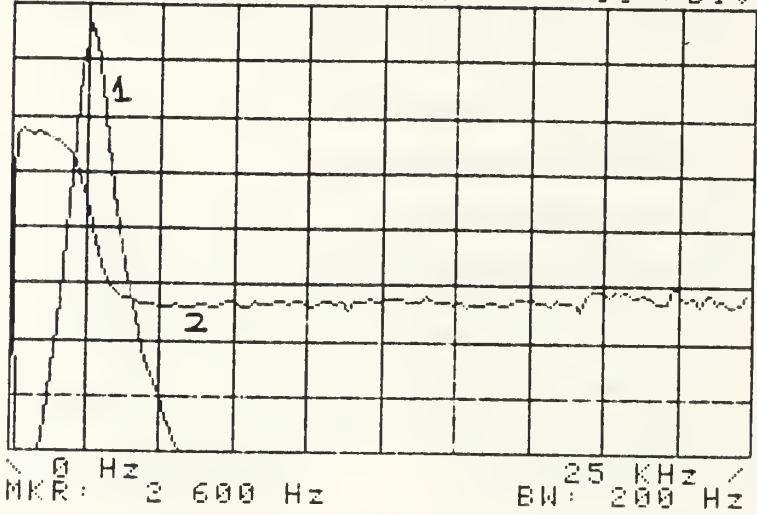
XFR FCTN MKR: 2.0dB 2 dB/DIV
XFR FCTN: 00 CENTER 500/DIV



0 Hz 25 KHz /
MKR: 6 000 Hz BW: 200 Hz

5.30 - BPF Phase/Amplitude Response.

XFR FCTN MKR: - .8dB 2 dB/DIV
XFR FCTN: 0° CENTER 500/DIV



- 1. Phase Response.
- 2. Amplitude Response.

XFR FCTN MKR: OFF SCALE 2 dB/DIV
XFR FCTN: 0° CENTER 500/DIV

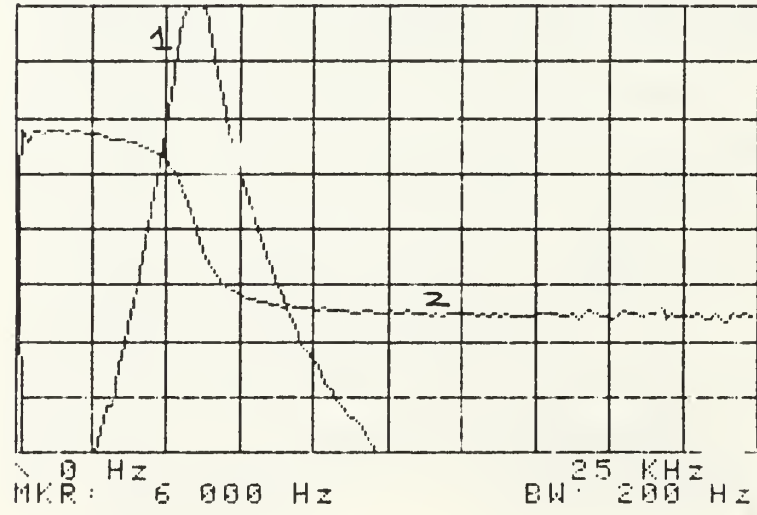
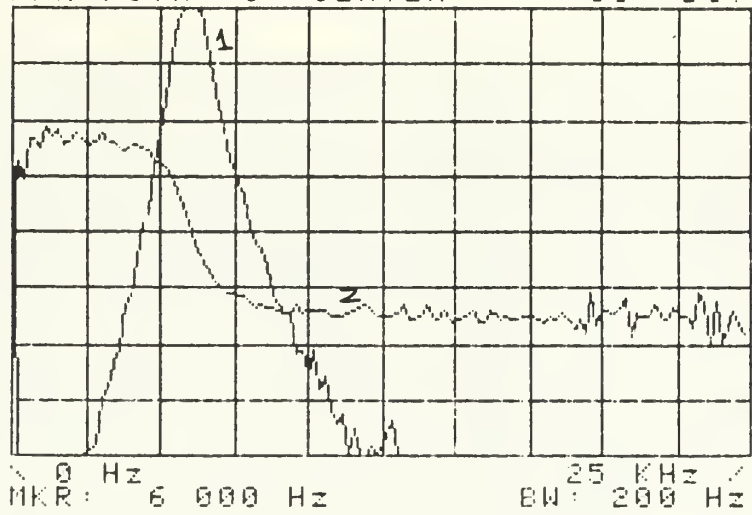


Fig. 5.31 - BPF Phase/Amplitude Response

XFR FCTN MKR: OFF SCALE 2 dB/DIV
XFR FCTN: 0° CENTER 50°/DIV



- 1. Phase Response.
- 2. Amplitude Response.

XFR FCTN MKR: OFF SCALE 2 dB/DIV
XFR FCTN: 0° CENTER 50°/DIV

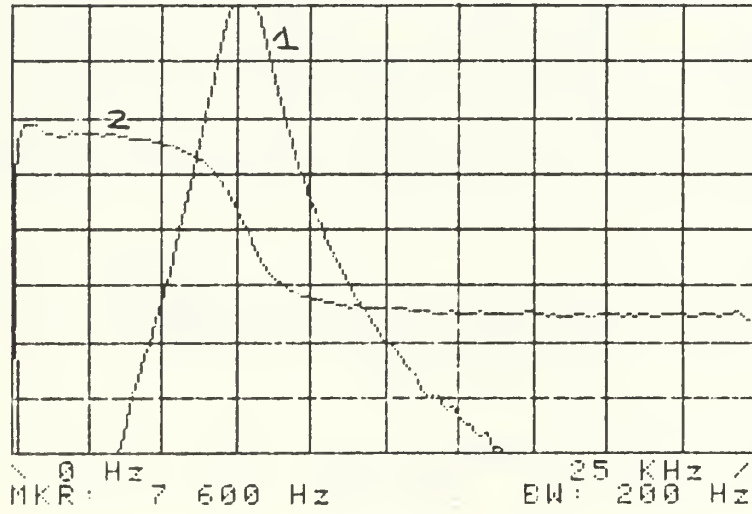


Fig. 5.32 - BPF Phase/Amplitude Response

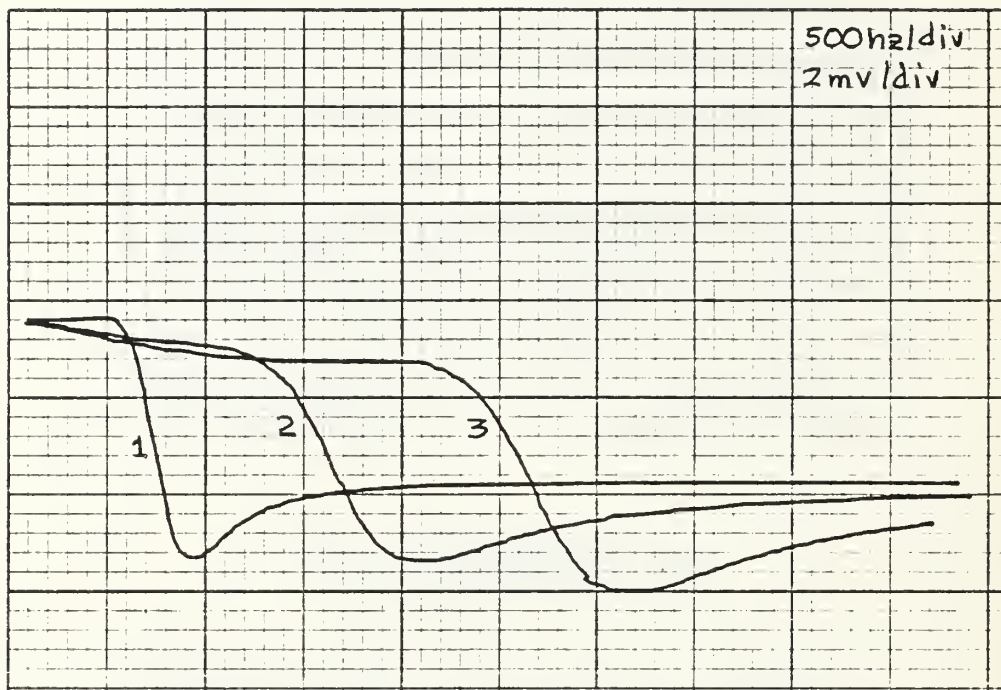
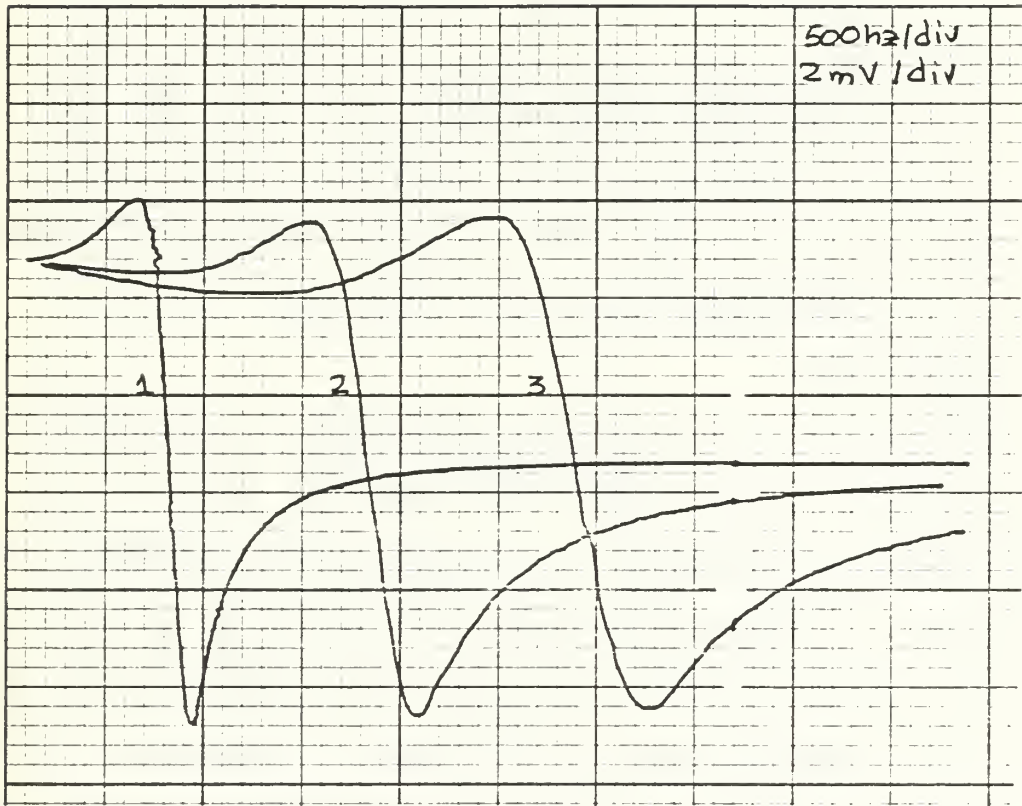


Fig. 5.33 - Notch Amplitude Response
 (R=1.6k), Q=4



- 1 - f = 0.99khz
- 2 - f = 1.99khz
- 3 - f = 3.83khz

Fig. 5.34 - Notch Amplitude Response
(R=1.6k)

illustrate the amplitude response for different frequencies and for $Q=4$, while Figs. (5.35) and (5.36) illustrate the amplitude response for $f=1\text{KHZ}$ and a variety of Q_s . Fig. (5.37) illustrate the phase response in addition to the amplitude one.

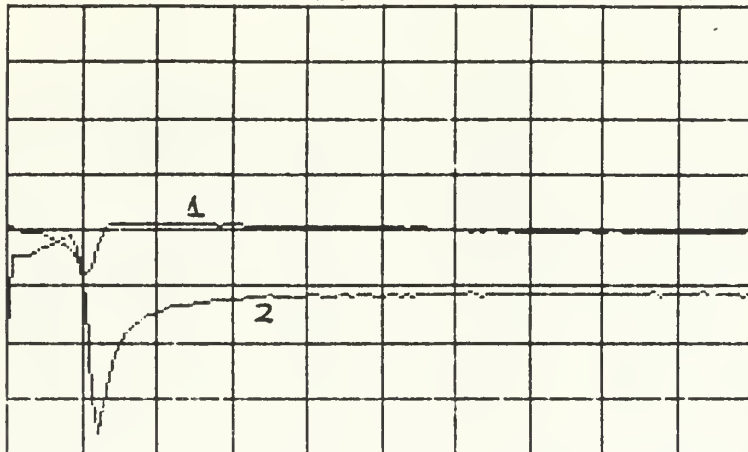
5. All Pass (AP) Realization

The topology-control bitword 100 realizes the All-Pass filter. Figs (5.38), (5.39) and (5.40) illustrate the plotted amplitude and phase responses.

B. CONCLUSION

The constructed circuit performed as predicted by the theoretical analysis and the computer simulations. This means that it realized all the desired filtering transfer functions LP, HP, BP, N, and AP. The effect of interference of the control switches nonideal performances which is more severe at high Q_s can be minimized by increasing the values of R (meaning that the values of R_q also increases and the values of C_s decreases).

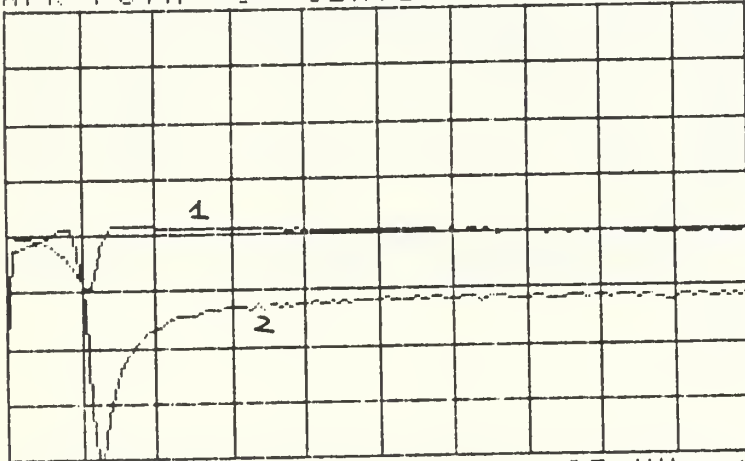
XFR FCTN MKR: - 5.2dB 2 dB/DIV
XFR FCTN: 0° CENTER 500°/DIV



0 Hz 25 KHz /
MKR: 3 000 Hz BW: 200 Hz

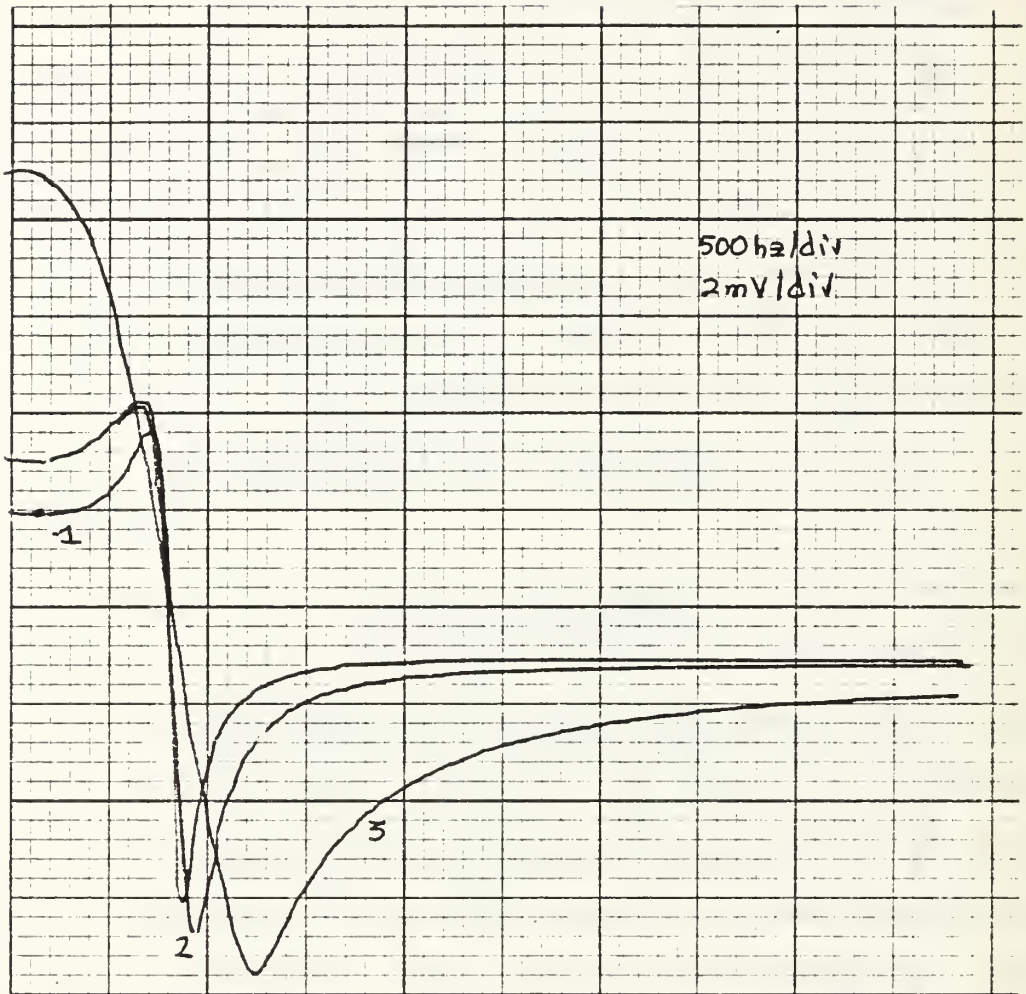
1. Phase Response.
2. Amplitude Response.

XFR FCTN MKR: OFF SCALE 2 dB/DIV
XFR FCTN: 0° CENTER 500°/DIV



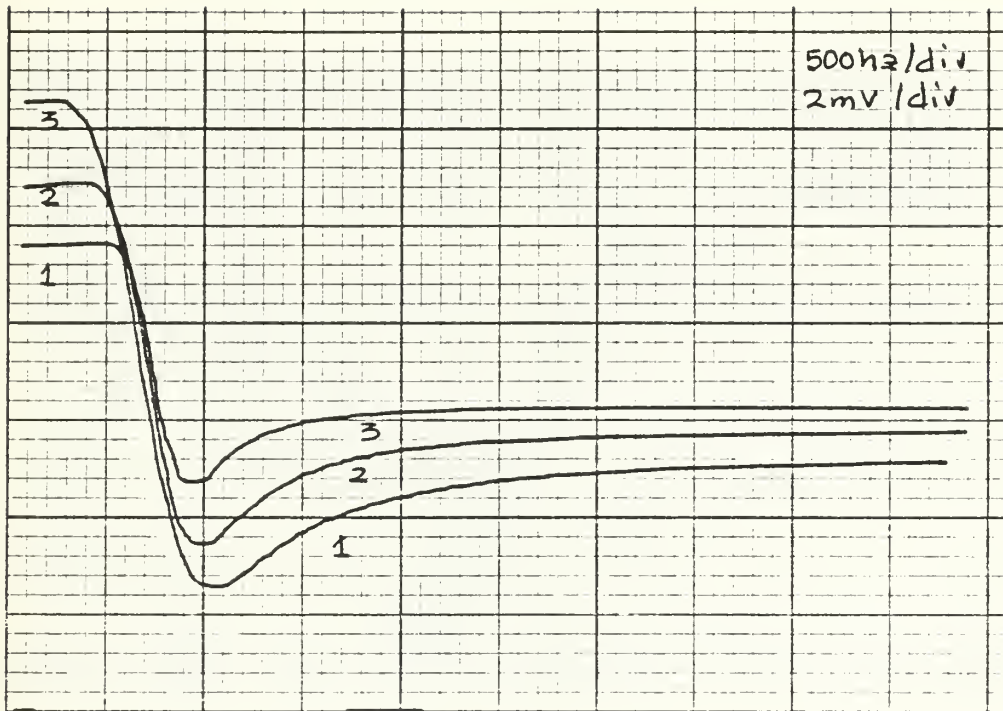
0 Hz 25 KHz /
MKR: 3 000 Hz BW: 200 Hz

Fig. 5.35 - Notch Phase/Amplitude Response
f=2.8kHz
(a) Q=7.5 (b) Q=5



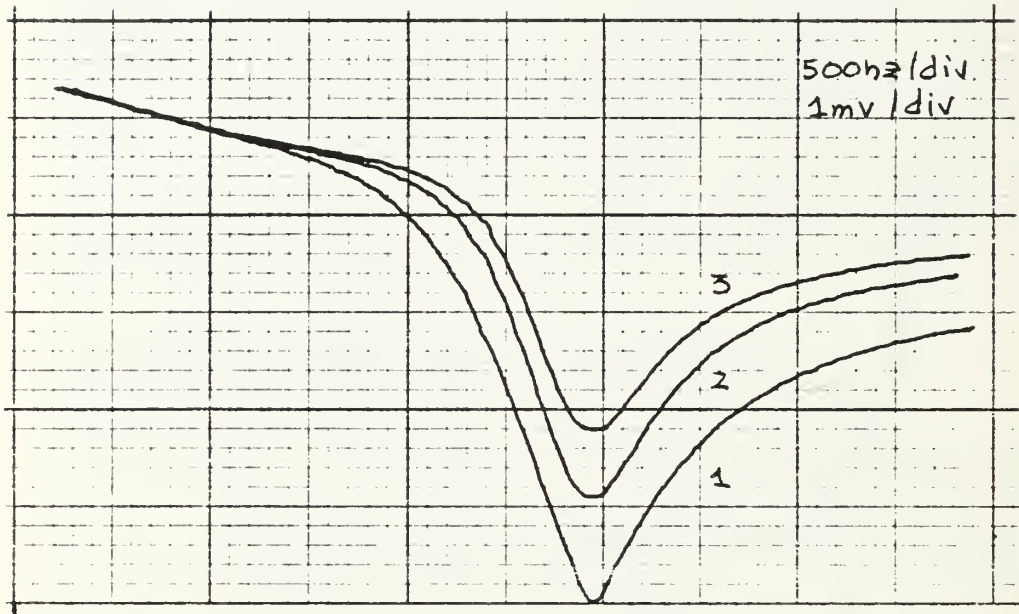
- 1 - Q = 2.0
- 2 - Q = 4.0
- 3 - Q = 8.0

Fig. 5.36 - Notch Amplitude Response
(R=1.6k), f=0.99khz



- 1 - $Q = 2.0$
- 2 - $Q = 4.0$
- 3 - $Q = 8.0$

· Fig. 5.37 - Notch Amplitude Response
($R=1.6k$), $f=0.99kHz$



- 1 - $Q = 4.0$
- 2 - $Q = 8.0$
- 3 - $Q = 12.0$

Fig. 5.38 - APF Amplitude Response
($R=1.6k$), $f=2.8kHz$

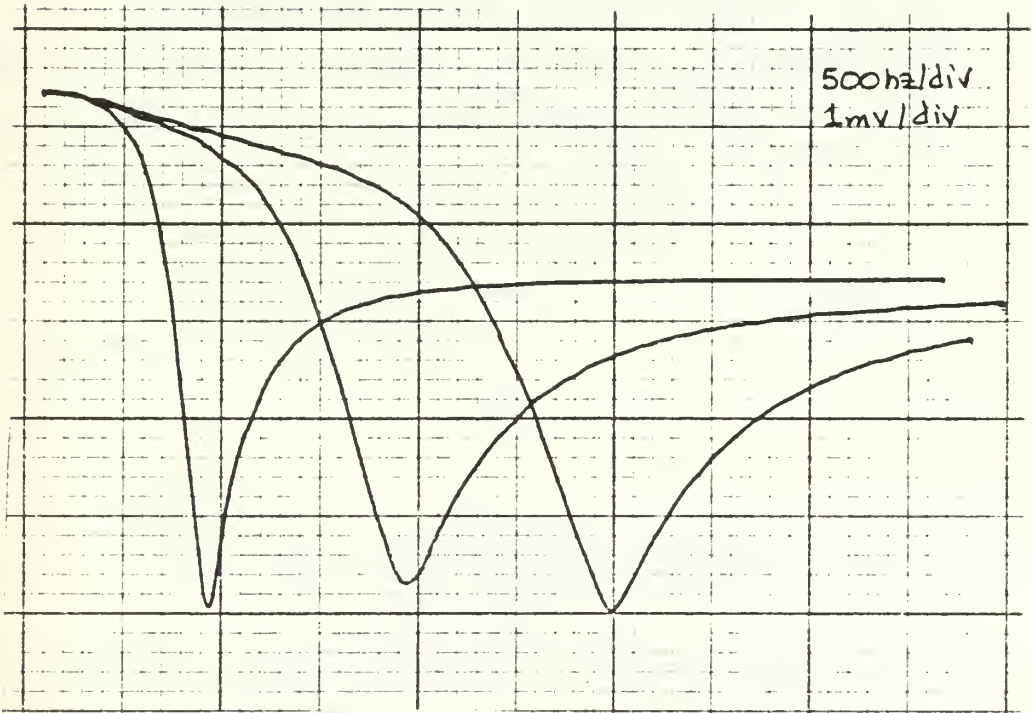
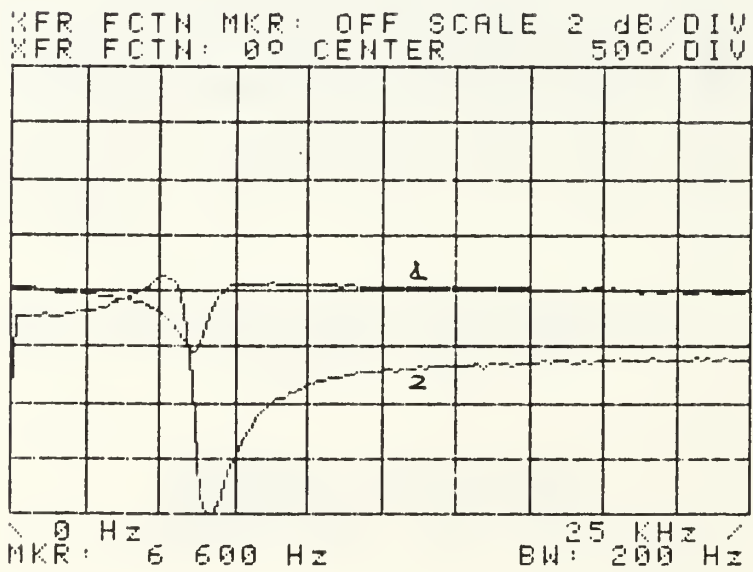
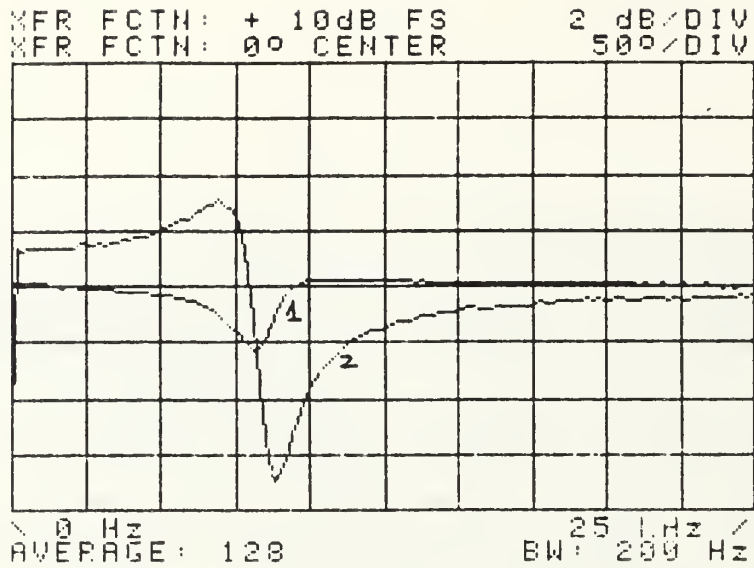


Fig. 5.39 - APF Amplitude Response
($R=1.6k$) for $f=0.99\text{kHz}$,
 $f=1.99\text{kHz}$, and $f=2.8\text{kHz}$



1. Phase.
2. Amplitude

Fig. 5.40 - APF Phase/Amplitude Response (Q=7.5)

VI. COMBINING HIGHER ORDER SECTIONS

By cascading two or more programmable filters, higher order transfer functions can be obtained. Fig. (6.1) illustrates two cascaded GIC programmable filters.

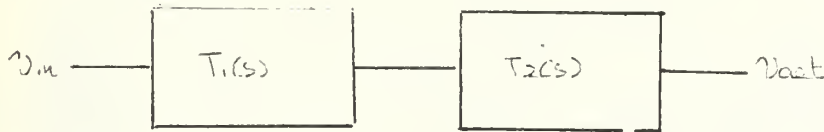


Fig. (6.1) Two Cascaded GIC Programmable Filters.
(Each Black box Stands for the Network
of Fig. (3.10))

25 different combinations of the two individual transfer functions $T_i(s)$ and $T_j(s)$ can be obtained as it is indicated in Table (4.3).

For Lp-LP combination and for ideal theoretical case ($A_1=A_2 \rightarrow \infty$) a fourth order low pass filter can be obtained with transfer function:

$$T_2(s) = \frac{\omega_p^4}{s^2 + \frac{\omega_p}{Q_p} s + \omega_p^2} \quad (6.1)$$

The computer simulation of the fourth order transfer function of a nonideal theoretical filter vs. the second order case is illustrated at Fig. (6.2). The experimental results taken from the properly designed and built circuit as illustrated in Fig. (6.3) are shown in Fig. (6.4).

Using the same procedure as above a fourth order HP-HP combination for the ideal theoretical response is given by

$$T_1(s) = 4 \frac{s^4}{\left\{ \omega_p^2 + \frac{\omega_p}{Q_p} s + s^2 \right\}^2} \quad (6.2)$$

which at ω_p takes the complex value of

$$T_1(j\omega_p) = -4jQ_p^2 \quad (6.3)$$

with magnitude of

$$|T_1(j\omega_p)| = 4Q_p^2 = 40 \log(2Q_p), \text{db} \quad (6.4)$$

Fig. (6.5) illustrates the fourth order nonideal theoretical HP filter response vs. the second order one. Both at $Q_p=2$ and $f_p=8\text{KHz}$, while fig. (6.6) illustrates the experimental responses. For $Q_p=2$ according to (6.4) and

L.P.F AMPL. RESPONSE(Q=2/F=4K)

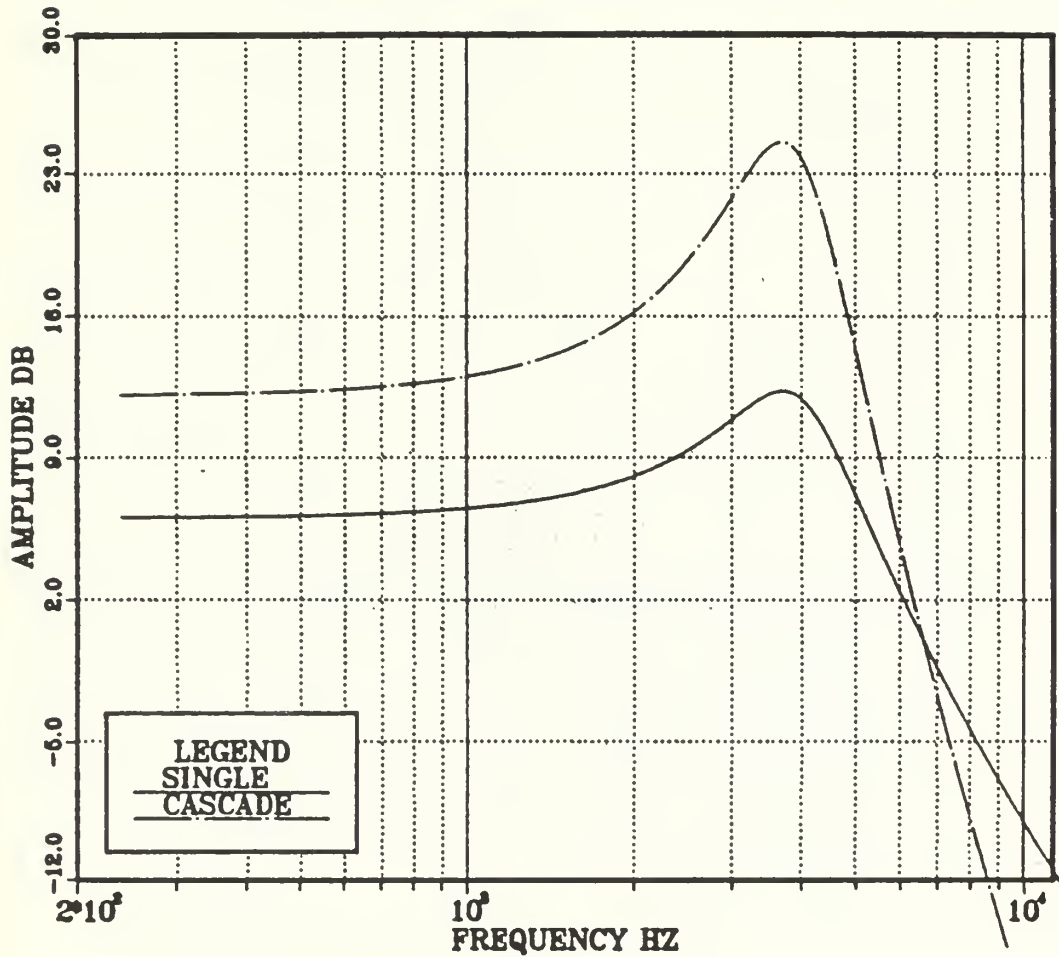


Fig. 6.2 - LPF Fourth Order vs. Second Order
Ideal Response from Computer Simulation.

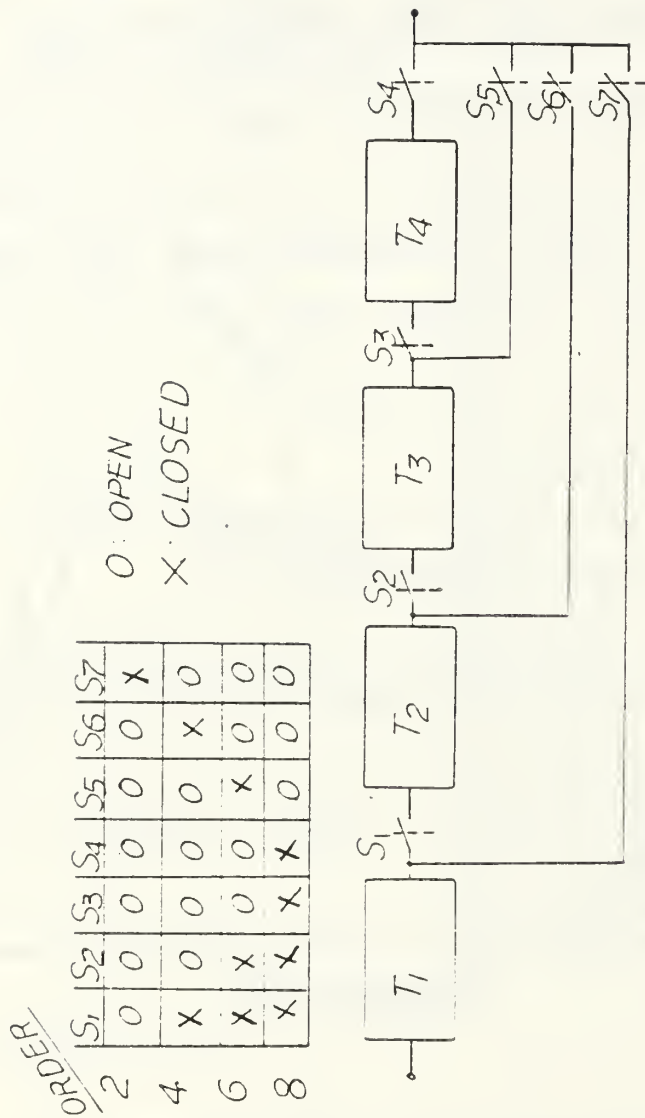
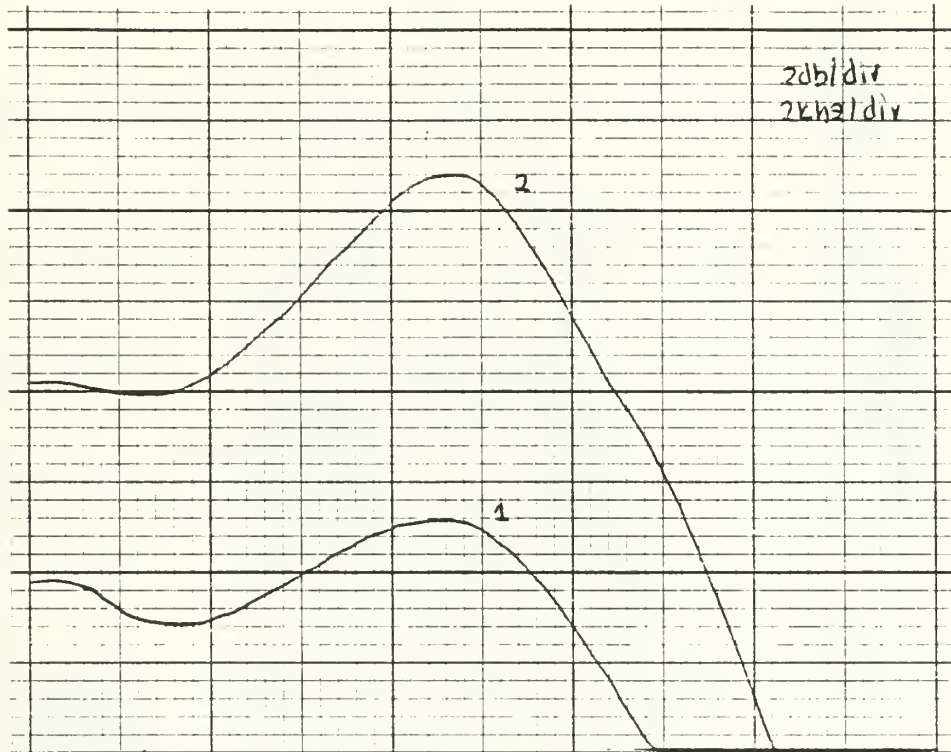


Fig. 6.3 - Network with Logic for Realizing n_p to 8th Order LP, HP, BP, N, and AP Transfer Functions.



1. Single
2. Cascade

Fig. 6.4 - 4th Order vs. 2nd Order
Experimental LPF Response
($Q=2$)

H.P.F AMPL.RESPONSE(Q=2/F=4K)

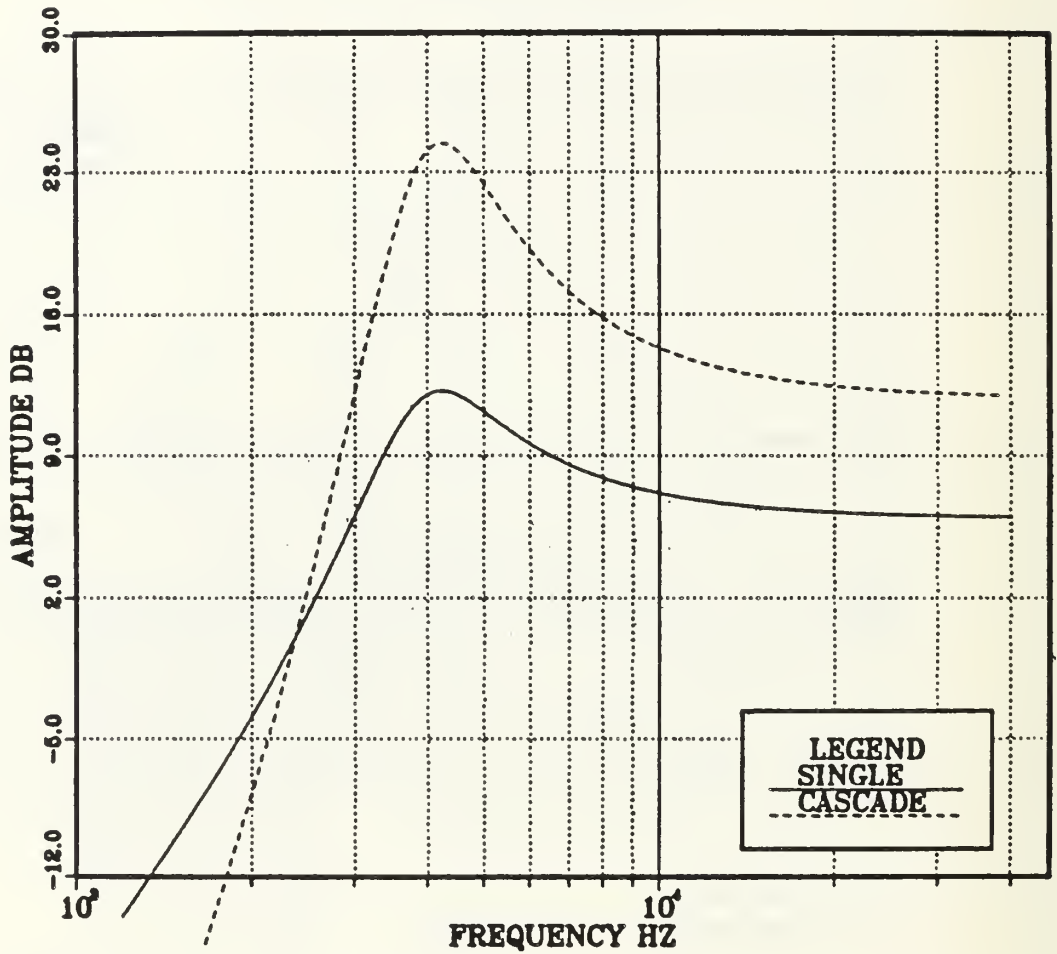


Fig. 6.5 - "Ideal" 4th vs. 2nd Order HPS Responses From Computer Simulation.

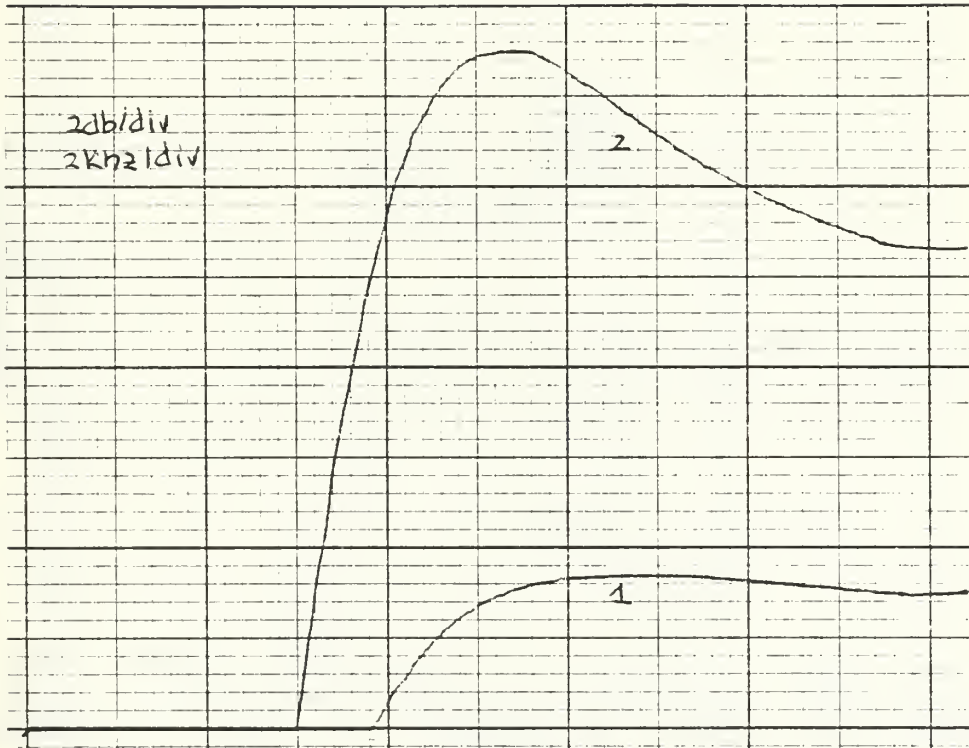


Fig. 6.6 - 4th Order vs. 2nd Order HPF obtained Responses from the Constructed Circuit.

(2.4) a difference of 12dB were expected between the second and fourth order filter which is approximately the case in both computer simulation and experimental results.

The BP-Bp combination leads to the theoretical "ideal" fourth order transfer function:

$$T_1(s) = 4 \frac{\left(\frac{\omega_p}{\phi_p}\right)^2 s^2}{\left\{s^2 + \frac{\omega_p}{\phi_p} s + \omega_p^2\right\}^2} \quad (6.5)$$

which takes the following value at ω_p :

$$T_1(j\omega_p) = 4 = 12\text{db} \quad (6.6)$$

According to this, a magnitude response of 12 dB approximately at ω_p , was expected from both experimental and computer simulation results. Fig. (6.7) illustrates the simulated response of a fourth order nonideal HP filter vs. a second-order one. A difference of 5.8 dB instead of 6 dB can be observed. Fig. (6.8) illustrates the experimental response, where a difference of 5.4 dB appears basically due to the interference of the control switches and the nonideally matched values of the capacitors which control the fp selection.

B.P.F AMPL. RESPONSE(Q=4/F=8K)

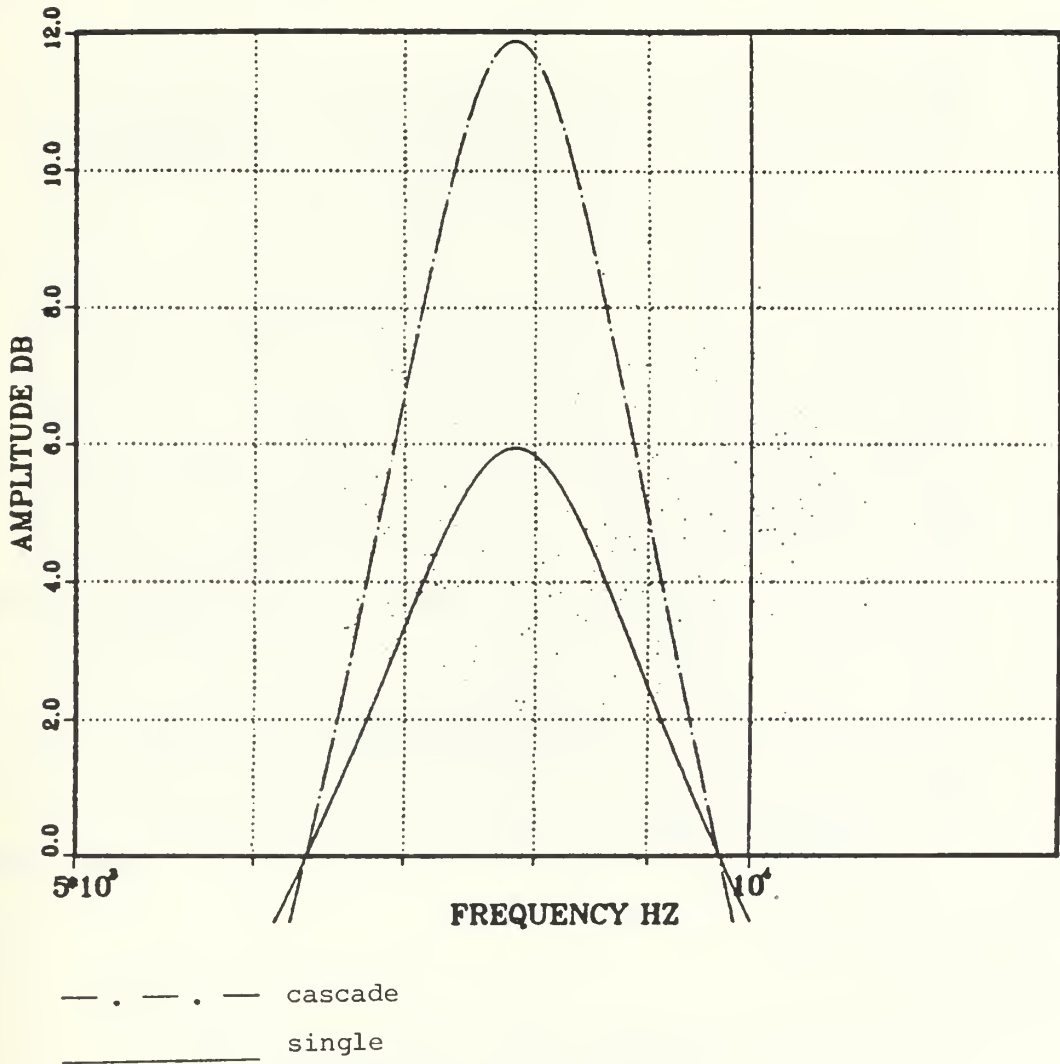


Fig. 6.7 - Fourth Order vs. Second Order BPF Amplitude Responses from Computer Simulation.

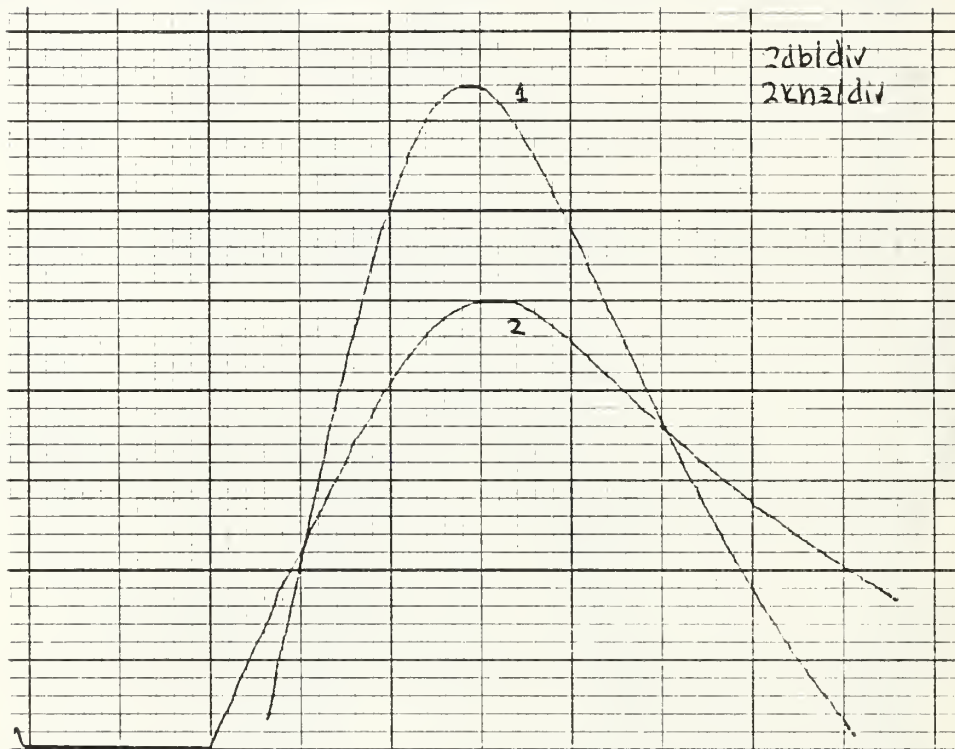


Fig. 6.8 - Fourth vs. Second Order BPF Responses Obtained from the Constructed Circuit.

The N-N combination for the ideal theoretical case ($A_1=A_2 \rightarrow \infty$) results the following transfer function:

$$T_2(s) = \frac{(s^2 + \omega_n)^2}{\left\{ s^2 + \frac{\omega_p}{Q_p} s + \omega_p^2 \right\}^2} \quad (6.7)$$

where ω_n is the Notch frequency.

Fig. (6.9) illustrates the fourth order "nonideal" Notch filter simulated response vs. the second order one.

The AP-AP combination for the theoretical ideal case result in the following transfer function:

$$T_1(s) = \frac{\left\{ s^2 - \frac{\omega_p}{Q_p} s + \omega_p^2 \right\}^2}{\left\{ s^2 + \frac{\omega_p}{Q_p} s + \omega_p^2 \right\}^2} \quad (6.8)$$

which takes the following values for $S=0$ and ∞ :

$$T_1(j0) = 1 \quad (6.9)$$

with amplitude and phase of

$$|T_1(j0)| = 1 = 0 \text{ db}, \quad \angle T_1(j0) = 360^\circ \quad (6.10)$$

N.F AMPLITUDE RESPONSE(Q=2./F=8K)

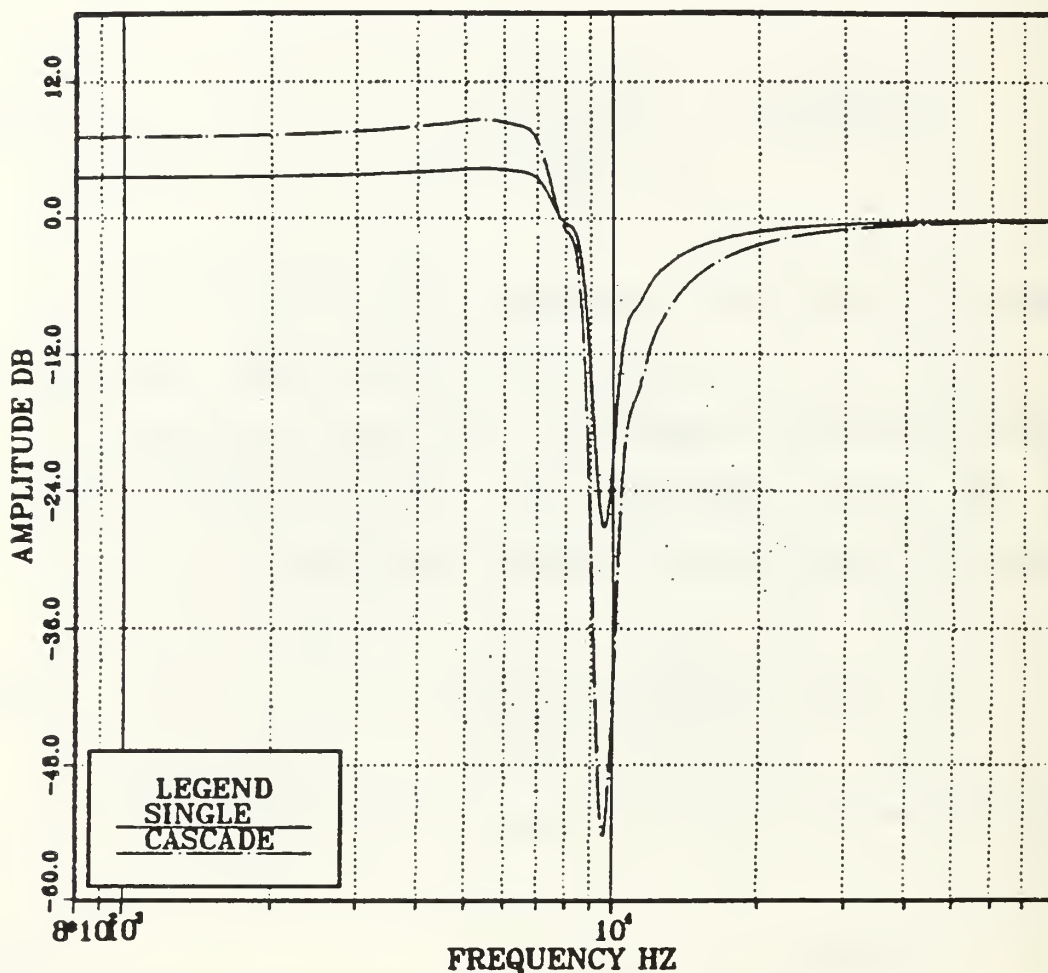


Fig. 6.9 - Fourth Order vs. Second Order Notch Filter Amplitude Response from Computer Simulation.

and

$$T_1(j\infty) = 2.25 \quad (6.11)$$

with amplitude and phase of

$$|T_1(j\infty)| = 7\text{db} , \quad \angle T_1(j\infty) = 0^\circ \text{db} \quad (6.12)$$

The computer simulation of nonideal fourth order all pass filter vs. a second order one which is illustrating at Fig. (6.10) matches the above.

Fig. (6.11) illustrates the resulting Chebychev filter from a BP-BP combination with $Q_p=4$ and different frequencies ($f_{p1}=8\text{KHZ}$ $f_{p2}=10\text{KHZ}$), while Figs. (6.12) and (6.13) illustrate the resulting Chebychev filters from the designed and built circuit. Fig. (6.14) illustrates the resulting response from a HP-LP combination.

A.P AMPLITUDE RESPONSE(Q=2)

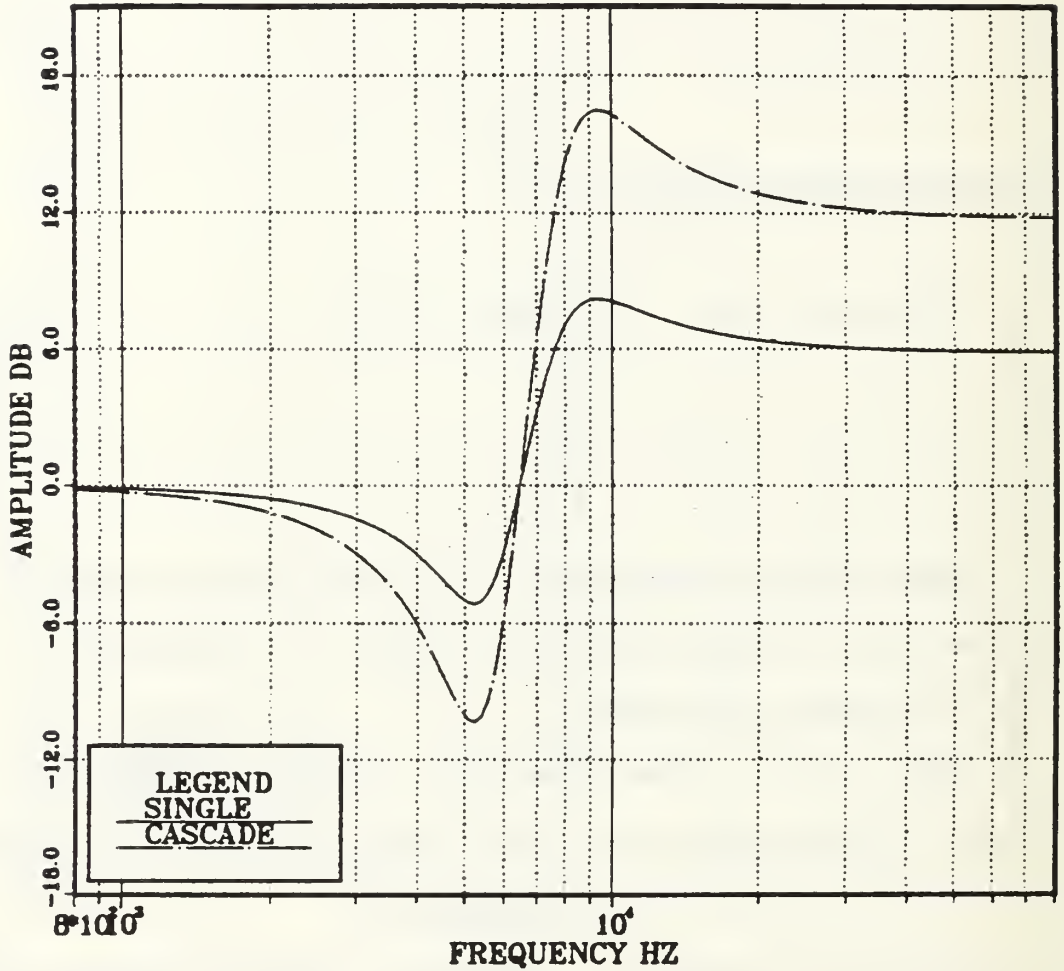


Fig. 6.10 - APF Fourth Order vs. Second Order Amplitude Response from Computer Simulation.

B.P.F AMPLITUDE RESPONSE(Q=4)

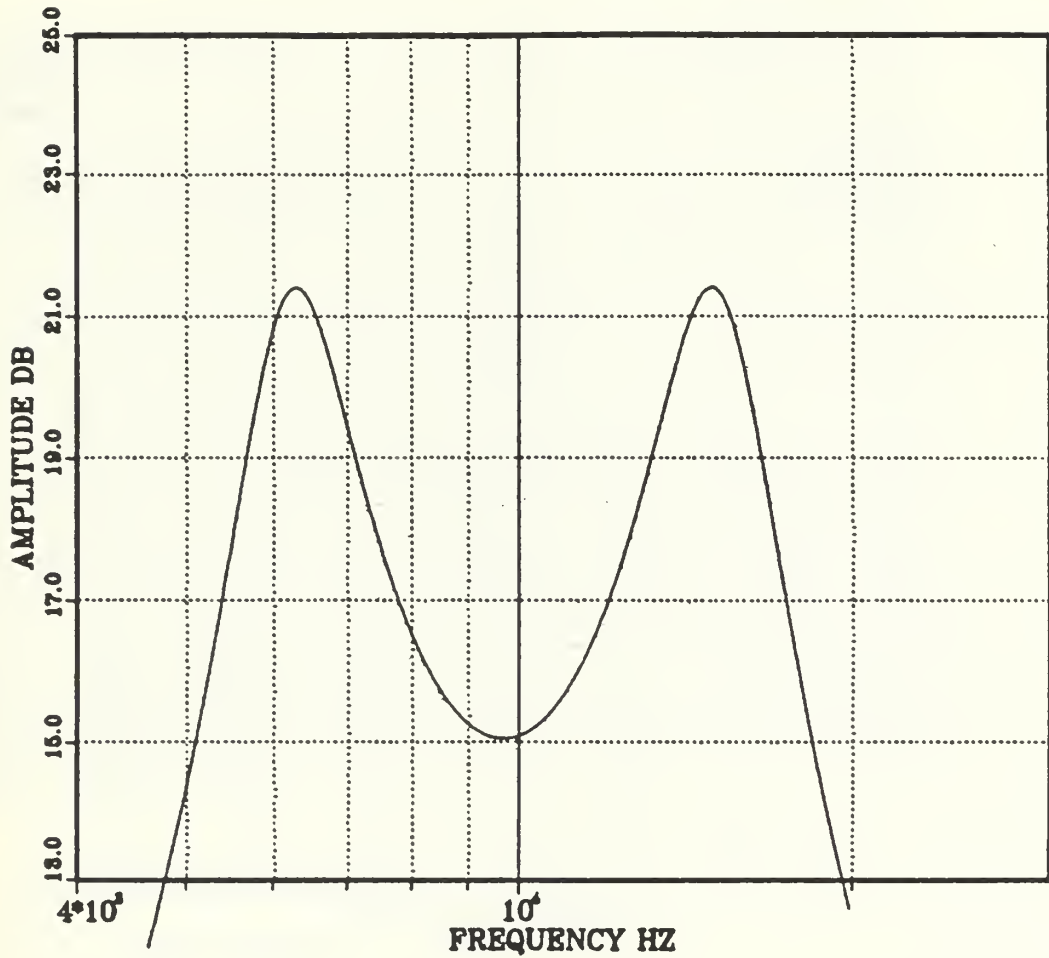


Fig. 6.11 - Chevycheb Response for $f_1=8k$,
 $f_2=10k$

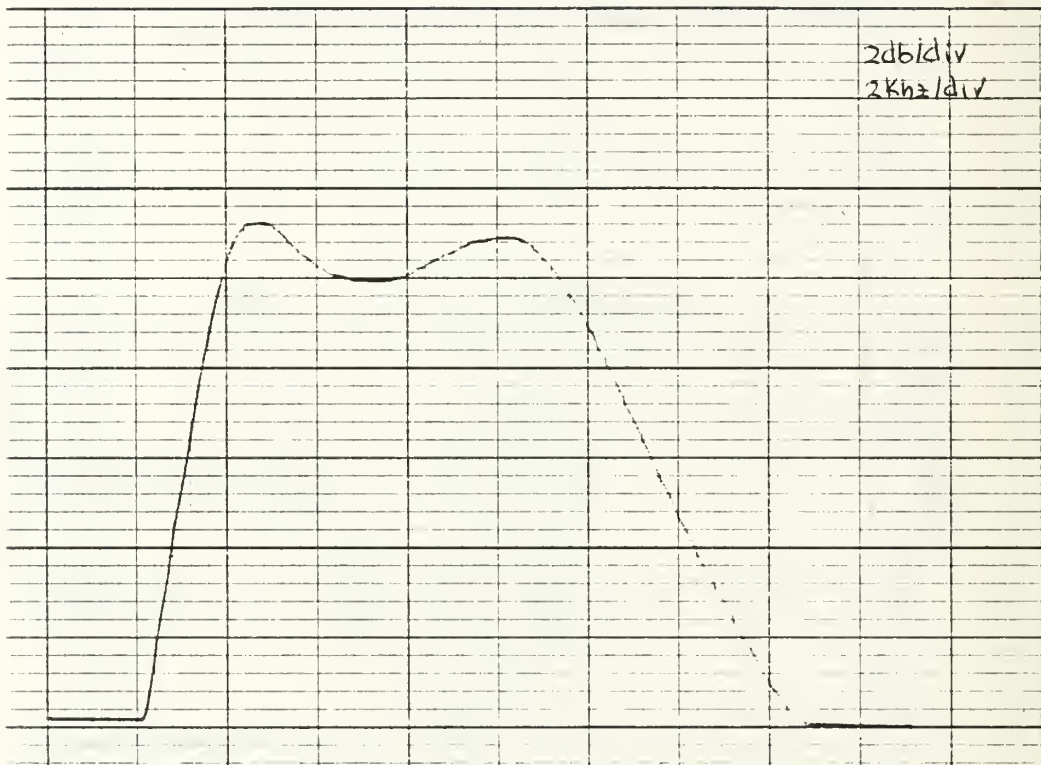


Fig. 6.12 - Chevychev Response Obtained by
Cascading BP-BP

$$f_1 = 6.65 \text{ kHz}$$

$$f_2 = 12.8 \text{ kHz}$$

$$Q_1 = 3$$

$$Q_2 = 3.5$$

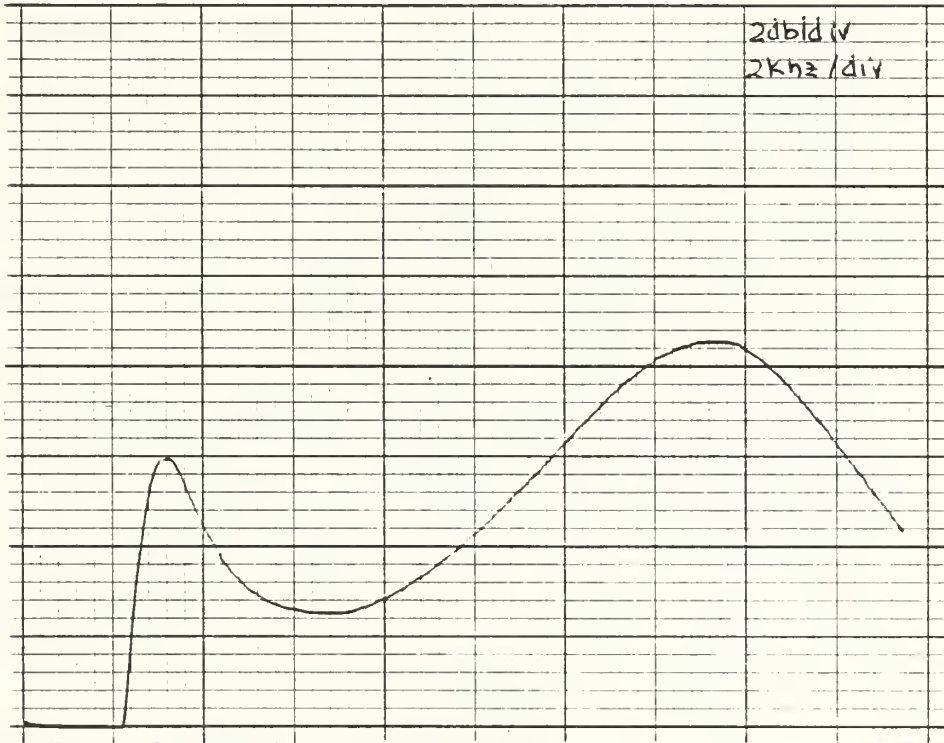


Fig. 6.13 - BP-BP Response $Q_1=Q_2=4$
($f_1=3\text{kHz}$, $f_2=15\text{kHz}$)

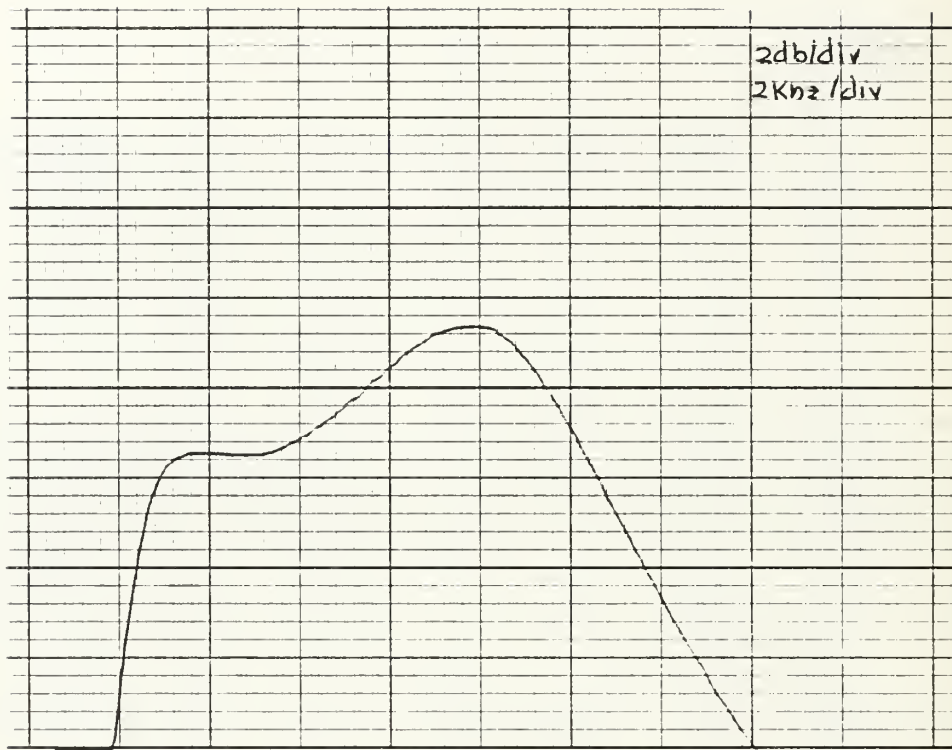


Fig. 6.14 - HP-LP Response $Q_1=Q_2=4$
($f_1=3\text{kHz}$, $f_2=9.0\text{kHz}$)

VII. APPLICATION OF THE PROPOSED GIC PROGRAMMABLE FILTER IN FREQUENCY HOPPING SYSTEMS

A. BACKGROUND

1. General Description of Frequency Hopping Signals

Frequency hopping is a spread spectrum modulation technique used to generate many possible carrier frequencies over a large bandwidth. Of all the possible carrier frequencies, only one is selected at a given time. However, all frequencies are eventually selected during some time interval.

Frequency hopping (FH) may be pictured as an RF carrier whose center frequency is "hopped" over many frequencies. The hopping may be either in a simple sequence or a pseudorandom sequence.

The hopping rate of a frequency hopping system does not affect the bandwidth of the output spectrum. In a direct sequence system the chip rate determines the total bandwidth. In a frequency hopping system, however, the bandwidth is determined by the highest and lowest frequencies of the frequency hopped carriers. For example, if the highest frequency carrier is at 15 MHz and the lowest frequency carrier is at 10 MHz, the total signal bandwidth is 5 MHz. This is the bandwidth regardless of the hopping rate. This allows wideband spread spectrum signal generation at low hopping rates.

2. Signal Generation

Frequency-hopped signals may be generated in several ways. The different methods are classified into two groups:

- (1) Direct synthesis, and
- (2) Indirect synthesis.

One important aspect of frequency hopping synthesis is coherency. coherent signal synthesis is defined as the establishment of a known and repeatable phase each time a new frequency is hopped to. Non-coherent signal synthesis is defined as the establishment of a random or unknown phase each time a new frequency is hopped to. some techniques, direct or indirect, of signal generation can be used as a coherent frequency source. In other techniques, the changing of frequencies creates non-coherent sources.

If a frequency hop system is a coherent, it will have a signal-to-noise advantage over a non-coherent system.

a. Direct Synthesis

The direct approach to signal synthesis utilizes techniques which enable direct synthesis of different frequencies. Examples of direct synthesis techniques are:

- (1) Frequency mixing, and
- (2) Surface acoustic wave devices.

Frequency mixing for single synthesis is a common technique used to generate many different frequencies. An example of the frequency mixing technique is show in Fig. (7.2).

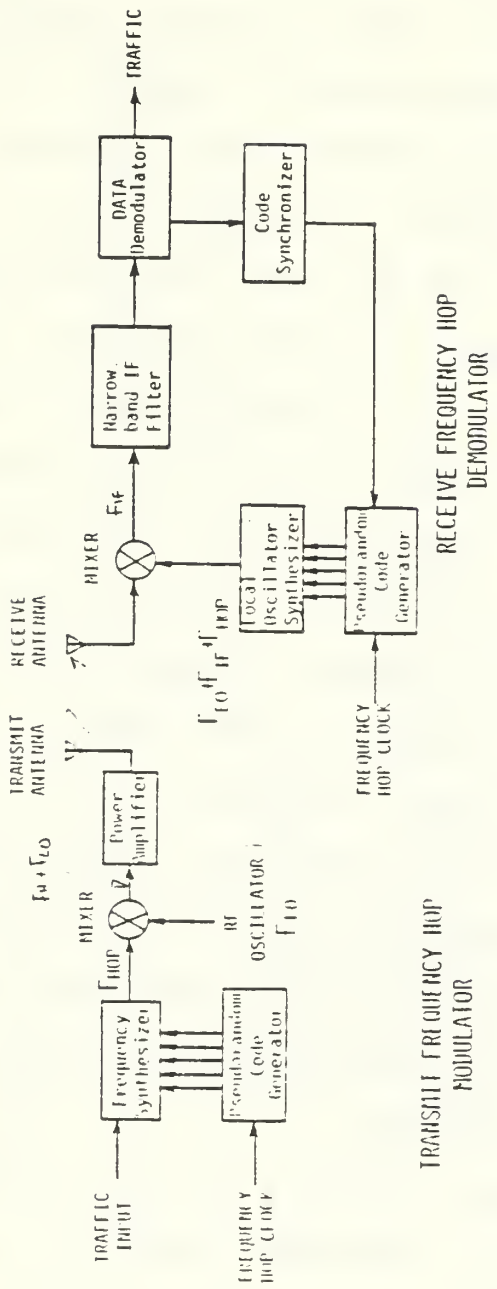


FIGURE 7.1 BLOCK DIAGRAM OF A FREQUENCY HOP MODEM

A pseudorandom code generator selects one of many transmit frequencies during a small time interval. The traffic modulates the carrier frequency which is spread over many different frequencies by the hopping action. The receiver dehops the input signal into a narrowband IF. The code synchronizer locks the pseudorandom code generator in the receiver to the received signal. A data demodulator removes the traffic from the IF amplifier output.

In Fig. (7.2), an RF switch selects one of several frequency inputs. Two of these input signals of different frequencies are multiplied together to generate a new output frequency. The device used to multiply the two signals together is called a frequency mixer. When two frequencies are mixed, the sum and the difference of the frequencies are generated. In order to select only one of these frequencies, a "filter is used to reject the unwanted frequency." A filter tuned to the desired frequency would allow selection of that frequency while rejecting the other. By selecting the mixing frequencies in the proper order, the output frequency can be stepped through several different frequencies. At each frequency mixer output, a filter is required to reject unwanted frequencies. The filters may require a short time for the signal to stabilize after it is selected. The time required for the filter to stabilize at each new frequency may ultimately determine the maximum hopping rate of the direct frequency synthesizer.

b. Indirect Synthesis

The indirect method of signal synthesis is defined as frequency synthesis through the use of phase-locked oscillators. One common indirect method for synthesis is shown in Fig. (7.3).

In this circuit a phase-locked loop is used to generate the numerous carrier frequencies. The phase-locked loop has an internal oscillator whose output frequency, F_0 ,

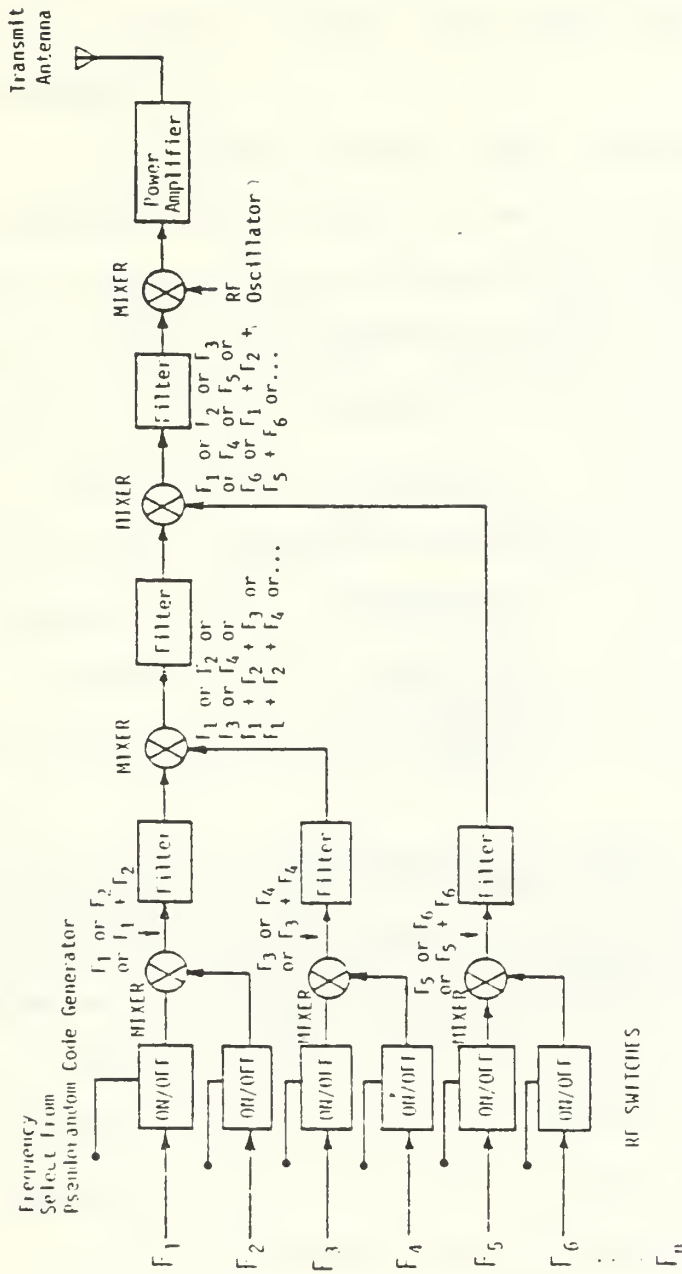


FIGURE 7.2 DIAGRAM OF A DIRECT FREQUENCY SYNTHESIZER

A pseudorandom sequence selects different combinations of F_1 through F_n , which are mixed together to form a new frequency. Each new frequency is mixed with the rf oscillator for transmission as one of the many hopping frequencies.

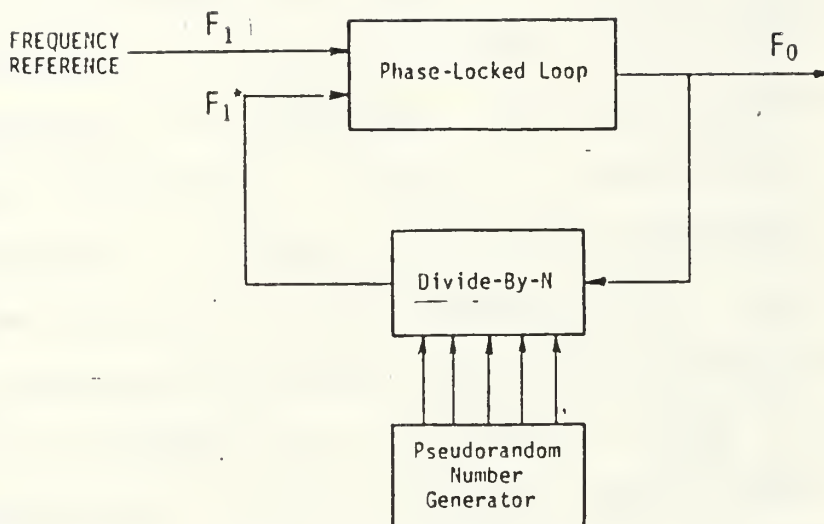


FIGURE 7.3 INDIRECT SIGNAL SYNTHESIS USING A PHASE-LOCKED LOOP

When the reference frequency, F_1 , is at the same frequency as F_1^* , the voltage-controlled oscillator produces a constant output frequency, F_0 . Since F_0 is divided by the programmable divider, F_0 is equal to N times F_1 . By changing the divider ratio, N , many output frequencies are possible.

is shown in Figure (7.3) as the phase-locked loop output. The divide-by-N circuit divides this oscillator frequency by a selected number, N.

The phase-locked loop internally adjust its output frequency F_o so that F_1^* is the same frequency as the reference frequency F_1 . If the divide-by-N circuit output frequency is initially lower than the reference frequency F_1 , the oscillator output frequency is automatically increased until F_1 and F_1^* are identical. When this occurs, the oscillator output frequency will become stable and remain at that frequency until the number, N, changes. When this number changes, the oscillator frequency is again automatically adjusted so that F_1 and F_1^* are again identical.

B. PROPOSED USES OF PROGRAMMABLE FILTER

A wide field of applications exist in FH systems for the programmable GIC filter. The outstanding performance of the filter (including sensitivity and stability) and its high speed response to the different inputs (due to the use of CMOS integrated circuits) make it very exceptional in this field. The first proposed use is indicated, in Fig. (7.4). The figure illustrates a receiver of a frequency hopping demodulator. The received frequency hopped signal after heterodyned by the RF mixer passes through the GIC filter in a BP realization (at this application the topology control network does not need to exist since the BP realization is

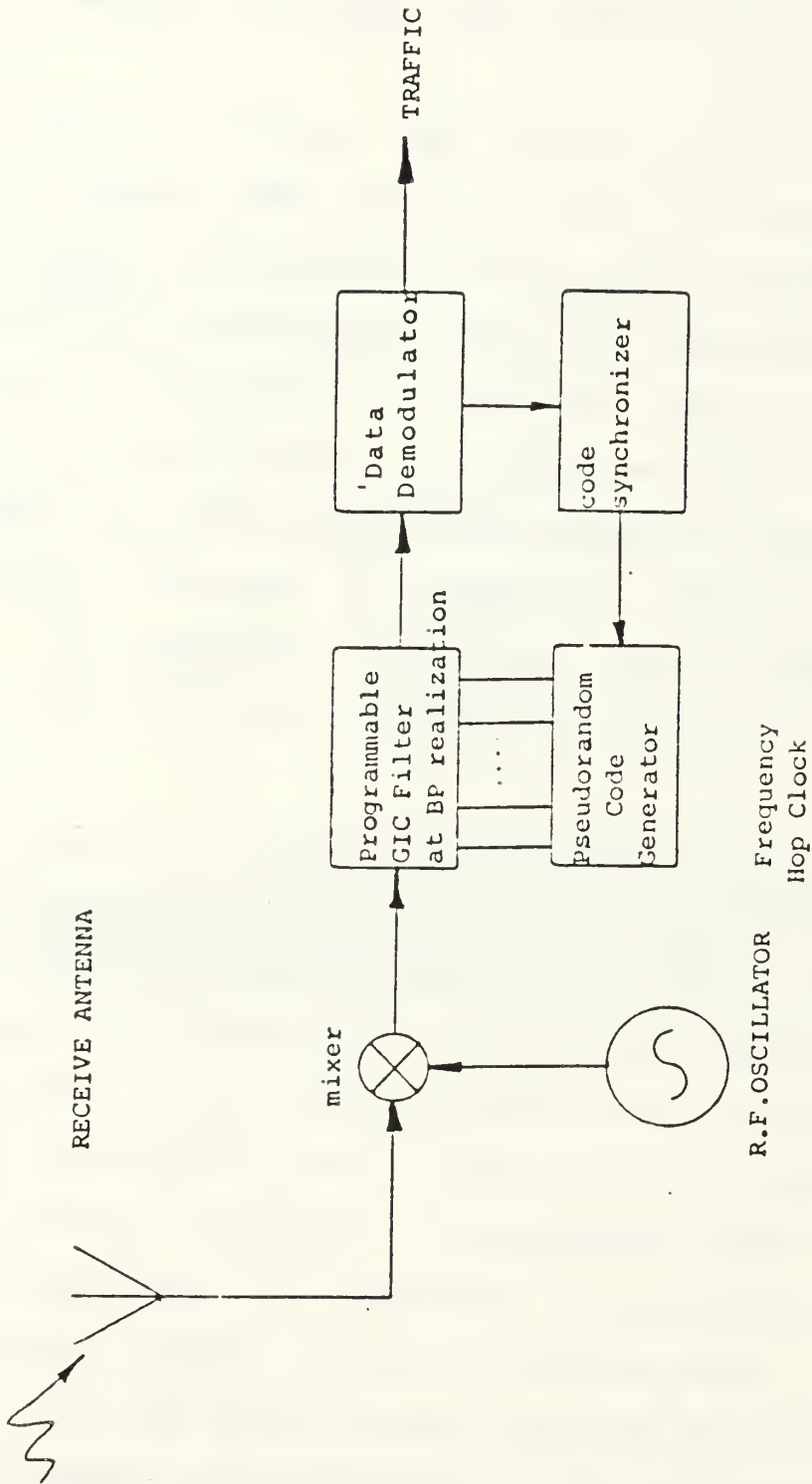


Fig. 7.4 - The Proposed Receiver of A Frequency Hopping System Using the Programmable GIC Filter

the only type to be used). The frequency shift of the filter is controlled by the synchronized pseudorandom code generator. This code generator also controls Q through some interfaced binary logic in order to correct the amplitude reduction which appears at high frequencies. The frequency shift problems can be easily corrected by the use of composite Op. Amp. Fig. (7.5) as it is extensively analyzed in Refs. [32], [34], and [35].

The programmable filter can also be used in the direct frequency synthesizer as it is illustrated at Fig. (7.2). At each frequency mixer output exists the need of a filter required to reject the unwanted frequencies. The frequencies to pass are not always the same, but they hop. the BP realization of the filter is used which center frequency can be controlled accordingly. The filter may require a short time for the signal to stabilize after it is selected. The time required for the filter to be stabilized at each new frequency may ultimately determine the maximum hopping rate of the direct frequency synthesizer.

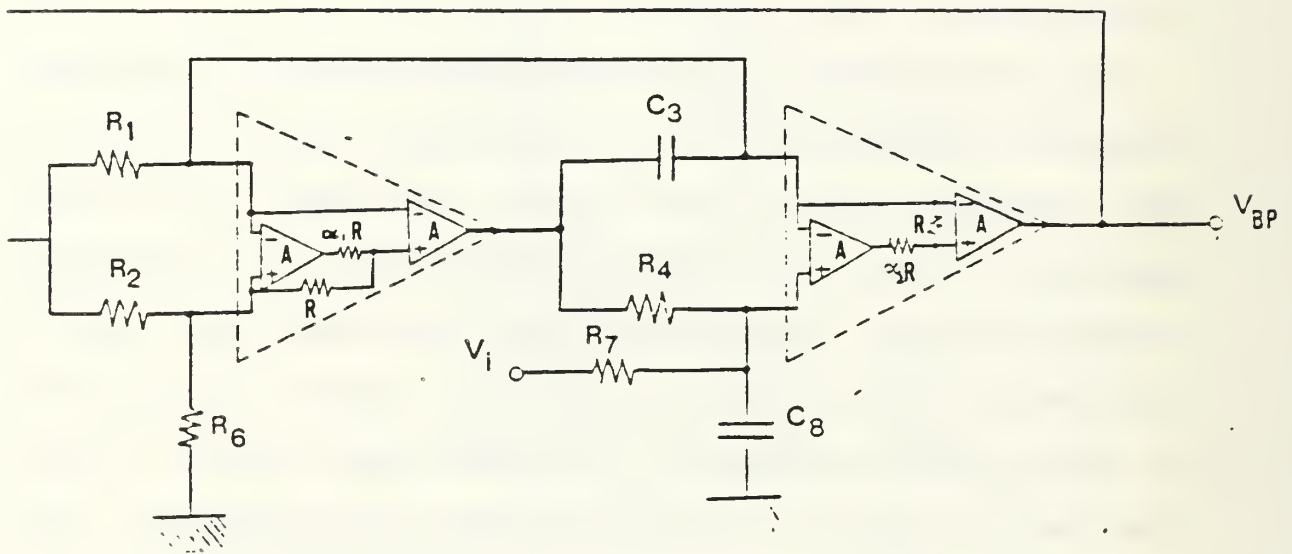


Fig. 7.5 Practical BP Filter Realization of the Composite GIC

VIII. CONCLUSION

The novel design described here has resulted in a universal programmable filter than can be digitally controlled to realize almost any practical filter specifications. This is done through the use of CMOS switches controlled by binary codes to program the order of the filter, the filter topology, the filter center frequency and selectivity. The design procedure required developing optimum switching arrangements for the minimum redundancy in components and least dependence of the filtering function on switching imperfections such as switches stray capacitances and non-zero and nonlinear switch-on resistance. The sensitivities of Q_p , W_p are found to be low with respect to the passive and active elements variations. The experimental result show close agreement between theory and practice. Further, these results indicate that these realizations are insensitive to temperature and power supply variations. A wide field of applications exists for the programmable filter beside the one discussed in Chapter VII.

- (1) Word recognition and speech synthesis;
- (2) Music applications;
- (3) Signal processing in communication;
- (4) Adaptive balancing.

Further investigation is needed to develop a programmable switched capacitor realization that can allow frequency scaling by changing clock frequency. Work can be also extended for developing a wide bandwidth programmable filter using the composite operational amplifier technique proposed by [39]. Such implementation would lead to a very useful monolithic device at moderate cost.

The research has yielded a paper that was presented at the 19th Annual Asilomar Conference on circuits, systems and computers, Monterey, California; November, 1985 (Appendix C).

APPENDIX A

```

$JOB
DIMENSION ATIS(100),PTIS(100),AT2S(100),PT2S(100)
*,AT3S(100),PT3S(100),FAT1(100),FAT2(100),FAT3(100)
DIMENSION AT1(100),PT1(100),AT2(100),PT2(100),AT3(100),
*,PT3(100),FPT1(100),FPT2(100),FPT3(100),
*,FTF1(100),FTF2(100),FTF3(100),FP1(100),FP2(100),FP3(100)
COMPLEX T1S,T2S,T3S,Y1S,Y2S,Y3S,Y4S,Y5S,Y6S,Y7S,Y8S,DS,K1S,K2S,
*,K3S,K4S,K5S,K6S
COMPLEX T1,T2,T3,Y1,Y2,Y3,Y4,Y5,Y6,Y7,Y8,D,K1,K2,K3,K4,K5,K6
DIMENSION FR(100),BT1S(100),HT1S(100),BT2S(100),HT2S(100)
*,BT3S(100),HT3S(100),FBT1(100),FBT2(100),FBT3(100)
DIMENSION BT1(100),HT1(100),BT2(100),HT2(100),BT3(100)
*,HT3(100),FHT1(100),FHT2(100),FHT3(100)
COMPLEX C1S,C2S,C3S,G1S,G2S,G3S,G4S,G5S,G6S,G7S,G8S,DDS,X1S,X2S,
*,X3S,X4S,X5S,X6S
COMPLEX C1,C2,C3,G1,G2,G3,G4,G5,G6,G7,G8,DD,X1,X2,X3,X4,X5,X6,S
OMEGA = 0.
DO 20 K = 1,100
OMEGA = OMEGA + 125.*20.
S = CMPLX( 0.0 , OMEGA )
C ***** DATA *****
R1 = 1600.
C1 = 200E-9
RQ1 = 3200.
R2 = 1600.
C2 = 50E-9
RQ2 = 3200.
R3 = 1600.
C3 = 12.5E-9
RQ3 = 3200.
R4 = 1600.
C4 = 3.12E-9
RQ4 = 3200.
A3 = A4 = A3S = A4S = 1E5
A1 = A2 = A1S = A2S = 1E5
J = 4
I = 4
L = 4
N = 4
C
C *****SELECT THE TYPE OF THE FOURTH FILTER *****
C DO CASE L
C CASE
C HPF
G1S = 1./R4
G2S = G1S
G3S = S*C4
G4S = G1S
G6S = G1S
G5S = 0.0
G7S = G3S
G8S = 1./RQ4
C CASE
C LPF
G1S = 1./R4
G2S = S*C4
G3S = G2S+ 1./RQ4
G4S = G1S
G6S = 0.0
G5S = G1S
G7S = 0.0
G8S =G1S
C CASE
C NOTCH
G1S = 1./R4
G2S = G1S
G3S = S*C4
G4S = G1S
G5S = G1S
G6S = 0.0
G7S = G3S

```

```

        G7S = G3S
        G8S = 1./RQ4
C      IF NONE DO
      BPF
        G1S = 1./R4
        G2S = G1S
        G3S = S*C4
        G4S = G1S
        G5S = 0.0
        G6S = G1S
        G7S = 1./RQ4
        G8S = S*C4
      END CASE
C
C ***** SELECT THE TYPE OF THE THIRD FILTER *****
      DO CASE N
C      CASE
      HPF
        G1 = 1./R3
        G2 = G1
        G3 = S*C3
        G4 = G1
        G6 = G1
        G5 = 0.0
        G7 = G3
        G8 = 1./RQ3
C      CASE
      LPF
        G1 = 1./R3
        G2 = S*C3
        G3 = G2 + 1./RQ3
        G4 = G1
        G6 = 0.0
        G5 = G1
        G7 = 0.0
        G8 = G1
C      CASE
      NOTCH
        G1 = 1./R3
        G2 = G1
        G3 = S*C3
        G4 = G1
        G5 = G1
        G6 = 0.
        G7 = G3
        G8 = 1./RQ3
C      IF NONE DO
      BPF
        G1 = 1./R3
        G2 = G1
        G3 = S*C3
        G4 = G1
        G5 = 0.0
        G6 = G1
        G7 = 1./RQ3
        G8 = S*C3
      END CASE
C ***** SELECT THE TYPE OF THE SECOND FILTER *****
      DO CASE I
C      CASE
      HPF
        Y1S = 1./R2
        Y2S = Y1S
        Y3S = S*C2
        Y4S = Y1S
        Y6S = Y1S
        Y5S = 0.0
        Y7S = Y3S
        Y8S = 1./RQ2
C      CASE
      LPF
        Y1S = 1./R2

```

```

Y2S = S*C2
Y3S = Y2S + 1./RQ2
Y4S = Y1S
Y6S = 0.0
Y5S = Y1S
Y7S = 0.0
Y8S = Y1S

```

```

C CASE
  NOTCH
    Y1S = 1./R2
    Y2S = Y1S
    Y3S = S*C2
    Y4S = Y1S
    Y5S = Y1S
    Y6S = 0.0
    Y7S = Y3S
    Y8S = 1./RQ2

```

```

C IF NONE DO
  BPF
    Y1S = 1./R2
    Y2S = Y1S
    Y3S = S*C2
    Y4S = Y1S
    Y5S = 0.0
    Y6S = Y1S
    Y7S = 1./RQ2
    Y8S = S*C2

```

```

END CASE

```

```

C ***** SELECT THE TYPE OF THE FIRST FILTER *****
C DO CASE J

```

```

C CASE
  HPF
    Y1 = 1./R1
    Y2 = Y1
    Y3 = S*C1
    Y4 = Y1
    Y6 = Y1
    Y5 = 0.0
    Y7 = Y3
    Y8 = 1./RQ1

```

```

C CASE
  LPF
    Y1 = 1./R1
    Y2 = S*C1
    Y3 = Y2 + 1./RQ1
    Y4 = Y1
    Y6 = 0.0
    Y5 = Y1
    Y7 = 0.0
    Y8 = Y1

```

```

C CASE
  NOTCH
    Y1 = 1./R1
    Y2 = Y1
    Y3 = S*C1
    Y4 = Y1
    Y5 = Y1
    Y6 = 0.
    Y7 = Y3
    Y8 = 1./RQ1

```

```

C IF NONE DO
  BPF
    Y1 = 1./R1
    Y2 = Y1
    Y3 = S*C1
    Y4 = Y1
    Y5 = 0.0
    Y6 = Y1
    Y7 = 1./RQ1
    Y8 = S*C1

```

```

END CASE

```

C*****

C

```

FR(K) = OMEGA/6.28
S = CMPLX(0.0, OMEGA)
K1S = Y1S*(1.+ 1./A2S)
K2S = (Y2S + Y5S + Y6S)
K3S = (Y4S + Y7S + Y8S)
K4S = Y4S + Y8S
K5S = Y1S + Y3S
K6S = Y5S + Y6S

```

C

```

K1 = Y1*(1.+ 1./A2)
K2 = (Y2 + Y5 + Y6)
K3 = (Y4 + Y7 + Y8)
K4 = Y4 + Y8
K5 = Y1 + Y3
K6 = Y5 + Y6

```

C

```

X1S = G1S*(1.+ 1./A4S)
X2S = (G2S + G5S + G6S)
X3S = (G4S + G7S + G8S)
X4S = G4S + G8S
X5S = G1S + G3S
X6S = G5S + G6S

```

C

```

X1 = G1*(1.+ 1./A4)
X2 = (G2 + G5 + G6)
X3 = (G4 + G7 + G8)
X4 = G4 + G8
X5 = G1 + G3
X6 = G5 + G6

```

C

C

```

DS = (K1S*K2S*K3S)/A1S + Y1S*Y4S*K6S + Y3S*K2S*K3S/(A1S*A2S) +
* Y2S*Y3S*Y4S/A2S + (Y2S/Y1S)*K1S*Y3S*(Y7S+Y8S) + Y3S*K6S*K3S/A2S
T1S = (Y1S*Y4S*Y5S + Y3S*Y5S*(Y7S-Y8S) + Y3S*Y7S*(Y2S+Y6S) + (Y7S*
* (Y1S+Y3S)*K2S)/A1S)/DS
T2S = (Y1S*Y5S*K4S - Y1S*Y7S*Y6S + Y3S*Y5S*K4S/A2S - Y3S*Y6S*Y7S/A2S
* + Y5S*Y7S*K5S/A1S + Y2S*Y3S*Y7S )/DS
T3S = (K1S*Y7S*K2S/A1S + K1S*Y4S*Y5S + Y3S*Y7S*K2S/A1S*A2S + Y3S*Y4S
* *Y5S/A2S + (Y1S/Y2S)*K1S*Y3S*Y7S + K6S*Y3S*Y7S/A2S)/DS

```

C

```

D = (K1*K2*K3)/A1 + Y1*Y4*K6 + Y3*K2*K3/(A1*A2) + Y2*Y3*Y4/A2 +
* (Y2/Y1)*K1*Y3*(Y7+Y8) + Y3*K6*K3/A2
T1 = (Y1*Y4*Y5 + Y3*Y5*(Y7-Y8) + Y3*Y7*(Y2+Y6) + (Y7*(Y1+Y3)*K2)/A1)/D
T2 = (Y1*Y5*K4 - Y1*Y7*Y6 + Y3*Y5*K4/A2 - Y3*Y6*Y7/A2 + Y5*Y7*K5/A2 +
* Y2*Y3*Y7 )/D
T3 = (K1*Y7*K2/A1 + K1*Y4*Y5 + Y3*Y7*K2/A1*A2 + Y3*Y4*Y5/A2 + (Y2/Y1)*
* K1*Y3*Y7 + K6*Y3*Y7/A2)/D

```

C

C

```

DDS = (X1S*X2S*X3S)/A3S + G1S*G4S*X6S + G3S*X2S*X3S/(A3S*A4S) +
* G2S*G3S*G4S/A4S + (G2S/G1S)*X1S*G3S*(G7S+G8S) + G3S*X6S*X3S/A4S
C1S = (G1S*G4S*G5S + G3S*G5S*(G7S-G8S) + G3S*G7S*(G2S+G6S) + (G7S*
* (G1S+G3S)*X2S)/A3S)/DDS
C2S = (G1S*G5S*X4S - G1S*G7S*G6S + G3S*G5S*X4S/A4S - G3S*G6S*G7S/A4S
* + G5S*G7S*X5S/A3S + G2S*G3S*G7S )/DDS
C3S = (X1S*G7S*X2S/A3S + X1S*G4S*G5S + G3S*G7S*X2S/A3S*A4S + G3S*G4S
* *G5S/A4S + (G1S/G2S)*X1S*G3S*G7S + X6S*G3S*G7S/A4S)/DDS

```

C

```

DD = (X1*X2*X3)/A3 + G1*G4*X6 + G3*X2*X3/(A3*A4) + G2*G3*G4/A4 +
* (G2/G1)*X1*G3*(G7+G8) + G3*X6*X3/A4
C1 = (G1*G4*G5 + G3*G5*(G7-G8) + G3*G7*(G2+G6) + (G7*(G1+G3)*X2)/A3)/DD
C2 = (G1*G5*X4 - G1*G7*G6 + G3*G5*X4/A4 - G3*G6*G7/A4 + G5*G7*X5/A4 +
* G2*G3*G7 )/DD
C3 = (X1*G7*X2/A3 + X1*G4*G5 + G3*G7*X2/A3*A4 + G3*G4*G5/A4 + (G2/G1)*
* X1*G3*G7 + X6*G3*G7/A4)/DD

```

C

C

```

AT1S(K) = 20.*ALOG10(CABS(T1S))
AT2S(K) = 20.*ALOG10(CABS(T2S))
AT3S(K) = 20.*ALOG10(CABS(T3S))

```

```

C      ART1S = REAL(T1S)
      ART2S = REAL(T2S)
      ART3S = REAL(T3S)
C
C      AIT1S = AIMAG(T1S)
      AIT2S = AIMAG(T2S)
      AIT3S = AIMAG(T3S)
C
C      PT1S(K) = ATAN2(AIT1S , ART1S)* 57.325
      PT2S(K) = ATAN2(AIT2S , ART2S)* 57.325
      PT3S(K) = ATAN2(AIT3S , ART3S)* 57.325
C
C      AT1(K) = 20.*ALOG10(CABS(T1))
      AT2(K) = 20.*ALOG10(CABS(T2))
      AT3(K) = 20.*ALOG10(CABS(T3))
C
C      ART1 = REAL(T1)
      ART2 = REAL(T2)
      ART3 = REAL(T3)
C
C      AIT1 = AIMAG(T1)
      AIT2 = AIMAG(T2)
      AIT3 = AIMAG(T3)
C
C      PT1(K) = ATAN2(AIT1 , ART1)* 57.325
      PT2(K) = ATAN2(AIT2 , ART2)* 57.325
      PT3(K) = ATAN2(AIT3 , ART3)* 57.325
C
C      FAT1(K) = AT1(K) + AT1S(K)
      FAT2(K) = AT2(K) + AT2S(K)
      FAT3(K) = AT3(K) + AT3S(K)
C
C      FPT1(K) = PT1(K) + PT1S(K)
      FPT2(K) = PT2(K) + PT2S(K)
      FPT3(K) = PT3(K) + PT3S(K)
C
C      BT1S(K) = 20.*ALOG10(CABS(C1S))
      BT2S(K) = 20.*ALOG10(CABS(C2S))
      BT3S(K) = 20.*ALOG10(CABS(C3S))
C
C      ART1S = REAL(C1S)
      ART2S = REAL(C2S)
      ART3S = REAL(C3S)
C
C      AIT1S = AIMAG(C1S)
      AIT2S = AIMAG(C2S)
      AIT3S = AIMAG(C3S)
C
C      HT1S(K) = ATAN2(AIT1S , ART1S)* 57.325
      HT2S(K) = ATAN2(AIT2S , ART2S)* 57.325
      HT3S(K) = ATAN2(AIT3S , ART3S)* 57.325
C
C      BT1(K) = 20.*ALOG10(CABS(C1))
      BT2(K) = 20.*ALOG10(CABS(C2))
      BT3(K) = 20.*ALOG10(CABS(C3))
C
C      ART1 = REAL(C1)
      ART2 = REAL(C2)
      ART3 = REAL(C3)
C
C      AIT1 = AIMAG(C1)
      AIT2 = AIMAG(C2)
      AIT3 = AIMAG(C3)
C
C      HT1(K) = ATAN2(AIT1 , ART1)* 57.325
      HT2(K) = ATAN2(AIT2 , ART2)* 57.325
      HT3(K) = ATAN2(AIT3 , ART3)* 57.325
C
C      FBT1(K) = BT1(K) + BT1S(K)
      FBT2(K) = BT2(K) + BT2S(K)
      FBT3(K) = BT3(K) + BT3S(K)

```

```

C      FHT1(K) = HT1(K) + HT1S(K)
      FHT2(K) = HT2(K) + HT2S(K)
      FHT3(K) = HT3(K) + HT3S(K)
C
      FTF1(K) = AT1(K) + BT1(K) + BT1S(K) + AT1S(K)
      FTF2(K) = FAT2(K) + FBT2(K)
      FTF3(K) = FAT3(K) + FBT3(K)
C
      FP1(K) = FHT1(K) + FPT1(K)
      FP2(K) = FHT2(K) + FPT2(K)
      FP3(K) = FHT3(K) + FPT3(K)
C
      WRITE(6,66) FR(K),FAT1(K),FBT1(K)
      #
      #      FHT3(K)
      #      ,FTF1(K),HT1(K),FHT1(K)
C
20    CONTINUE
66    FORMAT(6(1X,F9.3))
      STOP
      END
$ENTRY

```

APPENDIX B

```

$JOB
  DIMENSION AT1S(100),PT1S(100),AT2S(100),PT2S(100)
  *,AT3S(100),PT3S(100),FAT1(100),FAT2(100),FAT3(100).
  DIMENSION AT1(100),PT1(100),AT2(100),PT2(100),AT3(100),
  * PT3(100),FPT1(100),FPT2(100),FPT3(100),
  * FTF1(100),FTF2(100),FTF3(100),FP1(100),FP2(100),FP3(100)
  COMPLEX T1S,T2S,T3S,Y1S,Y2S,Y3S,Y4S,Y5S,Y6S,Y7S,Y8S,DS,K1S,K2S,
  *K3S,K4S,X5S,K6S
  COMPLEX T1,T2,T3,Y1,Y2,Y3,Y4,Y5,Y6,Y7,Y8,D,K1,K2,K3,K4,K5,K6
  DIMENSION FR(100),BT1S(100),HT1S(100),BT2S(100),HT2S(100)
  *,BT3S(100),HT3S(100),FBT1(100),FBT2(100),FBT3(100)
  DIMENSION BT1(100),HT1(100),BT2(100),HT2(100),BT3(100)
  *,HT3(100),FHT1(100),FHT2(100),FHT3(100)
  COMPLEX C1S,C2S,C3S,G1S,G2S,G3S,G4S,G5S,G6S,G7S,G8S,DDS,X1S,X2S,
  *X3S,X4S,X5S,X6S
  COMPLEX C1,C2,C3,G1,G2,G3,G4,G5,G6,G7,G8,DD,X1,X2,X3,X4,X5,X6,S
  OMEGA = 0.
  DO 20 K = 1,100
  OMEGA = OMEGA + 125.*20.
  S = CMPLX( 0.0 , OMEGA )
C***** DATA *****
  R1 = 1600.
  C1 = 200E-9
  RQ1 = 3200.
  R2 = 1600.
  C2 = 50E-9
  RQ2 = 3200.
  R3 = 1600.
  C3 = 12.5E-9
  RQ3 = 3200.
  R4 = 1600.
  C4 = 3.12E-9
  RQ4 = 3200.
W1 = W1S = "SET VALUE "
  A3 = A4 = A3S = A4S = W1/S
  A1 = A2 = A1S = A2S = W1S/S
  J = 4
  I = 4
  L = 4
  N = 4
C
C
C *****SELECT THE TYPE OF THE FOURTH FILTER *****
  DO CASE L
  CASE
  HPF
    G1S = 1./R4
    G2S = G1S
    G3S = S*C4
    G4S = G1S
    G6S = G1S
    G5S = 0.0
    G7S = G3S
    G8S = 1./RQ4
  CASE
  LPF
    G1S = 1./R4
    G2S = S*C4
    G3S = G2S + 1./RQ4
    G4S = G1S
    G6S = 0.0
    G5S = G1S
    G7S = 0.0
    G8S = G1S
  CASE
  NOTCH
    G1S = 1./R4
    G2S = G1S
    G3S = S*C4
    G4S = G1S
    G5S = G1S
    G6S = 0.0

```

```

      G7S = G3S
      G8S = 1./RQ4
C     IF NONE DO
      BPF
      G1S = 1./R4
      G2S = G1S
      G3S = S*C4
      G4S = G1S
      G5S = 0.0
      G6S = G1S
      G7S = 1./RQ4
      G8S = S*C4
      END CASE
C
C*****SELECT THE TYPE OF THE THIRD FILTER*****
      DO CASE N
      CASE
      HPF
      G1  = 1./R3
      G2  = G1
      G3  = S*C3
      G4  = G1
      G6  = G1
      G5  = 0.0
      G7  = G3
      G8  = 1./RQ3
C     CASE
      LPF
      G1  = 1./R3
      G2  = S*C3
      G3  = G2 + 1./RQ3
      G4  = G1
      G6  = 0.0
      G5  = G1
      G7  = 0.0
      G8  = G1
C     CASE
      NOTCH
      G1  = 1./R3
      G2  = G1
      G3  = S*C3
      G4  = G1
      G5  = G1
      G6  = 0.
      G7  = G3
      G8  = 1./RQ3
      IF NONE DO
      BPF
      G1  = 1./R3
      G2  = G1
      G3  = S*C3
      G4  = G1
      G5  = 0.0
      G6  = G1
      G7  = 1./RQ3
      G8  = S*C3
      END CASE
C *****SELECT THE TYPE OF THE SECOND FILTER*****
      DO CASE I
      CASE
      HPF
      Y1S = 1./R2
      Y2S = Y1S
      Y3S = S*C2
      Y4S = Y1S
      Y6S = Y1S
      Y5S = 0.0
      Y7S = Y3S
      Y8S = 1./RQ2
C     CASE
      LPF
      Y1S = 1./R2

```



```

Y2S = S*C2
Y3S = Y2S + 1./RQ2
Y4S = Y1S
Y6S = 0.0
Y5S = Y1S
Y7S = 0.0
Y8S = Y1S
C CASE
NOTCH
Y1S = 1./R2
Y2S = Y1S
Y3S = S*C2
Y4S = Y1S
Y5S = Y1S
Y6S = 0.0
Y7S = Y3S
Y8S = 1./RQ2
C IF NONE DO
BPF
Y1S = 1./R2
Y2S = Y1S
Y3S = S*C2
Y4S = Y1S
Y5S = 0.0
Y6S = Y1S
Y7S = 1./RQ2
Y8S = S*C2
END CASE
C
C***** SELECT THE TYPE OF THE FIRST FILTER *****
DO CASE J
CASE
HPF
Y1 = 1./R1
Y2 = Y1
Y3 = S*C1
Y4 = Y1
Y6 = Y1
Y5 = 0.0
Y7 = Y3
Y8 = 1./RQ1
C CASE
LPF
Y1 = 1./R1
Y2 = S*C1
Y3 = Y2 + 1./RQ1
Y4 = Y1
Y6 = 0.0
Y5 = Y1
Y7 = 0.0
Y8 = Y1
C CASE
NOTCH
Y1 = 1./R1
Y2 = Y1
Y3 = S*C1
Y4 = Y1
Y5 = Y1
Y6 = 0.
Y7 = Y3
Y8 = 1./RQ1
C IF NONE DO
BPF
Y1 = 1./R1
Y2 = Y1
Y3 = S*C1
Y4 = Y1
Y5 = 0.0
Y6 = Y1
Y7 = 1./RQ1
Y8 = S*C1
END CASE

```

C*****

C

```

FR(K) = OMEGA/6.28
S = CMPLX(0.0,OMEGA)
K1S = Y1S*(1.+ 1./A2S)
K2S = (Y2S + Y5S + Y6S)
K3S = (Y4S + Y7S + Y8S)
K4S = Y4S + Y8S
K5S = Y1S + Y3S
K6S = Y5S + Y6S

```

C

```

K1 = Y1*(1.+ 1./A2)
K2 = (Y2 + Y5 + Y6)
K3 = (Y4 + Y7 + Y8)
K4 = Y4 + Y8
K5 = Y1 + Y3
K6 = Y5 + Y6

```

C

```

X1S = G1S*(1.+ 1./A4S)
X2S = (G2S + G5S + G6S)
X3S = (G4S + G7S + G8S)
X4S = G4S + G8S
X5S = G1S + G3S
X6S = G5S + G6S

```

C

```

X1 = G1*(1.+ 1./A4)
X2 = (G2 + G5 + G6)
X3 = (G4 + G7 + G8)
X4 = G4 + G8
X5 = G1 + G3
X6 = G5 + G6

```

C

C

```

DS = (K1S*K2S*K3S)/A1S + Y1S*Y4S*K6S + Y3S*K2S*K3S/(A1S*A2S) +
* Y2S*Y3S*Y4S/A2S + (Y2S/Y1S)*K1S*Y3S*(Y7S+Y8S) + Y3S*K6S*K3S/A2
T1S = (Y1S*Y4S*Y5S + Y3S*Y5S*(Y7S-Y8S) + Y3S*Y7S*(Y2S+Y6S) + (Y7S*
* (Y1S+Y3S)*K2S)/A1S)/DS
T2S = (Y1S*Y5S*K4S - Y1S*Y7S*Y6S + Y3S*Y5S*K4S/A2S - Y3S*Y6S*Y7S/A2S
* + Y5S*Y7S*K5S/A1S + Y2S*Y3S*Y7S )/DS
T3S = (K1S*Y7S*K2S/A1S + K1S*Y4S*Y5S + Y3S*Y7S*K2S/A1S*A2S + Y3S*Y4S
* *Y5S/A2S + (Y1S/Y2S)*K1S*Y3S*Y7S + K6S*Y3S*Y7S/A2S)/DS

```

C

```

D = (K1*K2*K3)/A1 + Y1*Y4*K6 + Y3*K2*K3/(A1*A2) + Y2*Y3*Y4/A2 +
* (Y2/Y1)*K1*Y3*(Y7+Y8) + Y3*K6*K3/A2
T1 = (Y1*Y4*Y5 + Y3*Y5*(Y7-Y8) + Y3*Y7*(Y2+Y6) + (Y7*(Y1+Y3)*K2)/A1)/
T2 = (Y1*Y5*K4 - Y1*Y7*Y6 + Y3*Y5*K4/A2 - Y3*Y6*Y7/A2 + Y5*Y7*K5/A2 +
* Y2*Y3*Y7 )/D
T3 = (K1*Y7*K2/A1 + K1*Y4*Y5 + Y3*Y7*K2/A1*A2 + Y3*Y4*Y5/A2 + (Y2/Y1)
* K1*Y3*Y7 + K6*Y3*Y7/A2)/D

```

C

C

```

DDS = (X1S*X2S*X3S)/A3S + G1S*G4S*X6S + G3S*X2S*X3S/(A3S*A4S) +
* G2S*G3S*G4S/A4S + (G2S/G1S)*X1S*G3S*(G7S+G8S) + G3S*X6S*X3S/A4
C1S = (G1S*G4S*G5S + G3S*G5S*(G7S-G8S) + G3S*G7S*(G2S+G6S) + (G7S*
* (G1S+G3S)*X2S)/A3S)/DDS
C2S = (G1S*G5S*X4S - G1S*G7S*G6S + G3S*G5S*X4S/A4S - G3S*G6S*G7S/A4S
* + G5S*G7S*X5S/A3S + G2S*G3S*G7S )/DDS
C3S = (X1S*G7S*X2S/A3S + X1S*G4S*G5S + G3S*G7S*X2S/A3S*A4S + G3S*G4S
* *G5S/A4S + (G1S/G2S)*X1S*G3S*G7S + X6S*G3S*G7S/A4S)/DDS

```

C

```

DD = (X1*X2*X3)/A3 + G1*G4*X6 + G3*X2*X3/(A3*A4) + G2*G3*G4/A4 +
* (G2/G1)*X1*G3*(G7+G8) + G3*X6*X3/A4
C1 = (G1*G4*G5 + G3*G5*(G7-G8) + G3*G7*(G2+G6) + (G7*(G1+G3)*X2)/A3)/DD
C2 = (G1*G5*X4 - G1*G7*G6 + G3*G5*X4/A4 - G3*G6*G7/A4 + G5*G7*X5/A4 +
* G2*G3*G7 )/DD
C3 = (X1*G7*X2/A3 + X1*G4*G5 + G3*G7*X2/A3*A4 + G3*G4*G5/A4 + (G2/G1)
* X1*G3*G7 + X6*G3*G7/A4)/DD

```

C

C

```

AT1S(K) = 20.*ALOG10(CABS(T1S))
AT2S(K) = 20.*ALOG10(CABS(T2S))
AT3S(K) = 20.*ALOG10(CABS(T3S))

```

```

C      ART1S = REAL(T1S)
      ART2S = REAL(T2S)
      ART3S = REAL(T3S)

C      AIT1S = AIMAG(T1S)
      AIT2S = AIMAG(T2S)
      AIT3S = AIMAG(T3S)

C      PT1S(K) = ATAN2(AIT1S , ART1S)* 57.325
      PT2S(K) = ATAN2(AIT2S , ART2S)* 57.325
      PT3S(K) = ATAN2(AIT3S , ART3S)* 57.325

C      AT1(K) = 20.*ALOG10(CABS(T1))
      AT2(K) = 20.*ALOG10(CABS(T2))
      AT3(K) = 20.*ALOG10(CABS(T3))

C      ART1 = REAL(T1)
      ART2 = REAL(T2)
      ART3 = REAL(T3)

C      AIT1 = AIMAG(T1)
      AIT2 = AIMAG(T2)
      AIT3 = AIMAG(T3)

C      PT1(K) = ATAN2(AIT1 , ART1)* 57.325
      PT2(K) = ATAN2(AIT2 , ART2)* 57.325
      PT3(K) = ATAN2(AIT3 , ART3)* 57.325

C      FAT1(K) = AT1(K) + AT1S(K)
      FAT2(K) = AT2(K) + AT2S(K)
      FAT3(K) = AT3(K) + AT3S(K)

C      FPT1(K) = PT1(K) + PT1S(K)
      FPT2(K) = PT2(K) + PT2S(K)
      FPT3(K) = PT3(K) + PT3S(K)

C      BT1S(K) = 20.*ALOG10(CABS(C1S))
      BT2S(K) = 20.*ALOG10(CABS(C2S))
      BT3S(K) = 20.*ALOG10(CABS(C3S))

C      ART1S = REAL(C1S)
      ART2S = REAL(C2S)
      ART3S = REAL(C3S)

C      AIT1S = AIMAG(C1S)
      AIT2S = AIMAG(C2S)
      AIT3S = AIMAG(C3S)

C      HT1S(K) = ATAN2(AIT1S , ART1S)* 57.325
      HT2S(K) = ATAN2(AIT2S , ART2S)* 57.325
      HT3S(K) = ATAN2(AIT3S , ART3S)* 57.325

C      BT1(K) = 20.*ALOG10(CABS(C1))
      BT2(K) = 20.*ALOG10(CABS(C2))
      BT3(K) = 20.*ALOG10(CABS(C3))

C      ART1 = REAL(C1)
      ART2 = REAL(C2)
      ART3 = REAL(C3)

C      AIT1 = AIMAG(C1)
      AIT2 = AIMAG(C2)
      AIT3 = AIMAG(C3)

C      HT1(K) = ATAN2(AIT1 , ART1)* 57.325
      HT2(K) = ATAN2(AIT2 , ART2)* 57.325
      HT3(K) = ATAN2(AIT3 , ART3)* 57.325

C      FBT1(K) = BT1(K) + BT1S(K)
      FBT2(K) = BT2(K) + BT2S(K)
      FBT3(K) = BT3(K) + BT3S(K)

```

```

C      FHT1(K) = HT1(K) + HT1S(K)
      FHT2(K) = HT2(K) + HT2S(K)
      FHT3(K) = HT3(K) + HT3S(K)
C
      FTF1(K) = AT1(K) + BT1(K) + BT1S(K) + AT1S(K)
      FTF2(K) = FAT2(K) + FBT2(K)
      FTF3(K) = FAT3(K) + FBT3(K)
C
      FP1(K) = FHT1(K) + FPT1(K)
      FP2(K) = FHT2(K) + FPT2(K)
      FP3(K) = FHT3(K) + FPT3(K)
C
      WRITE(6,66) FR(K),FAT1(K),FBT1(K)
      *                                     ,FTF1(K),HT1(K),FHT1(K)
      * FHT3(K)
C 20 CONTINUE
66  FORMAT(6(1X,F9.3))
      STOP
      END
$ENTRY

```


due to the absence of negative terms in $D(s)$. Therefore the zeros of $D(s)$ will remain in the left-half s -plane and low frequency unstable modes cannot arise during activation.

Function programmability:

The objective of this research was to develop a device that is capable of realizing the following transfer functions: LP where $T(s) = K/D(s)$, BP where $T(s) = KS/D(s)$, HP where $T(s) = KS^2/D(s)$, AP where $T(s) = [s^2 - s(\omega_p/Q_p) + \omega_p^2]/D(s)$ and N where $T(s) = (s^2 + \omega_z^2)/D(s)$. By optimizing the design of the filter, it was found that all of the above functions can be realized by the second order GIC section using four resistors, two capacitors and two OAs as shown in Table 1. These passive elements are connected to different nodes to achieve the various realizations. A set of CMOS bilateral switches controlled by digital binary word, are used to relocate the same elements in different ways to achieve the desired filtering functions according to Fig. 2. The truth table of the switches control logic is shown in Table 2, while Fig. 3 illustrates the corresponding minimized CMOS logic circuit used for passive elements relocation.

Parameter programmability:

While four of the resistors are equal and of value R each, the fifth resistor is the Q_p determining resistor and of value $R_q = RQ_p$. The two capacitors are equal and of value $c = 1/(\omega_p R)$ each. Two equal banks of capacitors are used to control ω_p . Each bank contains n binary-weighted capacitors connected in series with n CMOS switches as shown in Fig. 4. Using n bit binary word to control the switches, 2^n different values of c can be obtained that corresponds to 2^n different values of ω_p . Using a similar technique, the value of R_q can be controlled by an m bit digital word that yields 2^m different values of Q_p , as illustrated in Fig. 5. Thus, full independent control of the pole pair ω_p and Q_p are achieved by programming the digital words controlling the switches to obtain the corresponding c and R_q . The complete second order programmable filter is shown in Fig. 6, where the function programmability as well as the parameter programmability are demonstrated.

Higher order programmability:

Active filters design procedure can be classified as direct or cascade. In direct synthesis procedures the transfer function is realized as a single section [7]. In cascade synthesis procedures a high order transfer function is expressed as a product of first and second order transfer functions and each of these is realized independently. The overall network is obtained by cascading the individual sections. The cascade method of synthesis offers two practical advantages (a) simple network tuning (b) a few number of universal sections can be designed which can realize a multitude of network specifications.

The second order GIC network structure lends itself to the cascade synthesis procedure since it does not require additional isolating amplifiers. Fig. 6.b shows a block diagram of a programmable higher order filter that utilizes the second procedure by cascading 2 or more sections of the filter network shown in Fig. 6.a. The result is a high order fully programmable general purpose filter, that can be tailored to match almost any proposed specification.

3. COMPUTER SIMULATIONS AND EXPERIMENTAL VERIFICATIONS:

Fig. 7 shows different computer simulation outputs of the programmable filter. The plots simulate the filter responses assuming ideal OAs with infinite Gain Bandwidth Products (GBWP), as well as practical filter responses assuming OA's finite GBWPs of 1 MHz as of that of the LM741 OA. A single pole OA model was utilized to approximate the filter transfer functions in the later case. The approximation was found adequate since the simulation results of the nonideal response were found to be of close proximity to the experimental results of Fig. 8. The experimental results were obtained using a three bit word for filter topology programmability to select the type of transfer functions. A two words, four bits each, were used for filter parameters programmability where ω_p and Q_p are controlled independently as given in Table 3. Fig. 7 also illustrates a higher order programmability where a fourth order characteristics are shown for a LPF and a Chebychev BPF.

4. CONCLUSION

The novel design described here has resulted in a universal programmable filter that can be digitally controlled to realize almost any practical filter specifications. This is done through the use of CMOS switches controlled by binary codes to program the order of the filter, the filter topology, the filter center frequency and selectivity. The design procedure required developing optimum switching arrangements for the minimum redundancy in components and the least dependence of the filtering function on switching imperfections such as switches stray capacitances and non-zero and non-linear switch-on resistance. Further investigation is being conducted to develop a programmable switched capacitor realization that can allow frequency scaling by changing clock frequency. Work is also in progress for developing an extended bandwidth programmable filter using the composite operational amplifier technique proposed earlier by the author. Such implementation would lead to a very useful monolithic device at moderate cost.

5. REFERENCES

1. R.W. Brodersen, P.R. Gray, and D.A. Hodges, "MOS Switched Capacitor Filters", IEEE Proceedings, Volume 67, No 1 pp 61-75, Jan., 1979.
2. D.J. Allstot, R.W. Brodersen, and P.R. Gray, "An Electronically Programmable Switched Capacitor Filter", IEEE Journal of Solid State Circuits, Volume SC-14, No. 6, pp. 1034-1041, Dec. 1979.
3. P.B. Denyer, J. Mavor and J.W. Arthur, "Miniature Programmable Transversal Filter using CCD MOS Technology", IEEE Proceedings, Volume 67, No. 1, pp 42-50, Jan 1979.
4. Sherif Michael, "Composite Operational Amplifiers and Their Applications in Active Networks" PhD Dissertation, West Virginia University, WV pp 95-138, Aug 1983.

5. B.B. Bhattacharyya, Wasfy B. Miknael and A. Antoniou, "Design of RC-Active Networks by Using Generalized-impittance Converters", Proceedings of the 1974 International Symposium on Circuit Theory pp 290-293, April 1973.

6. A.K. Mitra and U.K. Aatre, "A Note on Frequency and Q Limitations of Active Filters", IEEE Transactions CAS, Volume CAS-24, pp 215-218, April 1977.

7. L.T. Bruton, "Biquadratic Sections Using Generalized Impedance Converters", The Radio and Electronic Engr, Vol. 41, No 11, pp 510-512, Nov 1971.

switch control				Op	Op	switch control				C	fp
5a	5b	5c	5d	Kq		5e	5b	5c	5d	Op	fpz
0	0	0	0	24.0	15	0	0	0	0	5.94	16.493
0	0	0	1	22.4	14	0	0	0	1	6.34	15.703
0	0	1	0	20.8	13	0	0	1	0	7.16	13.887
0	0	1	1	15.2	12	0	0	1	1	7.72	12.875
0	1	0	0	17.6	11	0	1	0	0	8.42	11.816
0	1	0	1	16.0	10	0	1	0	1	9.20	10.856
0	1	1	0	14.4	9	0	1	1	0	10.00	10.043
0	1	1	1	12.8	8	0	1	1	1	11.00	9.047
1	0	0	0	11.2	7	1	0	0	0	15.10	6.650
1	0	0	1	5.6	6	1	0	0	1	17.40	5.637
1	0	1	0	8.0	5	1	0	1	0	20.80	4.823
1	0	1	1	6.4	4	1	0	1	1	24.00	3.828
1	1	0	0	4.8	3	1	1	0	0	35.50	2.805
1	1	1	1	3.2	2	1	1	0	1	55.00	1.816
1	1	1	0	1.6	1	1	1	1	0	100.00	.952

Table 3. Binary Words Controlling Op & fp

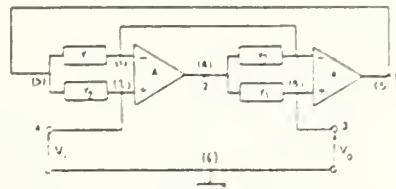


Fig. 1 The Generalized Impedance Converter

Filter Type	Y1	Y2	Y3	Y4	Y5	Y6	Y7	Y8	Transfer Function
LP	C	C	C	C	C	0	0	C	$T_1 = 2\omega p^2 / (1 + \omega^2)$
HP	C	C	C	C	0	C	C	$\frac{C}{1 + \omega^2}$	$T_1 = 2\omega^2 / (1 + \omega^2)$
BP	C	C	C	0	C	0	C	$\frac{C}{\omega}$	$T_1 = 2(\omega p / \omega_0)^2 / (1 + \omega^2)$
B	C	L	C	C	0	0	C	$\frac{C}{1 + \omega^2}$	$T_2 = (1 + \omega_m^2) / (1 + \omega^2)$
AL	C	C	C	C	0	0	C	$\frac{C}{2\omega}$	$T_1 = \frac{1}{\omega} - \frac{\omega}{2\omega_0} + \omega p^2 / (1 + \omega^2)$

Table 1.

The Elements Values for Different Realizations

where $T(s) = N(s)/D(s)$ and $D(s) = s^2 + (\omega_p/\Q)s + \omega_p^2$

To be Connected in Case of	Components Represented	Components & Switches	Components Represented	To be connected in case of
L, H, B, H	R_1, R_2, R_3		R_1, R_2, R_3	H, B, L, H = A
H, L, H, B	R_1, R_2, R_3		R_1, R_2, R_3	H, B = B
H, B, H = A	C_1, C_2, C_3		C_1, C_2, C_3	L, H = A
L, H, B, H = A	$R_1, R_2, R_3, C_1, C_2, C_3$		$R_1, R_2, R_3, C_1, C_2, C_3$	L, B, H, H = A
H, L, H	R_1, R_2		None	L, H, B = C

Fig. 2 Elements Relocation Switches for topology programmability

Binary Input	Filter	Switch													
		S1	S2	S3	S4	S5	S6	S7	S8	S9	S10				
0000	Low Pass	0	1	0	1	1	0	0	1	0	0	1	0	0	1
0001	High Pass	1	0	1	0	0	1	0	0	1	0	1	0	1	0
0100	Band Pass	1	0	1	0	0	0	1	0	1	0	1	0	1	0
0101	Notch	0	1	1	0	0	1	0	0	1	0	1	1	0	0
1000	All Pass	0	1	1	0	1	0	0	1	1	1	1	0	1	0

Table 2. The Truth Table of the Logic Controlling Elements Relocation Switches

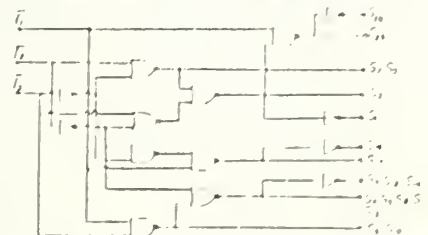


Fig. 3 The logic controlling figure 2 switches

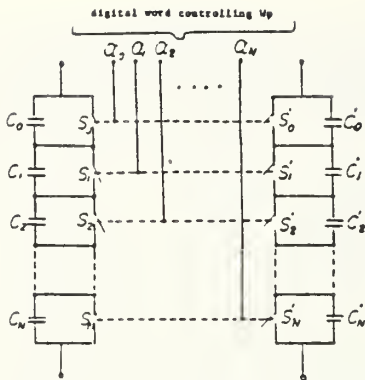
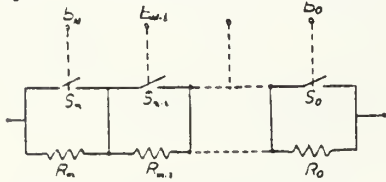


Fig. 4 Capacitors Banks for Frequency Programmability



(For linear Op control, $E_{j+1}=2E_j$, resulting to $R_{Op} = \sum_{j=0}^n E_j b_j$)

Fig. 5 The Programmable Rq Resistor

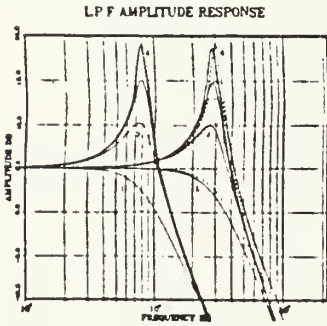


Fig. 7.a

Ideal vs. nominal L.P.F. amplitude response for frequencies 17.96, 36.167 and variety of Q.

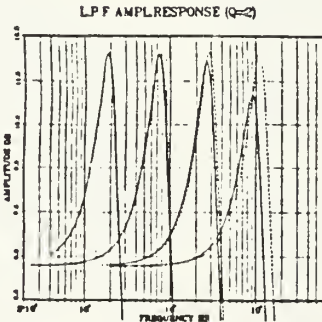


Fig. 7.b

Ideal vs. nominal L.P.F. amplitude response for Q=2 and frequencies 11.876, 7.964, 10.166 and 117.182.

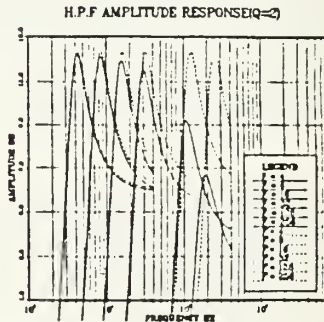


Fig. 7.c

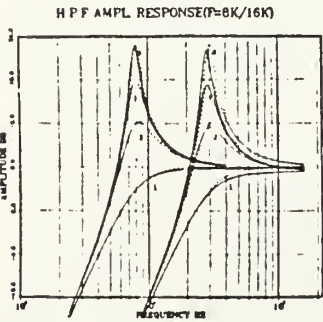


Fig. 7.d

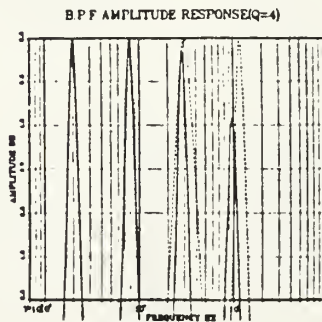


Fig. 7.e

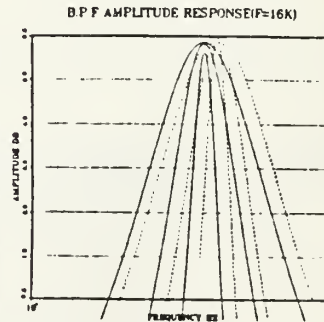


Fig. 7.f

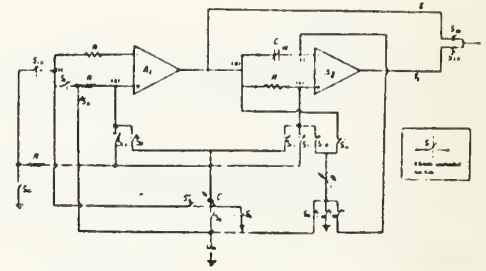


Fig. 6.a The General Second Order GIC Section

ORDER

2	S ₁	S ₂	S ₃	S ₄	S ₅	S ₆	S ₇	
4	O	O	O	O	O	X	O	
6	X	O	O	O	O	X	O	
8	X	X	X	X	O	O	O	

O OPEN
X CLOSED

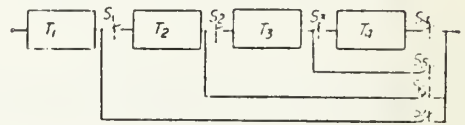


Fig. 6.b Higher Order Programmability of the GIC Sections

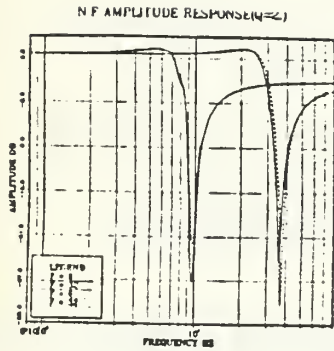


Fig. 7.g

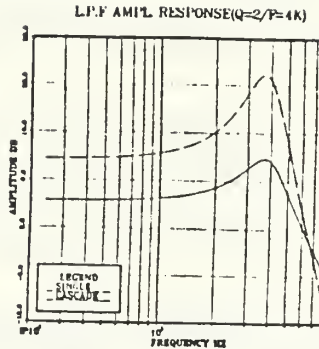


Fig. 7.h

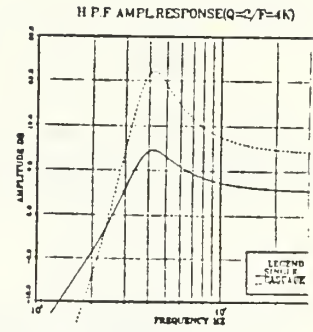


Fig. 7.k

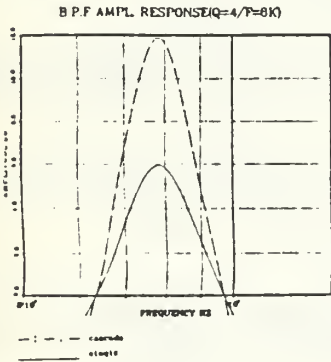


Fig. 7.l

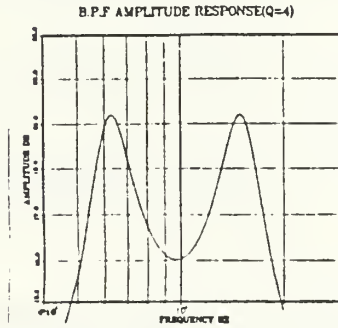


Fig. 7.m

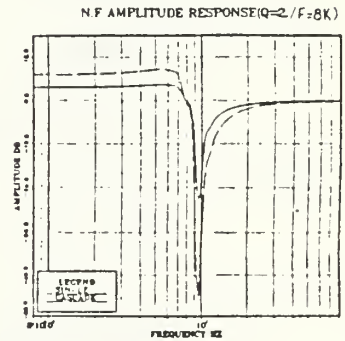


Fig. 7.n

Fig. 7 Computer Simulation's Results.

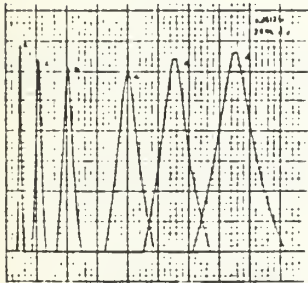


Fig. 8.a

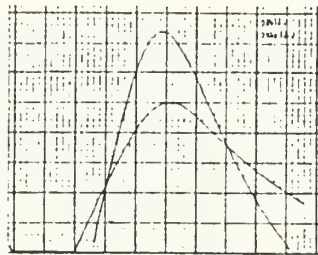


Fig. 8.b

2nd order & 4th order B.P.F

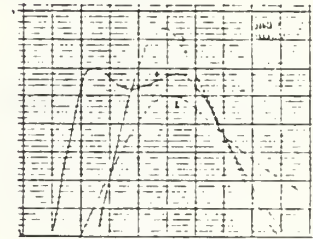


Fig. 8.c

B.P.F. Realization for different frequencies

Fig. 8 Experimental Results

LIST OF REFERENCES

1. Su, K. L., Active Network Synthesis, McGraw-Hill, New York, 1965.
2. Huelsman, L. P., Theory and Design of Active RC Circuits, McGraw-Hill, New York, 1968.
3. Haykin, S. S., Synthesis of RC Active Filter Networks, McGraw-Hill, New York, 1969.
4. Newcomb, R. W., Active Integrated Circuit Synthesis, Englewood Cliffs, N.J., Prentice-Hall, 1968.
5. Mitra, S. K., Analysis and Synthesis of Linear Active Networks, Wiley, New York, 1969.
6. Sedra, A. S. and Smith, K. C., "A Second-Generation Current Conveyor and its Applications," IEEE Trans. Circuit Theory, Vol. CT-17, pp. 132-134, 1970.
7. Sedra, A. S., "A New Approach to Active Network Synthesis," PhD Thesis, Department of Electric Engineering, University of Toronto, 1969.
8. Moschytz, G. S., Linear Integrated Networks: Fundamentals, Van Nostrand Reinhold, New York, 1975.
9. Heinlein, W. E. and Holmes, W. H., Active Filters for Integrated Circuits, R. Oldenbourg Verlag, Munich, 1974.
10. Mitra, S. K., Analysis and Synthesis of Linear Active Networks, Wiley, New York, 1959.
11. Gorski-Popiel, J., "RC-Active Synthesis Using Positive-Immittance Converters", Electron. Letts, Vol. 3, pp. 381-382, Aug. 1967.
12. Antoniou, A., "Realization of Gytrators Using Operational Amplifiers and Their Use in RC-Active Network Synthesis," Proc. Inst. Elec. Eng., Vol 116, pp. 1838-1850, Nov. 1969.
13. Riordan, R. H. S., "Simulated Inductors Using Differential Amplifiers," Electron. Letts., Vol 3, pp. 50-51, Feb. 1967.

14. Antoniou, A., "Stability Properties of Some Gyrator Circuits," Electron. Letts., Vol. 4, pp. 510-512, 1968.
15. Bruton, L. T., "Network Transfer Functions Using the Concept of Frequency-Dependent Negative Resistance," IEEE Trans. Circuit Theory, Vol. CT-16, pp. 406-408, Aug. 1969.
16. Antoniou, A., "Novel RC-Active Network Synthesis Using Generalized-Immittance Converters," IEEE Trans. Circuit Theory, Vol. CT-17, No. 2, pp. 212-217, May 1970.
17. Orchard, H. J., and Sheahan, D. F., "Introducorless Band-Pass Filters," IEEE J. Solid-State Circuits, Vol. SC-5, pp. 108-118, June 1970.
18. Cobb, D. R., and Su, K. L., "Open-Circuit Voltage Transfer Function Synthesis Using the Generalized Positive Impedance Converter," Proc. International Symposium on Circuit Theory, pp. 345-349, Apr. 1972.
19. Mikhael, W. B., and Bhattacharyya, B. B., "New Minimal-Capacitor Low-Sensitivity RC-Active Synthesis Procedure," Electron. Letts., Vol. 7, pp. 694-696, Nov. 1971.
20. Mikhael, W. B., and Bhattacharyya, B. B., "Stability Properties of Some RC-Active Realizations," Electron. Letts., Vol. 8, No. 11, pp. 288-289, June 1972.
21. Tarmi, R., and Ghausi, M. S., "Very High-Q Insensitive Active RC Networks," IEEE Trans. Circuit Theory, Vol. CT-17, pp. 358-366, Aug. 1970.
22. Kerwin, W. J., Huelsman, L. P., and Newcomb, R. W., "State-Variable Synthesis for Insensitive Integrated Circuit Transfer Functions," IEEE J. Solid State Circuits, Vol. SC-2, pp. 87-92, Sept. 1967.
23. Tow, J., "A Step-By-Step Active Filter Design," IEEE Spectrum, Vol. 6, pp. 64-68, Dec. 1969.
24. Moschytz, G. S., "FEN Filter Design Using Tantalum and Silicon Integrated Circuits," Proc. IEEE, Vol. 58, pp. 550-566, Apr. 1970.
25. Thomas, L. C., "The Biquad, Part I-Some Practical Design Considerations," IEEE Trans. Circuit Theory, Vol. CT-18, pp. 350-357, May 1971.

26. Thomas, L. C., "The Biquad, Part II-A Multi-Purpose Active Filtering System," IEEE Trans. Circuit Theory, Vol CT-18, pp. 358-361, May 1971.
27. Hamilton, T. A., and Sedra, A. S., "Some New Configurations for Active Filters," IEEE Trans. Circuit Theory, Vol. CT-19, pp. 25-33, Jan. 1972.
28. Bruton, L. T., "Biquadratic Sections Using Generalized Impedance Converters," The Radio and Electronic Engr., Vol. 41, No. 11, pp. 510-512, Nov. 1971.
29. Sheahan, D. F., and Orchard, H. J., "Band-Pass Filter Realization Using Gytrators," Electron. Letts., Vol. 3, pp. 40-42, 1967.
30. Valihora, J., "Modern Technology Applied to Network Implementation," Proc. International Symposium on Circuit Theory, pp. 169-173, Apr. 1972.
31. Bhattacharyya, B. B., Mikhael, W. B., and Antoniou, A., "Design of RC-Active Networks by Using Generalized-Immittance Converters," Proceedings of the 1974 International Symposium on Circuit Theory, pp. 290-392, April 1973.
32. Michael-Nessim, Sherif, "Composite Op. Amp. and Their Applications in Active Networks," PhD Dissertation, West Virginia University, WV, Aug. 1983.
33. Serpa, A. S., Brackett, P. O., Filter Theory and Design: Active and Passive, Matrix Publishers, Inc., 1978.
34. Luczac, Michael A., "Composite Op. Amp. and Their Use in Improving Bandwidth, Speed and Accuracy in Active Network," Thesis, NPGS, 1985.
35. Gariano, Patric, "Generation of an Optimum High Speed High Accuracy Op. Amp.," Thesis, NPGS, 1985.
36. Brodersen, R. W., Gray, P. R., and Hodges, D. A., "MOS Switched Capacitor Filters," IEEE Proceedings, Vol. 67, No. 1, pp. 61-75, Jan 1979.
37. Allstot, D. J., Brodersen, R. W., and Gray, P. R., "An Electronically Programmable Switched Capacitor Filter," IEEE Journal of Solid State Circuits, Vol. SC-14-No. 6, pp. 1034-1041, Dec. 1979.

38. Denyer, P. B., Mavor, J., and Arthur, J. W.,
"Miniature Programmable Transversal Filter Using CCD
MOS Technology," IEEE Proceedings, Vol. 67, No. 1,
pp. 42-50, Jan. 1979.
39. Michael, Sherif, and Panagiotis, Andresakis,
"Digitally Controlled Programmable Active Filters,"
19th Annual Asilomar Conference on Circuits, Systems
and Computers, Monterey, California, Nov. 1985.

INITIAL DISTRIBUTION LIST

	No. Copies
1. Library, Code 0142 Naval Postgraduate School Monterey, California 93943	2
2. Defense Technical Information Center Cameron Station Alexandria, Virginia 22304-6145	2
3. Hellenic Navy General Staff Genico Epitelio Nautikou Stratpedo Popagou Athens, Greece	4
4. Professor Sherif Michael, Code 62 Naval Postgraduate School Monterey, California 93943	4
5. Professor Gerald D. Ewing, Code 62 Naval Postgraduate School Monterey, California 93943	2
6. Department Chairman, Code 62 Naval Postgraduate School Monterey, California 93943	1
7. LT P. Andresakis, H.N. 15 Gr. Labraki Street Pireaus, 18533 Greece	6

215856

Thesis
A4952
c.1

Andresakis

Digitally controlled
"programmable" active
filters.

8 SEP 87

33446

215856

Thesis
A4952
c.1

Andresakis

Digitally controlled
"programmable" active
filters.



thesA4952

Digitally controlled programmable acti



3 2768 000 64635 0

DUDLEY KNOX LIBRARY